Generalized two-field α-attractor models from geometrically finite hyperbolic surfaces

C. I. Lazaroiu[1] **and C. S. Shahbazi**[2]

[1] *Center for Geometry and Physics, Institute for Basic Science, Pohang 37673, Republic of Korea*
[2] *Institut für Theoretische Physik, Leibniz Universität Hannover, Germany.*

E-mail: calin@ibs.re.kr, carlos.shahbazi@itp.uni-hannover.de

Abstract: We consider four-dimensional gravity coupled to a non-linear sigma model whose scalar manifold is a non-compact geometrically finite surface Σ endowed with a Riemannian metric of constant negative curvature. When the space-time is an FLRW universe, such theories produce a very wide generalization of two-field α-attractor models, being parameterized by a positive constant α, by the choice of a finitely-generated surface group $\Gamma \subset \mathrm{PSL}(2,\mathbb{R})$ (which is isomorphic with the fundamental group of Σ) and by the choice of a scalar potential defined on Σ. The traditional two-field α-attractor models arise when Γ is the trivial group, in which case Σ is the Poincaré disk. We give a general prescription for the study of such models through uniformization in the so-called "non-elementary" case and discuss some of their qualitative features in the gradient flow approximation, which we relate to Morse theory. We also discuss some aspects of the SRST approximation in these models, showing that it is generally not well-suited for studying dynamics near cusp ends. When Σ is non-compact and the scalar potential is "well-behaved" at the ends, we show that, in the *naive* local one-field truncation, our generalized models have the same universal behavior as ordinary one-field α-attractors if inflation happens near any of the ends of Σ where the extended potential has a local maximum, for trajectories which are well approximated by non-canonically parameterized geodesics near the ends; we also discuss spiral trajectories near the ends. Generalized two field α-attractors illustrate interesting consequences of nonlinear sigma models whose scalar manifold is not simply connected. They provide a large class of tractable cosmological models with non-trivial topology of the scalar field space.

Keywords: Non-linear sigma models, cosmology, hyperbolic geometry, uniformization, mathematical physics.

Contents

Introduction

Inflation in the early universe can be described reasonably well by so-called α-attractor models [1–6]. In their two-field version (see, for example, [5, 6]), such models arise from cosmological solutions of four-dimensional gravity coupled to a nonlinear sigma model whose scalar manifold Σ (i.e. the target manifold of the system of two real scalar fields) is the open unit disk endowed with its unique complete metric $\mathcal{G}$ (which determines the kinetic energy term of the scalar fields) of constant Gaussian curvature K equal to $-\frac{1}{3\alpha}$, where α is a positive constant. The "universal" behavior of such models in the radial one-field truncation close to the conformal boundary of the unit disk is a consequence of the hyperbolic character of $\mathcal{G}$ [4–6].

While ordinary one-field[1] models suffice to explain current cosmological data [7], there are at least a few good reasons to study the inflationary and post-inflationary dynamics of two-field (and of more general multi-field) models, which form a subject of active and continued interest [8–24]. First, it is possible that higher precision observations in the medium future may detect deviations from one-field model predictions. Second, it is considerably easier to produce multi-field models in fundamental theories of gravity (such as string theory) than it is to produce one-field models. Third, multi-field models are of theoretical interest in themselves. In particular, it is well-known that such models display behavior which is qualitatively new with respect to that of one-field models; this happens due to the higher-dimensionality of the target manifold of the system of real scalar fields.

In this paper, we initiate a systematic study of two-field cosmological models whose target manifold is an arbitrary borderless, connected, oriented and non-compact two-dimensional smooth manifold Σ endowed with a complete Riemannian metric $\mathcal{G}$ of constant negative curvature. Similar to the case of ordinary two-field α-attractor models, the Gaussian curvature K of $\mathcal{G}$ can be parameterized by a positive constant α which is defined though the relation $K = -\frac{1}{3\alpha}$. Since the open unit disk endowed with its unique complete metric of constant and fixed negative Gaussian curvature K provides the simplest example of such a Riemannian two-manifold, the cosmological models considered in this paper can form an extremely wide generalization of ordinary two-field α-attractors, so we shall call them *two-field generalized α-attractor models*.

Writing $\mathcal{G} = 3\alpha G$ produces a Riemannian metric G on Σ whose Gaussian curvature is constant and equal to -1. Thus (Σ, G) is an (oriented, connected, non-compact and borderless) *hyperbolic surface* and the two-field cosmological model defined by $(\Sigma, \mathcal{G})$ is equivalently parameterized by the real positive number α and by (Σ, G). The geometry and topology of non-compact hyperbolic surfaces are extremely rich. For example, such a surface can have infinite genus as well as a (countable) infinity of Freudenthal ends [25–27]; a simple example of this phenomenon is provided by the surface $\Sigma = \mathbb{C} \setminus \mathbb{Z}$, which has infinite genus and whose set of ends can be identified with the set of integer numbers. A full topological classification of oriented, borderless, connected and non-compact surfaces is provided by the so-called Kerékjártó-Stoilow model (see [28]). By the uniformization theorem of Poincaré and Koebe (see [29] for a modern account), a hyperbolic surface (Σ, G) is parameterized

[1] We count the number of *real* scalar fields present in the model.

up to isometry by the choice of the conjugacy class of a finitely-generated surface group $\Gamma \subset \mathrm{PSL}(2,\mathbb{R})$ (i.e. a discrete subgroup of $\mathrm{PSL}(2,\mathbb{R})$ without elliptic elements). Since there exists a continuous infinity of such conjugacy classes, it follows that the number of distinct choices of scalar manifold is continuously infinite for any fixed constant α. From this perspective, traditional two-field α-attractor models represent just *one* type of a continuous infinity of geometrically distinct models.

To simplify matters, in this paper we shall mostly focus on so-called *geometrically finite*[2] hyperbolic surfaces, defined as those hyperbolic surfaces (Σ, G) whose fundamental group $\pi_1(\Sigma)$ is finitely generated (but has an infinity of elements); such surfaces necessarily have finite genus as well as a finite number of ends. Even with this limitation, coupling four-dimensional gravity to the scalar sigma model with target space given by $(\Sigma, \mathcal{G})$ (while including an arbitrary smooth scalar potential $\Phi : \Sigma \to \mathbb{R}$) produces a theory whose cosmological solutions define a very wide generalization of ordinary two-field α-attractor models.

When (Σ, G) is geometrically finite, uniformization theory implies that the local form of the hyperbolic metric G on certain canonically-defined neighborhoods of each end has an explicit form in certain local coordinates defined on that neighborhood; the number of such allowed local forms is small and determines the so-called "hyperbolic type" of the end (see, for example [30]). Using this fact, we show that two-field cosmological models defined by geometrically finite hyperbolic surfaces have the same universal behavior as ordinary α-attractors for certain special trajectories, in the leading slow-roll approximation considered in the *naive* one-field truncation near each end, provided that the scalar potential is "well-behaved "and "locally maximal" at that end in the sense that it extends smoothly to a vicinity of the end considered in the Kerékjártó-Stoilow [27, 28] compactification of Σ and that its extension has a local maximum at the corresponding ideal point. This further supports our choice of name for such models. Given this similarity to ordinary two-field α-attractors, generalized models of this type may provide interesting candidates for a description of inflation in the early universe. More precisely, one finds (see [31, 32] for explicit numerical analysis in certain examples) that inflationary trajectories producing 50-60 e-folds can usually be found provided that inflation takes place within the canonical neighborhood of an end. This is of course not surprising given the naive universality property mentioned above. However, unlike the ordinary models, generalized two-field α-attractors allow for much more flexibility since Σ can have more than one end (as well as different types of ends). Of course, potential interest in such models is no way limited to their inflationary behavior. As for ordinary one-field models, one must also consider post-inflationary dynamics. It turns out that the cosmological trajectories of the models considered in this paper display quite intricate behavior away from the ends of Σ, which is partly due to the non-trivial topology of the surface; this is illustrated qualitatively in Section 4 and quantitatively in much more detail in the examples analyzed in references [31, 32].

The paper is organized as follows. In Section 1, we give the global formulation of two-field cosmological models with arbitrary Riemann surface targets and discuss a series of

[2] Sometimes called *topologically finite*.

increasingly restrictive approximations which are useful for analyzing them. The so-called "gradient flow approximation" described in that section will be used in Section 4 to give a qualitative picture of cosmological trajectories and a relation to Morse theory. We stress that the well-known SRST (slow-roll – slow-turn) approximation [8, 9] turns out to be too restrictive for a proper study of this class of models (for example, it can fail near cusp ends, as we show in Subsection 2.4). Due to this fact, we discuss a series of weaker approximations (which include, but are not limited to, the gradient flow approximation). Some of the approximations in this series do not seem to have been considered in detail in the literature, but they may turn out to be useful for deeper studies of the models considered in the present paper. Section 2 discusses classical cosmological trajectories in generalized two-field α-attractor models with geometrically finite hyperbolic surface targets. We show that the naive one-field truncation for certain special trajectories has universal behavior in the slow-roll approximation near all ends where the scalar potential is "well-behaved" and "locally maximal". We also discuss some aspects of the SRST approximation near the ends (showing that it can fail near cusp ends) and illustrate a form of spiral inflation which can occur within canonical neighborhoods of the ends. In Section 3, we propose a general method for studying such models which relies on lifting the cosmological equations to the Poincaré disk or to the upper half plane[3]. This approach assumes knowledge of a fundamental polygon for the uniformizing surface group Γ, the general computation of which is an open problem when (Σ, G) has infinite hyperbolic area (in the sense that no general stopping algorithm for computing such a polygon is known for a general infinite area geometrically finite hyperbolic surface). Section 4 gives a qualitative description of inflationary trajectories in the gradient flow approximation using the topological pants decomposition induced by Morse theory. In Section 5, we discuss some phenomenological aspects of our models and certain examples which are studied in detail in references [31, 32]. Finally, Section 6 concludes. Appendix A summarizes some useful formulas in isothermal and semi-geodesic coordinates, which are often used in various computations within this paper. The remaining appendices summarize certain classical results of uniformization theory (many of which go back to Poincaré). These are used throughout the paper but some of them may be unfamiliar to the cosmology community. Appendix B recalls some fundamental results on the uniformization of smooth (but not necessarily compact) Riemann surfaces. Appendix C summarizes relevant classical results regarding topologically finite surfaces and their Kerékjártó-Stoilow compactification (which is a closed surface). It also recalls some fundamental results regarding topologically finite surfaces endowed with a conformal structure and their conformal compactification (which generally is a surface with boundary). The Kerékjártó-Stoilow and conformal compactifications are conceptually important for understanding the behavior of our models near the ends of Σ. In Appendix D, we recall some classical results on geometrically finite hyperbolic surfaces, paying special attention to certain canonical neighborhoods of their ends, on which the hyperbolic metric can be brought to one of a few explicit forms. This paper assumes some basic familiarity with

[3] This relates a subclass of our models to the "modular inflation models" considered in [11, 12]. See [32] for a detailed discussion of the precise connection in the case of the hyperbolic triply-punctured sphere.

the notion of Freudenthal end of a manifold, for which we refer the reader to [25, 26]. For the case of surfaces, the Freudenthal theory of ends reduces to the classical theory of "ideal boundary points" developed by Kerékjártó and Stoilow (see [27, 28]).

Notations and conventions. All manifolds considered are smooth, connected, oriented and paracompact (hence also second-countable). All homeomorphisms and diffeomorphisms considered are orientation-preserving. By definition, a Lorentzian four-manifold has "mostly plus" signature.

1 Cosmological models with two real scalar fields minimally coupled to gravity

In this section, we give the general description of cosmological models with two real scalar fields minimally coupled to gravity, allowing for scalar manifolds of non-trivial topology. Our formulation is globally valid (in particular, it is coordinate free), since we allow for arbitrary topology of the target manifold Σ. Some of the local formulas are standard, but the reader should pay attention to the mathematical aspects involved in the global approach. We also discuss certain increasingly restrictive approximations which are useful when studying inflation in such models, the strictest of which is the well-known SRST approximation (which, as shown in Subsection 2.4, turns out to be of limited usefulness for such models). The so-called "gradient flow approximation" will be used in Section 4. The reader may notice that some of the approximations discussed in this section are not usually considered in the cosmology literature; they may be useful for our class of models due to the fact that the SRST approximation fails near cusp ends.

1.1 Two-dimensional scalar manifolds and scalar potentials

Let $(\Sigma, \mathcal{G})$ be any oriented, connected and complete two-dimensional Riemannian manifold without boundary (called the *scalar manifold*) and $\Phi : \Sigma \to \mathbb{R}$ be a smooth function (called the *scalar potential*).

Remark. The condition that Σ be orientable is physically unimportant and can be relaxed; we make this assumption merely for simplicity. We do *not* assume that Σ is compact; as we shall see below, allowing Σ to be non-compact is of direct relevance to cosmological applications. We require that the scalar manifold metric $\mathcal{G}$ be complete in order to avoid problems with conservation of energy.

With such weak assumptions, the topology of Σ can be quite involved. When Σ is compact, its (oriented) diffeomorphism class[4] is completely determined by its genus g. In that case, the fundamental group $\pi_1(\Sigma)$ is finitely generated on $2g$ generators and its Abelianization $H_1(\Sigma, \mathbb{Z})$ is isomorphic with $\mathbb{Z}^{2g}$. The topological classification is much more subtle when Σ is non-compact. In that case, the fundamental group can be infinitely

[4] The homeomorphism and diffeomorphism classifications of two-manifolds coincide as implied by Kirby's torus trick.

generated[5] and Σ can have an infinite number of ends in the sense of Freudenthal [25, 26]. The ends correspond to the "ideal points" of the "ideal boundary" of the so-called *end compactification* (a.k.a. *Kerékjártó-Stoilow compactification*) $\hat{\Sigma}$ of Σ (see [27]). The ideal boundary is a totally-disconnected, compact and separable topological space, containing a closed subset corresponding to "non-planar" ends. Together with this subspace, the ideal boundary determines the topology of Σ. In fact, every pair of nested totally disconnected, compact and separable spaces occurs as the ideal boundary of some orientable non-compact surface [27]. Moreover, Σ admits a canonical *Stoilow presentation* (or *Stoilow model*) [28] as the surface obtained by removing from the Riemann sphere $\mathbb{C} \sqcup \{\infty\} \simeq \mathbb{CP}^1$ a compact totally disconnected set B of points lying on the real axis (where B corresponds to the ideal boundary) and a finite or countable collection of pairs of mutually-disjoint disks which are symmetric with respect to the real axis and whose bounding circles can accumulate only on the set B, after which the bounding circles are pairwise identified. In latter sections of the paper, we will focus for simplicity on the case when Σ is *topologically finite*, which means that its fundamental group $\pi_1(\Sigma)$ is finitely-generated. In that case, the genus of Σ is finite and the ideal boundary consists of a finite number of points $p_1, \ldots, p_n$, all of which correspond to planar ends; in this situation, the end compactification $\hat{\Sigma}$ is a compact oriented surface from which Σ is obtained by removing the points p_j (see Appendix C for details). The case of compact Σ arises when the ideal boundary is empty, i.e. when Σ has no ends; in that case, one has $\hat{\Sigma} = \Sigma$.

1.2 The Einstein-Scalar theory defined by $(\Sigma, \mathcal{G}, \Phi)$

Any triplet $(\Sigma, \mathcal{G}, \Phi)$ as above allows one to define an Einstein-Scalar theory on any four-dimensional oriented manifold X which admits Lorentzian metrics. This theory includes four-dimensional gravity (described by a Lorentzian metric g defined on X) and a smooth map $\varphi : X \to \Sigma$ (which locally describes two real scalar fields), with action:

$$S[g, \varphi] = \int_X \mathcal{L}(g, \varphi) \mathrm{vol}_g \quad , \tag{1.1}$$

where vol_g is the volume form of (X, g) and $\mathcal{L}(g, \varphi)$ is the Lagrange density:

$$\mathcal{L}(g, \varphi) \stackrel{\text{def.}}{=} \frac{M^2}{2} \mathrm{R}(g) - \frac{1}{2} \mathrm{Tr}_g \varphi^*(\mathcal{G}) - \Phi \circ \varphi \quad . \tag{1.2}$$

Here $\mathrm{R}(g)$ is the scalar curvature of g and M is the reduced Planck mass. The notation $\varphi^*(\mathcal{G})$ denotes the pull-back through φ of the metric $\mathcal{G}$ (this pull-back is a symmetric covariant 2-tensor field defined on X), while $\mathrm{Tr}_g \varphi^*(\mathcal{G})$ denotes the trace of the tensor field of type $(1, 1)$ obtained by raising one of the indices of $\varphi^*(\mathcal{G})$ using the metric g. The notation $\Phi \circ \varphi$ denotes the smooth map from X to $\mathbb{R}$ obtained by composing φ with Φ. The formulation (1.2) allows one to define such a theory globally for any topology of the oriented scalar manifold Σ and any topology of the oriented space-time X. For any fixed

[5] A simple example is provided by the planar non-compact surface $\Sigma = \mathbb{C} \setminus \mathbb{Z}$, which has infinitely generated fundamental group.

Lorentzian metric g, the Lagrange density:

$$\mathcal{L}_g(\varphi) \stackrel{\text{def.}}{=} -\frac{1}{2}\mathrm{Tr}_g\varphi^*(\mathcal{G}) - \Phi\circ\varphi$$

defines the non-linear sigma model with source (X, g), target space $(\Sigma, \mathcal{G})$ and scalar potential Φ.

Local expressions in real coordinates on Σ. If $(U, (x^\mu)_{\mu=0\ldots3})$ and $(V, (y^\alpha)_{\alpha=1,2})$ are local coordinate systems on X and Σ such that $\varphi(U) \subset V$, then the map φ has locally-defined components:

$$\varphi^\alpha(x) = (y^\alpha \circ \varphi)(x) \quad \text{for} \quad x \in U$$

and the metrics g and $\mathcal{G}$ have squared line elements:

$$\mathrm{d}s_g^2 = g_{\mu\nu}\mathrm{d}x^\mu\mathrm{d}x^\nu \quad , \quad \mathrm{d}s_{\mathcal{G}}^2 = \mathcal{G}_{\alpha\beta}\mathrm{d}y^\alpha\mathrm{d}y^\beta \quad .$$

Moreover, we have:

$$\mathrm{Tr}_g\varphi^*(\mathcal{G}) = g^{\mu\nu}\mathcal{G}_{\alpha\beta}\partial_\mu\varphi^\alpha\partial_\nu\varphi^\beta \quad , \quad (\Phi\circ\varphi)(x) = \Phi(\varphi^1(x), \varphi^2(x)) \quad .$$

Hence $\mathcal{L}(g, \varphi)$ coincides locally with the usual expression for the Lagrange density of two real scalar fields minimally coupled to gravity.

Local expressions in a $\mathcal{G}$-compatible complex coordinate on Σ. By definition, a *conformal structure* on Σ is a conformal equivalence class of metrics on Σ. Since Σ is a surface, any almost complex structure J on Σ has vanishing Nijenhuis tensor and hence is integrable (i.e. it is a complex structure). Moreover, any two-form on Σ is closed and hence any J-Hermitian metric on Σ is Kähler. Recall that the set of conformal equivalence classes of Riemannian metrics on Σ is in bijection with the set of orientation-compatible complex structures on Σ. This bijection takes the conformal equivalence class of a Riemannian metric $\mathcal{G}$ into the unique orientation-compatible complex structure J which has the property that $\mathcal{G}$ is Hermitian (and hence Kähler) with respect to J. Endowing Σ with the complex structure J determined by $\mathcal{G}$, let z be a local J-holomorphic coordinate on Σ, defined on an open subset $V \subset \Sigma$. Since $\mathcal{G}$ is Hermitian with respect to J, we have $\mathrm{d}s_{\mathcal{G}}^2|_V = \lambda(z, \bar{z})^2|\mathrm{d}z|^2$ for some positive function $\lambda(z, \bar{z}) > 0$ (See Appendix A). Choosing a local chart $(U, (x^\mu))$ of X such that $\varphi(U) \subset V$ and setting $z(x) \stackrel{\text{def.}}{=} z(\varphi(x))$, the map φ is described locally by the complex-valued scalar field $z(x)$ and the Lagrange density takes the local form:

$$\mathcal{L}(g, z) = \frac{M^2}{2}\mathrm{R}(g) - \frac{1}{2}\lambda^2(z, \bar{z})g^{\mu\nu}\partial_\mu z\partial_\nu\bar{z} - \Phi(z, \bar{z}) \quad . \tag{1.3}$$

1.3 Cosmological models defined by $(\Sigma, \mathcal{G}, \Phi)$

By definition, a *cosmological model* defined by $(\Sigma, \mathcal{G}, \Phi)$ is a solution of the equations of motion of the theory (1.1)-(1.2) when (X, g) is an FLRW universe and φ depends only on the cosmological time. We shall assume for simplicity that the spatial section is flat and simply connected. With these assumptions, the cosmological models of interest are defined by the following conditions:

1. X is diffeomorphic with $\mathbb{R}^4$, with global coordinates (t, x^1, x^2, x^3)
2. The squared line element of g has the form:

$$\mathrm{d}s_g^2 = -\mathrm{d}t^2 + a(t)^2 \sum_{i=1}^{3} (\mathrm{d}x^i)^2 \quad , \tag{1.4}$$

   where $a(t) > 0$. In particular, the space-time metric g is determined by the single function $a(t)$.
3. φ depends only on t.
4. $(a(t), \varphi(t))$ are such that (g, φ) is a solution of the equations of motion derived from the action functional (1.1).

Let $||\cdot||_{\mathcal{G}}$ denote the norm induced by $\mathcal{G}$ on the fibers of the tensor and exterior powers of the tangent bundle $T\Sigma$ and of the cotangent bundle $T^*\Sigma$. Since φ depends only on t, it describes a smooth curve $\varphi : \mathfrak{I} \to \Sigma$ in Σ, where $\mathfrak{I}$ is a maximal interval of definition of the solution. Setting $\dot{} \stackrel{\text{def.}}{=} \frac{\mathrm{d}}{\mathrm{d}t}$, let $H \stackrel{\text{def.}}{=} \frac{\dot{a}}{a}$ denote the Hubble parameter and let $\dot{\varphi}(t) \stackrel{\text{def.}}{=} \frac{\mathrm{d}\varphi(t)}{\mathrm{d}t} \in T_{\varphi(t)}\Sigma$ for $t \in \mathfrak{I}$. Let σ be the proper length along this curve measured starting from $t = t_0 \in \mathfrak{I}$:

$$\sigma(t) \stackrel{\text{def.}}{=} \int_{t_0}^{t} \mathrm{d}t' ||\dot{\varphi}(t')||_{\mathcal{G}} \implies \dot{\sigma}(t) = ||\dot{\varphi}(t)||_{\mathcal{G}} \quad (t \in \mathfrak{I}) \quad .$$

We assume that $||\dot{\varphi}(t)||$ does not vanish for $t \in \mathfrak{J}$. The equations of motion derived from the action (1.1) when g is given by (1.4) and φ depends only on t reduce to:

$$\nabla_t \dot{\varphi} + 3H\dot{\varphi} + (\mathrm{grad}_{\mathcal{G}}\Phi) \circ \varphi = 0 \quad , \tag{1.5}$$

$$\frac{1}{3}\dot{H} + H^2 - \frac{\Phi \circ \varphi}{3M^2} = 0 \quad , \tag{1.6}$$

$$\dot{H} + \frac{\dot{\sigma}^2}{2M^2} = 0 \quad , \tag{1.7}$$

where:

$$\nabla_t \stackrel{\text{def.}}{=} \nabla_{\dot{\varphi}(t)}$$

is the covariant derivative with respect to $\dot{\varphi}(t)$. Assuming $H(t) > 0$, equations (1.6) and (1.7) give:

$$H(t) = \frac{1}{\sqrt{6}M} \left[||\dot{\varphi}(t)||_{\mathcal{G}}^2 + 2\Phi(\varphi(t)) \right]^{1/2} \quad . \tag{1.8}$$

This allows us to eliminate $H(t)$, thus reducing the system (1.5)-(1.7) to the single non-linear equation:

$$\nabla_t \dot{\varphi}(t) + \frac{1}{M}\sqrt{\frac{3}{2}} \left[||\dot{\varphi}(t)||_{\mathcal{G}}^2 + 2\Phi(\varphi(t)) \right]^{1/2} \dot{\varphi}(t) + (\mathrm{grad}_{\mathcal{G}}\Phi)(\varphi(t)) = 0 \quad . \tag{1.9}$$

The initial conditions at cosmological time $t_0 \in \mathfrak{I}$ take the form:

$$\varphi(t_0) = \varphi_0 \quad , \quad \dot{\varphi}(t_0) = v_0 \in T_{\varphi_0}\Sigma \quad , \tag{1.10}$$

where φ_0 is a point of Σ and v_0 is a vector tangent to Σ at that point. Together with the initial conditions (1.10), equation (1.9) determines the function $\varphi(t)$, which also determines $H(t)$ through relation (1.8).

1.4 Conditions for inflation

Equation (1.7) shows that $\dot{H}$ is negative. As usual, define the *first slow-roll parameter* through:

$$\epsilon(t) \stackrel{\text{def.}}{=} -\frac{\dot{H}(t)}{H(t)^2} > 0 \quad . \tag{1.11}$$

Then:

$$\frac{\ddot{a}}{a} = \dot{H} + H^2 = H^2(1-\epsilon)$$

and the condition for inflation $\ddot{a} > 0$ amounts to $\epsilon(t) < 1$. By definition, inflation occurs for time intervals during which $H > 0$ and $\epsilon < 1$, i.e. for intervals where a is a (strictly) convex and increasing function of the cosmological time t. Using (1.11), equation (1.6) becomes:

$$H(t)^2(1 - \frac{\epsilon(t)}{3}) = \frac{1}{3M^2}\Phi(\varphi(t))$$

and the conditions for inflation read:

$$H > 0 \ \text{ and } \ \Phi > 2M^2H^2 \iff \Phi(\varphi(t)) > 0 \ \text{ and } \ 0 < H(t) < \frac{1}{M}\sqrt{\frac{\Phi(\varphi(t))}{2}} \quad . \tag{1.12}$$

Using (1.8), these amount to $H(t) > 0$ together with the condition:

$$||\dot{\varphi}(t)||^2_{\mathcal{G}} < \Phi(\varphi(t)) \quad .$$

When $H(t) > 0$, we have:

$$\epsilon(t) \ll 1 \ \text{ iff } \ ||\dot{\varphi}(t)||^2_{\mathcal{G}} \ll \Phi(\varphi(t)) \quad .$$

1.5 The gradient flow approximation

In this subsection, we discuss an approximation in which cosmological trajectories of the model are replaced by reparameterized gradient flow lines of the scalar potential Φ. This allows one to derive qualitative features of the model using the well-known properties of gradient flows on Riemann surfaces, which is especially useful when Φ is a Morse function (see Section 4 for an application of this approximation). We stress that the approximation discussed in this subsection is much less restrictive than the well-known SRST approximation [8, 9]. The latter is used traditionally when studying cosmological perturbations in two-field models but turns out to be ill-suited for understanding deeper aspects of generalized two-field α-attractors (see Subsection 2.4 for how the SRST approximation can fail near cusp ends).

Assuming $H(t) > 0$, define the *gradient flow vector parameter* through:

$$\eta(t) \stackrel{\text{def.}}{=} -\frac{1}{H\dot{\sigma}}\nabla_t\dot{\varphi} = -\frac{1}{H}\frac{\nabla_t\dot{\varphi}}{||\dot{\varphi}||_{\mathcal{G}}} = -M\sqrt{6}\left[||\dot{\varphi}(t)||^2_{\mathcal{G}} + 2\Phi(\varphi(t))\right]^{-1/2}\frac{\nabla_t\dot{\varphi}}{||\dot{\varphi}||_{\mathcal{G}}} \quad , \tag{1.13}$$

i.e.:

$$\eta(t) = 3\frac{\left[||\dot{\varphi}(t)||^2_{\mathcal{G}} + 2\Phi(\varphi(t))\right]^{1/2}\dot{\varphi}(t) + M\sqrt{\frac{2}{3}}(\mathrm{grad}_{\mathcal{G}}\Phi)(\varphi(t))}{||\dot{\varphi(t)}||_{\mathcal{G}}\left[||\dot{\varphi}(t)||^2_{\mathcal{G}} + 2\Phi(\varphi(t))\right]^{1/2}} \quad . \tag{1.14}$$

Using (1.13), equation (1.5) becomes:

$$3H||\dot{\varphi}||_{\mathcal{G}}(\vartheta - \frac{\eta}{3}) + \mathrm{grad}_{\mathcal{G}}\Phi = 0 \quad , \tag{1.15}$$

where:

$$\vartheta(t) \stackrel{\mathrm{def.}}{=} \frac{\dot{\varphi}(t)}{||\dot{\varphi}(t)||_{\mathcal{G}}} \tag{1.16}$$

is the unit tangent vector to the curve φ at time t. Since $||\vartheta||_{\mathcal{G}} = 1$, the term proportional to η can be neglected in this equation when the *kinematic gradient flow condition*:

$$||\eta||_{\mathcal{G}} \ll 1 \tag{1.17}$$

is satisfied. When (1.17) holds, equation (1.15) reduces to:

$$\dot{\varphi}(t) \simeq -\frac{1}{3H(t)}(\mathrm{grad}_{\mathcal{G}}\Phi)(\varphi(t)) \iff \frac{\mathrm{d}\varphi(q)}{\mathrm{d}q} \simeq -(\mathrm{grad}_{\mathcal{G}}\Phi)(\varphi(q)) \quad , \tag{1.18}$$

which shows that φ can be approximated by a gradient flow trajectory $\varphi_\bullet(q)$ of the potential Φ with respect to the metric $\mathcal{G}$ and the parameter:

$$q(t) \stackrel{\mathrm{def.}}{=} q_0 + \int_{t_0}^{t} \mathrm{d}t' \frac{1}{3H(t')} \quad . \tag{1.19}$$

In this expression, we assumed that t_0 is chosen within a time interval on which the gradient flow approximation holds and we set $q(t_0) = q_0$. Using (1.18), relation (1.8) reduces to the algebraic equation:

$$H^4 - \frac{\Phi}{3M^2}H^2 - \frac{||\mathrm{d}\Phi||^2_{\mathcal{G}}}{54M^2} = 0 \quad ,$$

which gives:

$$H(t(q)) = \frac{1}{M\sqrt{6}}\left(\Phi(\varphi_\bullet(q)) + \sqrt{\Phi(\varphi_\bullet(q))^2 + \frac{2}{3}M^2||(\mathrm{d}\Phi)(\varphi_\bullet(q))||^2_{\mathcal{G}}}\ \right)^{1/2} \quad , \tag{1.20}$$

where we assumed $H(t) > 0$. Thus (1.19) reduces to:

$$t - t_0 = \frac{1}{M}\sqrt{\frac{3}{2}}\int_{q_0}^{q} \mathrm{d}q \left(\Phi(\varphi_\bullet(q)) + \sqrt{\Phi(\varphi_\bullet(q))^2 + \frac{2}{3}M^2||(\mathrm{d}\Phi)(\varphi_\bullet(q))||^2_{\mathcal{G}}}\ \right)^{1/2} \quad . \tag{1.21}$$

This relation can be used to determine t as a function of q given the approximating gradient flow trajectory $\varphi_\bullet(q)$.

Let us assume that $\Phi(\varphi(t)) > 0$, as required by the first inflation condition in (1.12). Then the second inflation condition amounts to the following inequality in the gradient flow approximation:

$$M\frac{||(\mathrm{d}\Phi)(\varphi_\bullet(q))||_{\mathcal{G}}}{\Phi(\varphi_\bullet(q))} < \frac{3}{\sqrt{2}} \quad .$$

Together with (1.21), the last inequality can be used to determine the inflationary time intervals within the gradient flow approximation. Notice from (1.20) that H is determined by the point $\varphi_\bullet(q) \in \Sigma$ in this approximation.

A gradient flow trajectory is determined uniquely by the gradient flow equation:

$$\frac{\mathrm{d}\varphi_\bullet(q)}{\mathrm{d}q} = -(\mathrm{grad}_{\mathcal{G}}\Phi)(\varphi_\bullet(q)) \tag{1.22}$$

(which is a *first* order differential equation), together with the initial condition:

$$\varphi_\bullet(q_0) = \varphi_0 \quad .$$

Validity of the gradient flow approximation at $t = t_0$ requires $\frac{\mathrm{d}\varphi}{\mathrm{d}q}(q_0) = -(\mathrm{grad}_{\mathcal{G}}\Phi)(\varphi_0)$, i.e.:

$$v_0 = -\frac{(\mathrm{grad}_{\mathcal{G}}\Phi)(\varphi_0)}{3H_0} \quad , \tag{1.23}$$

where $H_0 \stackrel{\mathrm{def.}}{=} H(t_0)$ is determined from (1.20) as:

$$H_0 = \frac{1}{M\sqrt{6}}\left(\Phi(\varphi_0) + \sqrt{\Phi(\varphi_0)^2 + \frac{2}{3}M^2||(\mathrm{d}\Phi)(\varphi_0)||^2_{\mathcal{G}}}\right)^{1/2} \quad . \tag{1.24}$$

In particular, the gradient flow approximation constrains the initial velocity v_0 in terms of the initial value φ_0, as expected from the fact that, in this approximation, the second order equation (1.9) is replaced by the first order equation (1.22).

1.6 The potential gradient flow condition

In the gradient flow approximation, we have $||\dot{\varphi}||_{\mathcal{G}} = \frac{1}{3H}||\mathrm{d}\Phi||_{\mathcal{G}}$ and equation (1.7) gives:

$$\dot{H} \simeq -\frac{1}{18M^2H^2}||\mathrm{d}\Phi||^2_{\mathcal{G}} \quad .$$

Relation (1.19) implies:

$$\nabla_t = \nabla_{\dot{\varphi}(t)} \simeq \frac{1}{3H}\nabla_{\frac{\mathrm{d}\varphi_\bullet(q)}{\mathrm{d}q}} = -\frac{1}{3H}\nabla_{\mathrm{grad}_{\mathcal{G}}\Phi} \quad .$$

Thus:

$$\begin{aligned}\nabla_t\dot{\varphi} &= \nabla_t\left[\frac{1}{3H}\mathrm{grad}_{\mathcal{G}}\Phi\right] = -\frac{\dot{H}}{3H^2}\mathrm{grad}_{\mathcal{G}}\Phi + \frac{1}{3H}(\nabla_t\,\mathrm{grad}_{\mathcal{G}}\Phi) \simeq \\ &\simeq \frac{1}{9H^2}\left[\frac{1}{6M^2H^2}||\mathrm{d}\Phi||^2_{\mathcal{G}}\,\mathrm{grad}_{\mathcal{G}}\Phi - \nabla_{\mathrm{grad}_{\mathcal{G}}\Phi}\,\mathrm{grad}_{\mathcal{G}}\Phi\right]\end{aligned}$$

and:

$$\eta = -\frac{1}{H}\frac{\nabla_t\dot{\varphi}}{||\dot{\varphi}||_{\mathcal{G}}} \simeq -3\frac{\nabla_t\dot{\varphi}}{||\mathrm{d}\Phi||_{\mathcal{G}}} \simeq \frac{1}{3H^2}\frac{\nabla_{\mathrm{grad}_{\mathcal{G}}\Phi}\,\mathrm{grad}_{\mathcal{G}}\Phi}{||\mathrm{d}\Phi||_{\mathcal{G}}} - \frac{1}{18M^2H^4}||\mathrm{d}\Phi||_{\mathcal{G}}\,\mathrm{grad}_{\mathcal{G}}\Phi \quad .$$

This gives:

$$||\eta||^2_{\mathcal{G}} \simeq \frac{1}{9H^4}\frac{||\nabla_{\mathrm{grad}_{\mathcal{G}}\Phi}\,\mathrm{grad}_{\mathcal{G}}\Phi||^2_{\mathcal{G}}}{||\mathrm{d}\Phi||^2_{\mathcal{G}}} - \frac{1}{27M^2H^6}\mathcal{G}(\mathrm{grad}_{\mathcal{G}}\Phi, \nabla_{\mathrm{grad}_{\mathcal{G}}\Phi}\,\mathrm{grad}_{\mathcal{G}}\Phi) + \frac{||\mathrm{d}\Phi||^4_{\mathcal{G}}}{324M^4H^8} \quad . \tag{1.25}$$

Since $\mathcal{G}$ is covariantly constant with respect to its Levi-Civita connection ∇, the following relation holds for any vector field X defined on Σ:

$$\partial_X ||X||^2_{\mathcal{G}} = 2\mathcal{G}(X, \nabla_X X) \quad .$$

Using this relation for $X = \mathrm{grad}_{\mathcal{G}}\Phi$, equation (1.25) becomes:

$$||\eta||^2_{\mathcal{G}} \simeq \frac{1}{9H^4} \frac{||\nabla_{\mathrm{grad}_{\mathcal{G}}\Phi} \mathrm{grad}_{\mathcal{G}}\Phi||^2_{\mathcal{G}}}{||\mathrm{d}\Phi||^2_{\mathcal{G}}} - \frac{1}{54M^2H^6} \partial_{\mathrm{grad}_{\mathcal{G}}\Phi} ||\mathrm{d}\Phi||^2_{\mathcal{G}} + \frac{||\mathrm{d}\Phi||^4_{\mathcal{G}}}{324M^4H^8} \quad .$$

Hence consistency of the gradient flow approximation requires that the *potential gradient flow condition*:

$$\frac{1}{9H^4} \frac{||\nabla_{\mathrm{grad}_{\mathcal{G}}\Phi} \mathrm{grad}_{\mathcal{G}}\Phi||^2_{\mathcal{G}}}{||\mathrm{d}\Phi||^2_{\mathcal{G}}} - \frac{1}{54M^2H^6} \partial_{\mathrm{grad}_{\mathcal{G}}\Phi} ||\mathrm{d}\Phi||^2_{\mathcal{G}} + \frac{||\mathrm{d}\Phi||^4_{\mathcal{G}}}{324M^4H^8} \ll 1 \tag{1.26}$$

is satisfied. In this relation, H^2 can be expressed in terms of Φ and $||\mathrm{d}\Phi||_{\mathcal{G}}$ using relation (1.20), thus obtaining a condition involving only the metric $\mathcal{G}$ as well as Φ and its first and second order derivatives:

$$\frac{\begin{bmatrix} 12\,\|\mathrm{d}\Phi\|^6_{\mathcal{G}}\,M^4 - 12\,\|\mathrm{d}\Phi\|^2_{\mathcal{G}}\,M^4 \left(\Phi + \sqrt{\Phi^2 + \frac{2}{3}M^2\,\|\mathrm{d}\Phi\|^2_{\mathcal{G}}}\right) \partial_{\mathrm{grad}_{\mathcal{G}}\Phi}\,\|\mathrm{d}\Phi\|^2_{\mathcal{G}} + \\ +8M^4 \left[M^2\,\|\mathrm{d}\Phi\|^2_{\mathcal{G}} + 3\Phi \left(\Phi + \sqrt{\Phi^2 + \frac{2}{3}M^2\,\|\mathrm{d}\Phi\|^2_{\mathcal{G}}}\right)\right] \left\|\nabla_{\mathrm{grad}_{\mathcal{G}}\Phi}\mathrm{grad}_{\mathcal{G}}\Phi\right\|^2_{\mathcal{G}} \end{bmatrix}}{3\,\|\mathrm{d}\Phi\|^2_{\mathcal{G}} \left(\Phi + \sqrt{\Phi^2 + \frac{2}{3}M^2\,\|\mathrm{d}\Phi\|^2_{\mathcal{G}}}\right)^4} \ll 1 \ .$$

The potential gradient flow condition is necessary for validity of the gradient flow approximation.

1.7 Decomposition in a Frenet frame

The equations of Subsection 1.3 define globally a two-field cosmological model with non-canonical kinetic term. As usual in the theory of curves, it is convenient to choose a *framing* of φ, which in this case is a unit norm smooth vector field $n \in \Gamma(\mathfrak{I}, \varphi^*(T\Sigma))$ which is everywhere orthogonal to the unit tangent vector (1.16):

$$n(t) \perp \vartheta(t) = 0 \quad , \text{ i.e. } \mathcal{G}(n(t), \vartheta(t)) = 0 \quad , \quad \forall t \in \mathfrak{I} \quad .$$

We have $\vartheta(t), n(t) \in T_{\varphi(t)}\Sigma$ for all $t \in \mathfrak{I}$. Since Σ is oriented, we can choose n so that $(\vartheta(t), n(t))$ is a positively-oriented orthonormal basis of $T_{\varphi(t)}\Sigma$ for all t. The Frenet-Serret equations of φ read:

$$\nabla_t \vartheta(t) = \dot{\sigma}\,\kappa\,n \quad , \quad \nabla_t n(t) = -\dot{\sigma}\,\kappa\,\vartheta \quad , \tag{1.27}$$

where $\kappa(t)$ is the extrinsic curvature of φ. Using the first of equations (1.27) and the relation $\dot{\varphi} = \dot{\sigma}\vartheta$ gives:

$$\nabla_t \dot{\varphi} = \ddot{\sigma}\vartheta + \dot{\sigma}^2 \kappa n \quad . \tag{1.28}$$

Thus:

$$\eta = \eta_{\|}\vartheta + \eta_{\perp} n \quad , \tag{1.29}$$

where

$$\eta_{\|} \stackrel{\text{def.}}{=} \mathcal{G}(\vartheta, \eta) = -\frac{\ddot{\sigma}}{H\dot{\sigma}} \quad , \quad \eta_{\perp} \stackrel{\text{def.}}{=} \mathcal{G}(n, \eta) = -\frac{\dot{\sigma}}{H}\kappa = \frac{\partial_n \Phi}{H\dot{\sigma}}$$

are known [10] as the *second slow-roll parameter* ($\eta_{\|}$) and the *first slow-turn parameter* ($\eta_{\perp}$). Using (1.28) and the relation $\dot{\varphi} = \dot{\sigma}\vartheta$ shows that (1.5) is equivalent with the system:

$$\ddot{\sigma} + 3H\dot{\sigma} + \partial_{\vartheta}\Phi = 0 \quad , \tag{1.30}$$

$$\kappa = -\frac{1}{\dot{\sigma}^2}\partial_n \Phi \quad . \tag{1.31}$$

Notice that $\dot{\Phi} \stackrel{\text{def.}}{=} \frac{\mathrm{d}}{\mathrm{d}t}(\Phi \circ \varphi) = (\mathrm{d}\Phi)(\dot{\varphi}) = \dot{\sigma}\partial_{\vartheta}\Phi$. Using (1.29), the system becomes:

$$\begin{aligned} 3(1 - \frac{\eta_{\|}}{3})H\dot{\sigma} &= -\partial_{\vartheta}\Phi \quad , \\ \eta_{\perp} H\dot{\sigma} &= \partial_n \Phi \quad . \end{aligned} \tag{1.32}$$

Since $||\eta||_{\mathcal{G}} = \sqrt{\eta_{\|}^2 + \eta_{\perp}^2}$, the gradient flow condition $||\eta||_{\mathcal{G}} \ll 1$ amounts to $|\eta_{\|}| \ll 1$ and $|\eta_{\perp}| \ll 1$.

1.8 The slow gradient flow approximation

In this subsection, we discuss an approximation which is more restrictive than the gradient flow approximation in that it implies the latter. This consists of approximating cosmological trajectories by gradient flow lines and further assuming that the motion along such lines is "slow".

Formally, the *slow gradient flow approximation* is defined by the *kinematic slow gradient flow conditions*:

$$\epsilon \ll 1 \ \text{ and } \ ||\eta||_{\mathcal{G}} \ll 1 \quad . \tag{1.33}$$

Notice that these are more restrictive than the kinematic gradient flow condition.

Proposition. When (1.33) hold, we have $\vartheta \simeq \frac{\mathrm{grad}_{\mathcal{G}}\Phi}{||\mathrm{d}\Phi||_{\mathcal{G}}}$ and the scalar potential Φ satisfies the *potential slow gradient flow conditions*:

$$M|\partial_n \log \Phi| \ll 1 \quad , \tag{1.34}$$

$$\left|\frac{\partial_n \Phi}{\partial_{\vartheta}\Phi}\right| \ll 1 \quad , \tag{1.35}$$

$$M^2 \frac{\mathrm{Hess}(\Phi)(\vartheta, \vartheta)}{\Phi} \ll 1 \quad , \tag{1.36}$$

where $\mathrm{Hess}(\Phi)$ is the Hessian of Φ.

Proof. Using the first slow-roll parameter, equations (1.6) and (1.7) become:

$$\dot{\sigma} = MH\sqrt{2\epsilon} \text{ and } \Phi = 3M_p^2H^2\left(1+\frac{\epsilon}{3}\right) \quad . \tag{1.37}$$

Assume that $\eta_{\|} \ll 1$. Then the first term of equation (1.30) can be neglected and (1.30) becomes:

$$H\dot{\sigma} \simeq -\frac{1}{3}\partial_\vartheta\Phi \implies \eta_\perp = -\frac{3\partial_n\Phi}{\partial_\vartheta\Phi} \quad .$$

Differentiating this relation with respect to t and dividing the resulting equation by H^2 gives:

$$\eta_{\|} + \epsilon = \frac{1}{3H^2}\nabla_\vartheta\partial_\vartheta\Phi = M^2\left(1+\frac{\epsilon}{3}\right)\frac{\nabla_\vartheta\partial_\vartheta\Phi}{\Phi} \quad , \tag{1.38}$$

where in the last equality we used (1.37). Let us further assume that $\epsilon \ll 1$. Then (1.38) gives $\eta_{\|} \simeq M^2\frac{\nabla_\vartheta\partial_\vartheta\Phi}{\Phi}$. In this case, the full gradient flow condition $||\eta||_{\mathcal{G}} \ll 1$ implies (1.35) and (1.36).

Now let us assume that the full conditions (1.33) hold. Then (1.22) applies, giving:

$$\dot{\sigma} \simeq ||\dot{\varphi}||_{\mathcal{G}} = \frac{|\partial_n\Phi|}{3H} \quad .$$

Substituting this into the relation $\epsilon = \frac{\dot{\sigma}^2}{2H^2M^2}$ gives:

$$\epsilon \simeq \frac{|\partial_n\Phi|^2}{18H^4M^2} \quad . \tag{1.39}$$

Since ϵ is small, the second relation in (1.37) implies $H^2 \simeq \frac{\Phi}{3M^2}$. Substituting this into (1.39) gives:

$$\epsilon \simeq \frac{M^2}{2}|\partial_n \log\Phi|^2 \quad . \tag{1.40}$$

Hence the slow gradient flow approximation also implies (1.34).

1.9 The SRST approximation

Following [8, 9, 13–19] (see [10] for a recent review), we end this section by briefly recalling the traditional SRST approximation, which is considerably more restrictive that the approximations discussed above[6]. Define the *third slow-roll parameter* $\xi_{\|}$ and the *second slow-turn parameter* $\xi_\perp$ through:

$$\xi_{\|} \stackrel{\text{def.}}{=} -\frac{\dddot{\sigma}}{H\ddot{\sigma}} \quad , \quad \xi_\perp \stackrel{\text{def.}}{=} -\frac{\dot{\eta_\perp}}{H\eta_\perp} \quad .$$

The *Hubble slow-roll parameters* are defined through:

$$\begin{aligned}
\epsilon_H &\stackrel{\text{def.}}{=} \epsilon \quad , \\
\eta_H &\stackrel{\text{def.}}{=} \eta_{\|} - \epsilon \quad , \\
\xi_H &\stackrel{\text{def.}}{=} -\frac{\dot{\eta_H}}{H\eta_H} = \frac{\eta_{\|}(\xi_{\|} - \eta_{\|} - 3\epsilon) + 2\epsilon^2}{\eta_{\|} - \epsilon} \quad .
\end{aligned}$$

[6] As we shall see below (see, for example, Subsection 2.4), this popular approximation is insufficient for the study of generalized two-field α-attractor models.

With these definitions, the *kinematical slow-roll (SR) approximation* corresponds to $|\epsilon_H|$,$|\eta_H|$, $|\xi_H| \ll 1$ while the *kinematical slow-turn (ST) approximation* corresponds to $|\eta_\perp|, |\xi_\perp| \ll 1$ (see [10]). The *kinematical slow-roll – slow-turn (SRST) approximation* corresponds to imposing all of these conditions simultaneously.

As explained in [10], the kinematical SRST approximation implies the *potential SRST conditions*:

$$M||\mathrm{d}\log\Phi||_{\mathcal{G}} \ll 1 \quad , \tag{1.41}$$

$$M^2\left|\frac{\mathrm{Hess}(\Phi)(\vartheta,\vartheta)}{\Phi}\right| \ll 1 \quad , \tag{1.42}$$

$$M^2\left|\frac{\mathrm{Hess}(\Phi)(n,\vartheta)}{\Phi}\right| \ll 1 \quad . \tag{1.43}$$

Since the conditions $\epsilon_H, \eta_H, \eta_\perp \ll 1$ imply $||\eta||_{\mathcal{G}} \ll 1$, the SRST approximation implies the slow gradient flow approximation and hence also the gradient flow approximation. However, the gradient flow approximation (which will be used in Section 4) is much less restrictive than the SRST approximation, since it requires only $|\eta_\parallel| \ll 1$ and $|\eta_\perp| \ll 1$, conditions which constrain only the second slow-roll parameter and the first slow-turn parameter. Similarly, the slow gradient flow approximation is considerably less restrictive than the SRST approximation. We stress that experience with explicit examples shows that the SRST approximation is generally quite ill-suited for a study of generalized two-field α-attractor models, for example if one wishes to study cosmological dynamics near cusp ends or within the compact core of Σ.

1.10 The strong potential SRST conditions

The potential SRST conditions are implied by the stronger conditions:

$$M||\mathrm{d}\log\Phi||_{\mathcal{G}} \ll 1 \quad , \quad M^2\frac{||\mathrm{Hess}(\Phi)||_{\mathcal{G}}}{|\Phi|} \ll 1 \quad , \tag{1.44}$$

which we shall call the *strong potential SRST conditions*. These conditions are convenient since they are easy to test. When these conditions are satisfied, it is reasonable to expect that the SRST approximation is valid [8–10].

2 Generalized two-field α-attractor models

In this section, we introduce two-field generalized α-attractor models and discuss some of their fundamental properties. This section makes free use of mathematical results and terminology which are summarized in Appendices B, C and D.

Let (Σ, G) be a geometrically finite hyperbolic surface with n ends. For any real positive number $\alpha > 0$, consider the rescaled hyperbolic metric:

$$\mathcal{G} \stackrel{\mathrm{def.}}{=} 3\alpha G \quad ,$$

which has Gaussian curvature $K = -\frac{1}{3\alpha}$. Let Φ be a smooth real-valued function defined on Σ. By definition, a *generalized two-field α-attractor model* defined by α and (Σ, G, Φ) is a cosmological model associated to the triplet $(\Sigma, \mathcal{G}, \Phi)$ as in Section 1.

When Σ is simply connected, the hyperbolic surface (Σ, G) is isometric with the Poincaré disk. In this case, G is uniquely determined and coincides with the Poincaré metric, hence the generalized two-field α-attractor model reduces to the two-field model discussed in [6]. When Σ is not simply connected, isometry classes of hyperbolic metrics on Σ with fixed type of ends form a moduli space. When Σ is non-elementary, this moduli space has real dimension equal to $6g - 6 + 3n_f + 2n_c$ (see [30]). In particular, generalized two-field α-attractor models form an *uncountably infinite* family of generalizations of the hyperbolic disk model of [6].

2.1 Symmetries

Isometries of the scalar manifold (Σ, G) which preserve the scalar potential Φ induce symmetries of the equations of motion of the generalized two-field α-attractor model. Restricting to orientation preserving isometries gives the symmetry group[7]:

$$\mathrm{Aut}^+(\Sigma, \mathcal{G}, \Phi) = \mathrm{Aut}^+(\Sigma, G, \Phi) = \{h \in \mathrm{Iso}^+(\Sigma, G) \mid \Phi \circ h = \Phi\} \ .$$

The results summarized in Appendix B.8 imply:

A. In the elementary case, the group $\mathrm{Aut}^+(\Sigma, G, \Phi)$ is infinite (namely, isomorphic with $\mathrm{U}(1)$) iff Φ is invariant under $\mathrm{Iso}^+(\Sigma, G) \simeq \mathrm{U}(1)$. This happens iff Φ depends only on $|u|$ when Σ is conformal to the disk $\mathbb{D}$, the hyperbolic punctured disk $\mathbb{D}^*$ or an annulus $\mathbb{A}(R)$. When Φ depends on both $|u|$ and $\arg u$, the group $\mathrm{Aut}^+(\Sigma, G, \Phi)$ is a finite cyclic group, which is trivial in the generic case.

B. In the non-elementary case, the symmetry group $\mathrm{Aut}^+(\Sigma, G, \Phi)$ is necessarily finite, being a normal subgroup of the finite group $\mathrm{Aut}(\Sigma, G) \simeq N(\Gamma)/\Gamma$, where Γ is the uniformizing Fuchsian group of Σ (see Apppendix B.8).

In particular, generalized two-field α-attractors based on non-elementary hyperbolic surfaces *cannot* admit D-term embeddings [33–35] in gauged $\mathcal{N} = 1$ supergravity with a single chiral multiplet, since the construction of the latter involves gauging a *continuous* group of isometries of $(\Sigma, \mathcal{G})$. However, such models do admit F-term embeddings in $\mathcal{N} = 1$ supergravity provided that the scalar potential is induced by a holomorphic superpotential.

2.2 Well-behaved scalar potentials

Let $\hat{\Sigma}$ be the end compactification of Σ (see Appendix C). A scalar potential $\Phi : \Sigma \to \mathbb{R}$ is called *well-behaved at the ideal point (or end) $p \in \hat{\Sigma} \setminus \Sigma$* if there exists a smooth function $\hat{\Phi}_p : \Sigma \sqcup \{p\} \to \mathbb{R}$ such that:

$$\Phi = \hat{\Phi}_p|_\Sigma \ .$$

[7] Note that these are only the 'obvious' symmetries of the model and not the most general Noether symmetries.

In this case, $\hat{\Phi}_p$ is uniquely determined by Φ through continuity and is called the *extension of* Φ to p. The potential $\hat{\Phi}$ is called *globally well-behaved* if there exists a globally-defined smooth function $\hat{\Phi} : \hat{\Sigma} \to \mathbb{R}$ such that:

$$\Phi = \hat{\Phi}|_{\Sigma} \quad .$$

In this case, $\hat{\Phi}$ is uniquely determined by Φ through continuity and is called the *global extension of* Φ to $\hat{\Sigma}$. Notice that Φ is globally well-behaved iff it is well-behaved at each end of Σ. As we shall see below, potentials which are well-behaved at p lead to the same universal expression for the spectral index and tensor to scalar ratio as ordinary α-attractor models in the leading order of the slow-roll approximation if an appropriate one-field truncation is performed in the vicinity of p.

Consider semi-geodesic coordinates (r, θ) near p in which the hyperbolic metric G has the asymptotic form (D.5). Setting:

$$\phi \stackrel{\text{def.}}{=} 2\,\mathrm{arccot}(r) \in (0, \pi) \iff r = \cot\left(\frac{\phi}{2}\right) \in (0, +\infty) \quad ,$$

the change of coordinates from (r, θ) to (ϕ, θ) induces a diffeomorphism $\mu_p : V_p \to \mathrm{S}^2 \setminus \{\nu, \sigma\}$ which identifies the punctured semi-geodesic coordinate neighborhood $V_p \subset \Sigma$ of p with the unit sphere with the north and south poles ν and σ removed. Here ϕ and θ are viewed as spherical coordinates on $\mathrm{S}^2 = \{(\sin\phi\cos\theta, \sin\phi\sin\theta, \cos\phi) \,|\, \phi \in [0, \pi], \theta \in [0, 2\pi)\} \subset \mathbb{R}^3$. The limit $r \to +\infty$ corresponds to $\phi \to 0$, i.e. to the north pole $\nu \in \mathrm{S}^2$, while the limit $r \to 0$ corresponds to $\phi \to \pi$, i.e. to the south pole $\sigma \in \mathrm{S}^2$. In particular, the north pole of S^2 corresponds to the ideal point p. A potential $\Phi : \Sigma \to \mathbb{R}$ is well-behaved at p iff there exists a smooth function $\bar{\Phi}_p : \mathrm{S}^2 \setminus \{\sigma\} \to \mathbb{R}$ such that $\Phi = \bar{\Phi}_p \circ \mu_p$, which gives:

$$\Phi(r, \theta) = \bar{\Phi}_p(2\,\mathrm{arccot}(r), \theta) \quad . \tag{2.1}$$

The condition that $\bar{\Phi}_p$ is smooth at the north pole implies that $\bar{\Phi}_p(\phi, \theta)$ has a finite limit for $\phi \to 0$ (which equals $\hat{\Phi}_p(p)$) and hence $\Phi(r, \theta)$ has a θ-independent limit for $r \to +\infty$. Moreover, (2.1) gives:

$$\begin{aligned}
&\partial_r\Phi = -\frac{2}{1+r^2}\partial_\phi\bar{\Phi}_p \quad , \\
&\partial_r^2\Phi = \frac{4r}{(1+r^2)^2}\partial_\phi\bar{\Phi}_p + \frac{4}{(1+r^2)^2}\partial_\phi^2\bar{\Phi}_p \quad , \\
&\partial_\theta\Phi = \partial_\theta\bar{\Phi}_p \quad , \quad \partial_\theta^2\Phi = \partial_\theta^2\bar{\Phi}_p \quad , \\
&\partial_r\partial_\theta\Phi = -\frac{2}{1+r^2}\partial_\phi\partial_\theta\bar{\Phi}_p \quad .
\end{aligned} \tag{2.2}$$

These relations imply the following asymptotics for $r \gg 1$:

$$\begin{aligned}
&\partial_r\Phi \simeq -\frac{2}{r^2}\partial_\phi\bar{\Phi}_p \quad , \quad \partial_r^2\Phi \simeq \frac{4}{r^3}\partial_\phi\bar{\Phi}_p \\
&\partial_\theta\Phi = \partial_\theta\bar{\Phi}_p \quad , \quad \partial_\theta^2\Phi = \partial_\theta^2\bar{\Phi}_p \quad , \quad \partial_r\partial_\theta\Phi \simeq -\frac{2}{r^2}\partial_\phi\partial_\theta\bar{\Phi}_p \quad .
\end{aligned} \tag{2.3}$$

The Laplace expansion of $\hat{\Phi}$. In this paragraph, we discuss a natural expansion for the extension of well-behaved scalar potentials, which gives a systematic way to approximate such potentials in our class of models. Some applications of this type of expansion can be found in references [31, 32]. Let $\mathfrak{c}$ be the conformal equivalence class of the hyperbolic metric G on Σ and let $\hat{\mathfrak{c}}$ be its prolongation to $\hat{\Sigma}$ (see Appendix C.2). Let $\hat{G}$ denote the canonical complete metric in the conformal class $\hat{\mathfrak{c}}$, which was defined in the same subsection. Notice that the restriction of $\hat{G}$ to Σ differs from G (in particular, this restriction is *not* a complete metric on Σ !). Since $\hat{\Sigma}$ is compact, the sign opposite $-\hat{\Delta}$ of the Laplacian $\hat{\Delta}$ of $\hat{G}$ is a positive operator with purely discrete spectrum, whose distinct eigenvalues $0 = \lambda_0 < \lambda_1 < \lambda_2 < \ldots$ accumulate only at $+\infty$. The eigenspace $\mathcal{H}_l$ of the eigenvalue λ_l is finite-dimensional and consists of all smooth functions $f : \hat{\Sigma} \to \mathbb{C}$ which satisfy:

$$\hat{\Delta} f = -\lambda_l f \quad .$$

For $l = 0$, all eigenfunctions are constant and we have $\mathcal{H}_0 = \mathbb{C}1$, where 1 denotes the constant unit function defined on $\hat{\Sigma}$. The Hilbert space $L^2(\hat{\Sigma}, \hat{G})$ of complex-valued square-integrable functions (modulo equivalence almost everywhere) with respect to the Lebesgue measure defined by $\hat{G}$ has an orthogonal direct sum decomposition:

$$L^2(\hat{\Sigma}, \hat{G}) = \overline{\bigoplus}_{l=0}^{\infty} \mathcal{H}_l$$

where $\overline{\bigoplus}_{l=0}^{\infty}$ denotes the completed direct sum. Let $M_l \stackrel{\text{def.}}{=} \dim_{\mathbb{C}} \mathcal{H}_l$ denote the multiplicity of the eigenvalue λ_l and let $u_{l1}, \ldots, u_{lM_l}$ denote an orthonormal basis of $\mathcal{H}_l$ for each $l \in \mathbb{N}$, where $M_0 = 1$ and $u_{01} = 1$. Since λ_l are real, the complex conjugates $\overline{u_{lm}}$ also form an orthonormal basis of $\mathcal{H}_l$, so we have:

$$\overline{u_{lm}} = \sum_{m'=1}^{M_l} q^{(l)}_{mm'} u_{lm'} \quad \forall m = 1, \ldots, M_l \quad ,$$

for some $q^{(l)}_{mm'} \in \mathbb{C}$, where $Q^{(l)} \stackrel{\text{def.}}{=} (q^{(l)}_{mm'})_{m,m'=1\ldots M_l}$ is a unitary and symmetric matrix[8] and $q^{(0)}_{11} = 1$.

Let Φ be a globally well-behaved scalar potential on Σ and let $\hat{\Phi}$ be its global extension to $\hat{\Sigma}$. Then $\hat{\Phi}$ can be expanded uniquely as:

$$\hat{\Phi} = \sum_{l=0}^{\infty} \sum_{m=1}^{M_l} C_{lm} u_{lm} \quad , \tag{2.4}$$

where C_{lm} are complex constants given by:

$$C_{lm} = \int_{\hat{\Sigma}} (\hat{\Phi}\, \overline{u_{lm}}) \mathrm{vol}_{\hat{G}}$$

and the series in the right hand side converges to the left hand side in the L^2 norm determined by $\hat{G}$. Since $\hat{\Phi}$ is real-valued, we have:

$$\overline{C_{lm}} q^{(l)}_{mm'} = C_{lm'} \quad .$$

[8] We have $[Q^{(l)}]^t = Q^{(l)}$ and $Q^{(l)}\overline{Q^{(l)}} = 1$.

The expansion (2.4) gives a systematic method to approximate globally well-behaved potentials by truncating away all modes with l larger than some given cutoff.

When Σ is a planar surface (i.e. when its genus g vanishes), the end compactification $\hat{\Sigma}$ is a sphere S^2 and the canonical complete metric $\hat{G}$ determined by the conformal prolongation $\hat{\mathfrak{c}}$ of the conformal class $\mathfrak{c}$ of G is the round metric of radius one. In this case, we have $\lambda_l = l(l+1)$ with $l \in \mathbb{N}$ and u_{lm} can be taken to be the spherical harmonics Y_{lm}. Thus (2.4) reduces to the classical Laplace-Fourier expansion on the sphere; some models of this type are discussed in [31, 32]. When Σ has genus one, the end compactification $\hat{\Sigma}$ endowed with the metric $\hat{G}$ and the complex structure $\hat{J}$ is a complex torus $\mathrm{T}^2 = \mathbb{C}/L$, where $L = \mathbb{Z} \oplus \mathbb{Z}\tau$ is the lattice generated by 1 and $\tau \in \mathbb{H}$, with $|\tau| \geq 1$ and $\mathrm{Re}(\tau) \leq \frac{1}{2}$ (see Appendix C.2). In this case, an orthonormal basis of eigenfunctions of $-\hat{\Delta}$ is given by $u_w(z) = e^{2\pi \mathbf{i}\langle w, z\rangle}$, where z is the complex coordinate induced from $\mathbb{C}$ and the 2-dimensional vector $w \in \mathbb{R}^2 \equiv \mathbb{C}$ runs over the elements of the dual lattice $L^\vee$. The eigenvalue of u_w is $\lambda_w = 4\pi^2 ||w||^2$. When the genus g of Σ is greater than one, the metric $\hat{G}$ is hyperbolic. In that case, a basis of eigenfunctions of $-\hat{\Delta}$ is sensitive to the hyperbolic geometry of $(\hat{\Sigma}, \hat{G})$ and cannot in general be determined explicitly. However, results from the well-developed spectral theory of compact hyperbolic surfaces [36] can in principle be applied to extract information about the spectrum and eigenfunctions of $-\hat{\Delta}$.

2.3 Naive local one-field truncations and "universality" for certain special trajectories near the ends

In this subsection, we briefly discuss "universality" of generalized two-field α-attractor models in the naive classical truncation near the ends. We stress that one-field truncations are far from sufficient when studying two-field generalized two-field α-attractors, which in our view cannot be understood properly unless one treats them systematically as two-field models. We also stress that we do not consider in detail the quantum perturbations of such models, since this subject lies outside the scope of the present paper.

Universality in one-field models. As explained in [4], α-attractor models with a *single* real scalar field have universal behavior[9] when:

- The scalar manifold is diffeomorphic with an open interval I, thus admitting a global real coordinate $x : I \xrightarrow{\sim} (0, 1)$.
- The coefficient $s(x)$ of the field space metric $\mathrm{d}s^2 = s(x)\mathrm{d}x^2$ has asymptotic form:

$$s(x) =_{x \ll 1} \frac{a}{x^p}(1 + \mathrm{O}(x)) \tag{2.5}$$

- The one-field scalar potential $W(x)$ has an asymptotic expansion:

$$W(x) =_{x \ll 1} W_0 \left(1 - cx + \mathrm{O}(x^2)\right) \quad , \tag{2.6}$$

[9] Near $x = 0$.

where $a > 0$ and $c > 0$ are constants. In this case, the spectral index n_s and the tensor to scalar ratio r in the leading order of the one-field slow-roll approximation in the region $x \ll 1$ are given by [4]:

$$n_s \approx 1 - \frac{p}{p-1}\frac{1}{N(t)}, \quad r \approx \frac{8c^{\frac{p-2}{p-1}}a^{\frac{1}{p-1}}}{(p-1)^{\frac{p}{p-1}}}\frac{1}{N^{\frac{p}{p-1}}} \quad , \tag{2.7}$$

where:

$$N \stackrel{\text{def.}}{=} \log\frac{a(t_1)}{a(t_0)}$$

is the number of e-folds (t_0 and t_1 being the cosmological times at which inflation starts and ends).

Universality in the truncated model on the hyperbolic disk. Consider the *two-field* α-attractor model based on the Poincaré disk:

$$\mathbb{D} = \{u \in \mathbb{C} |\ |u| < 1\} \quad .$$

At the classical level, this can be truncated to a one-field model by taking $\varphi(t) = (x(t), \theta_0)$, with θ_0 independent of t. Setting $u = (1-x)e^{\mathbf{i}\theta}$ (with $x \in (0,1)$ and $\theta \in \mathbb{R}/(2\pi\mathbb{Z})$), the rescaled Poincaré metric on $\mathbb{D}$ takes the form:

$$\mathrm{d}s^2_{\mathcal{G}} = \frac{3\alpha}{2}\frac{4}{x^2(2-x)^2}[\mathrm{d}x^2 + (1-x)^2\mathrm{d}\theta^2] \simeq_{x\ll 1} \frac{3\alpha}{2}\frac{1}{x^2}(\mathrm{d}x^2 + \mathrm{d}\theta^2)$$

and the *reduced* field $\varphi(t) = (x(t), \theta_0)$ "feels" only the radial metric:

$$\mathrm{d}s^2_{\mathcal{G}} = \frac{3\alpha}{2}\frac{4}{x^2(2-x)^2}\mathrm{d}x^2 =_{x\ll 1} \frac{3\alpha}{2}\left[\frac{1}{x^2} + \mathrm{O}(x^2)\right]\mathrm{d}x^2 \quad ,$$

which has the form (2.5) with $p = 2$ and $a = \frac{3\alpha}{2}$. Let us assume that $\Phi(x,\theta)$ has an asymptotic expansion of the form:

$$\Phi(x,\theta) =_{x\ll 1} a - b(\theta)x + \mathrm{O}(x^2) \quad , \tag{2.8}$$

where a is a non-zero constant and $b(\theta) > 0$ is a smooth function defined on the circle $\mathbb{R}/(2\pi\mathbb{Z})$. Then $W(x) \stackrel{\text{def.}}{=} \Phi(x,\theta_0)$ has an expansion of the form (2.6) for $x \leq 1$, where $W_0 = a$ and $c \stackrel{\text{def.}}{=} \frac{b(\theta_0)}{a}$ (the latter of which generally depends on θ_0). In this case, the argument of [4] shows that, to leading order of the slow-roll approximation for the *truncated* model, the quantities n_s and r are given by relation (2.7) with $p = 2$:

$$n_s \approx 1 - \frac{2}{N}, \quad r \approx \frac{12\alpha}{N^2} \quad , \tag{2.9}$$

which fit well current observational data.

Notice that the right hand sides of these expressions have no explicit dependence of the constant c (and hence of the choice of θ_0). However, the number N of e-folds realized during inflation can depend implicitly on c and hence on the choice of θ_0. A limit argument (based on taking W_0 to zero) shows that the same relations (2.7) are obtained when $a = 0$.

Universality for certain special trajectories in the naive local truncation of generalized two-field α-attractor models near the ends. A similar argument can be applied to generalized two-field α-attractor models in a punctured neighborhood of each ideal point $p \in \hat{\Sigma} \setminus \Sigma$. On a sufficiently small such neighborhood, the hyperbolic metric G has a U(1) symmetry, which in semi-geodesic coordinates (r, θ) acts by shifts of θ. Moreover, the hyperbolic metric can be approximated by (D.5) near the end, where the ideal point corresponds to $r \to +\infty$. The change of coordinates $r = -\log x$ (with $x = e^{-r} > 0$) places the ideal point at $x = 0$ and brings the rescaled asymptotic metric $\mathcal{G}$ to the form:

$$\mathrm{d}s^2_{\mathcal{G}} =_{x \ll 1} \begin{cases} \frac{3\alpha}{2}\frac{1}{x^2}\left[\mathrm{d}x^2 + \left(\frac{c_p}{4\pi}\right)^2 \mathrm{d}\theta^2\right] & \text{if } \epsilon_p = +1 \text{ (plane, horn, funnel end)} \\ \frac{3\alpha}{2}\frac{1}{x^2}\left[\mathrm{d}x^2 + \left(\frac{c_p}{4\pi}\right)^2 x^4 \mathrm{d}\theta^2\right] & \text{if } \epsilon_p = -1 \text{ (cusp end)} \end{cases}$$

Suppose that Φ is well-behaved at the end p. In this case, considering a small enough disk D_p centered at p, we have:

$$\Phi(r, \theta) = \hat{\Phi}_p(e^{-r}, \theta) \quad \text{for} \quad r \gg 1$$

for some smooth function $\hat{\Phi}_p : D_p \to \mathbb{R}$. Using the Taylor expansion of $\hat{\Phi}_p$ around $x = 0$, this implies that Φ has the asymptotic form (2.8), where $b(\theta) = -(\partial_{x_1}\hat{\Phi}_p|_{x=0})\cos\theta - (\partial_{x_2}\hat{\Phi}_p|_{x=0})\sin\theta$ (with $x_1 = x\cos\theta$ and $x_2 = x\sin\theta$). On such a small neighborhood of p, one can truncate the two-field model by setting $\varphi(t) = (x(t), \theta_0)$ with θ_0 independent of t. Such a truncation is justified when the inflationary trajectories near the end are well-approximated by non-canonically parameterized geodesics flowing from the end toward the compact core[10] of (Σ, G). The truncated model "feels" the metric:

$$\mathrm{d}s^2 \simeq_{x \ll 1} \frac{3\alpha}{2}\frac{\mathrm{d}x}{x^2} \quad ,$$

which has the same form for all types of ends. Assuming $b(\theta_0) > 0$ (so that inflation proceeds from the end toward the interior), the same argument as above shows that n_s and r are given by (2.9) in the leading order of the slow-roll approximation for the *truncated* model. Thus:

- *Suppose that Φ is well-behaved at an end of (Σ, G) where its extension has a local maximum and that inflation takes place near that end and proceeds away from the end. Then the generalized two-field α-attractor model admits a* naive *local truncation to a one-field model in a punctured vicinity of the corresponding ideal point for which the universal relations* (2.9) *apply in the leading order of the one-field slow-roll approximation, for the special trajectories described above.*

This shows that generalized two-field α-attractor models have the same kind of universal behavior as the disk models of [6] near each such end, at least in the naive one-field truncation discussed above.

[10] see Appendix D.2 for a definition of the compact core.

Of course, the classical local truncation to a one-field model used in the argument of [6] (as well as above) is somewhat simplistic. In particular, one may worry that quantum effects could destabilize the one-field trajectory and change the predictions for radiative corrections. For ordinary α-attractors (those models for which Σ is the hyperbolic disk $\mathbb{D}$), a resolution of this problem can be obtained when restricting to those α-attractor models which admit embeddings in $\mathcal{N}=1$ supergravity coupled to one chiral multiplet. For such models, it was argued in [5] that the naive truncation can be stabilized in a universal way provided that the superpotential is sufficiently well-behaved. As explained later on in Section 3, any generalized two-field α-attractor model can be lifted to a model defined on the hyperbolic disk by using the uniformization map $\pi_{\mathbb{D}} : \mathbb{D} \to \Sigma$. This lift is an ordinary α-attractor whose scalar potential is invariant under the action of the uniformizing surface group $\Gamma \subset \mathrm{PSL}(2,\mathbb{R})$. When the generalized two-field α-attractor model admits an F-term embedding in $\mathcal{N}=1$ supergravity coupled to a single chiral multiplet with superpotential $W : \Sigma \to \mathbb{C}$, the lifted model also admits such an embedding, with superpotential given by the lift $\tilde{W} \stackrel{\text{def.}}{=} W \circ \pi_{\mathbb{D}}$ of W, which is Γ-invariant. The cosmological trajectories of the model defined by Σ are the $\pi_{\mathbb{D}}$-images of the cosmological trajectories of this lifted model. The two models are related by the field redefinition induced by $\pi_{\mathbb{D}}$, which implements the quotient of the lifted model through the discrete group Γ. Provided that this discrete symmetry is preserved when quantizing perturbations of the lifted model around a classical solution, the effect of quantum perturbations of the model defined by Σ can be obtained from those of the lifted model by projection through the uniformization map (which implements the quotient through Γ). This implies that cosmological solutions of the generalized two-field α-attractor model have the same local properties as those of the lifted model, to which stabilization arguments such as those of [5] apply for radial trajectories on the Poincaré disk. The trajectories involved in the naive truncations near the ends of Σ lift to small portions of radial trajectories on $\mathbb{D}$ which are located near the conformal boundary of $\mathbb{D}$. In models which have appropriate F-term embeddings in supergravity one can thus expect that, at least near flaring ends, the local one-field truncations discussed above can be stabilized by constructions similar to those used for ordinary α-attractors, provided that the discrete Γ-symmetry of the lifted model is unbroken by such corrections. To make this argument rigorous, one must of course first classify F-term embeddings of generalized two-field α-attractors into $\mathcal{N}=1$ supergravity, a subject which we plan to discuss in a separate publication. Here, we mention only that generalized two-field α-attractors can admit F-term embeddings which are 'twisted' by a unitary character of the fundamental group of Σ, an aspect which must be taken into account when studying the corresponding supergravity models. We mention that universality in two-field α-attractors defined on the hyperbolic disk was recently studied for curved trajectories in reference [37] (such trajectories do not coincide with the lift to the hyperbolic disk of the very special trajectories considered in this subsection).

Notice, however, that generalized two-field α-attractors are intrinsically *two-field* models, since they are interesting precisely due to the non-trivial topology of the 2-manifold Σ. A proper understanding of the dynamics of such models simply cannot be attained by

considering one-field truncations, which in our opinion are of limited interest in this context (in particular, since such truncations cannot make sense globally when Σ is topologically non-trivial). In the next subsection, we briefly discuss the classical two-field dynamics of such models in the SRST approximation near the ends, showing that, in this approximation, the models have different behavior near cusp and flaring ends. In particular, we show that the SRST approximation can fail near cusp ends and hence (as already mentioned before) this approximation is insufficient for the study of generalized two-field α-attractors.

2.4 The strong potential SRST conditions near the ends

Let $\Phi : \Sigma \to \mathbb{R}$ be a scalar potential which is well-behaved at an ideal point $p \in \hat{\Sigma} \setminus \Sigma$ and assume that the smooth extension $\hat{\Phi}_p : \Sigma \sqcup \{p\} \to \mathbb{R}$ of Φ does not vanish at p. Consider semi-geodesic coordinates (r, θ) in a neighborhood of p. Using relation (D.5) of Appendix D.6, we find the following asymptotic expressions for $r \gg 1$:

$$\begin{aligned} &M||\mathrm{d}\log\Phi||_{\mathcal{G}} \simeq_{r\gg 1} \frac{M}{\sqrt{3\alpha}}\frac{\sqrt{(\partial_r\Phi)^2 + \left(\frac{4\pi}{c_p}\right)^2 e^{-2\epsilon_p r}(\partial_\theta\Phi)^2}}{|\Phi|} \\ &\frac{M_p^2}{|\Phi|}||\mathrm{Hess}(\Phi)||_{\mathcal{G}} \simeq_{r\gg 1} \\ &\frac{M^2}{3\alpha}\frac{\sqrt{(\partial_r^2\Phi)^2 + 2\left(\frac{4\pi}{c_p}\right)^2(\partial_r\partial_\theta\Phi)^2 e^{-2\epsilon_p r} + \left(\frac{4\pi}{c_p}\right)^4 e^{-4\epsilon_p r}(\partial_\theta^2\Phi)^2}}{|\Phi|} \end{aligned} \quad . \tag{2.10}$$

The quantities c_p and ϵ_p are defined in equation (D.6) of Appendix D.6. Below, we use the terminology and results of that appendix.

Flaring ends. When p corresponds to a flaring end, we have $\epsilon_p = +1$ and the exponential terms appearing in the right hand side of (2.10) are suppressed when $r \gg 1$, since we assume that Φ is well-behaved at p. In this case, we find:

$$\begin{aligned} &M||\mathrm{d}\log\Phi||_{\mathcal{G}} \simeq_{r\gg 1} \frac{M}{\sqrt{3\alpha}}\left|\frac{\partial_r\Phi}{\Phi}\right| \\ &\frac{M^2}{|\Phi|}||\mathrm{Hess}(\Phi)||_{\mathcal{G}} \simeq_{r\gg 1} \frac{M^2}{3\alpha}\left|\frac{\partial_r^2\Phi}{\Phi}\right| \end{aligned}$$

and the strong potential SRST conditions are satisfied on a pointed neighborhood of p provided that:

$$\frac{M}{\sqrt{3\alpha}}\left|\frac{\partial_r\Phi}{\Phi}\right| \ll 1 \quad \text{and} \quad \frac{M^2}{3\alpha}\left|\frac{\partial_r^2\Phi}{\Phi}\right| \ll 1 \quad \text{for} \quad r \gg 1 \quad . \tag{2.11}$$

Using relations (2.3) shows that (2.11) amount to the conditions:

$$\frac{2M}{r^2\sqrt{3\alpha}}\left|\frac{(\partial_\phi\bar{\Phi}_p)(\nu)}{\bar{\Phi}_p(\nu)}\right| \ll 1 \quad \text{and} \quad \frac{4M^2}{3\alpha r^3}\left|\frac{(\partial_\phi^2\bar{\Phi}_p)(\nu)}{\bar{\Phi}_p(\nu)}\right| \ll 1 \quad , \tag{2.12}$$

where $r = \cot(\frac{\phi}{2})$. These conditions are satisfied for $r \gg r_p$, where:

$$r_p \stackrel{\text{def.}}{=} \max\left[\left(\frac{2M}{\sqrt{3\alpha}}\left|\frac{(\partial_\phi \bar{\Phi}_p)(\nu)}{\bar{\Phi}_p(\nu)}\right|\right)^{1/2}, \left(\frac{4M^2}{3\alpha}\left|\frac{(\partial_\phi^2 \bar{\Phi}_p)(\nu)}{\bar{\Phi}_p(\nu)}\right|\right)^{1/3}\right] \quad .$$

In particular, the strong SRST conditions are always satisfied on a small enough vicinity of a flaring end (when the scalar potential is well-behaved at that end) and one can use the SRST approximation there.

Cusp ends. When p corresponds to a cusp end, we have $\epsilon_p = -1$ and $c_p = 2$. In this case, the strong potential SRST conditions hold on a pointed neighborhood of p provided that, beyond (2.11), the following conditions are also satisfied for $r \gg 1$:

$$\frac{2\pi M}{\sqrt{3\alpha}} e^r \left|\frac{\partial_\theta \Phi}{\Phi}\right| \ll 1 \quad , \quad \frac{(2\pi M)^2}{3\alpha} e^{2r} \left|\frac{\partial_\theta^2 \Phi}{\Phi}\right| \ll 1 \quad , \quad \frac{2^{3/2}\pi M^2}{3\alpha} e^r \left|\frac{\partial_r \partial_\theta \Phi}{\Phi}\right| \ll 1 \quad . \tag{2.13}$$

As before, conditions (2.11) are automatically satisfied on a small enough pointed neighborhood of p. On the other hand, conditions (2.13) require fine-tuning of the potential Φ in a neighborhood of the cusp. For example, these conditions are satisfied in the *non-generic* case when $\bar{\Phi}_p$ is independent of θ on some neighborhood of the north pole of S^2.

In particular, the strong SRST conditions fail to hold near a cusp end when Φ is a generic potential which is well-behaved at that end and hence the SRST approximation can fail near such ends. This shows that the SRST approximation is generally not well-suited for studying cosmological dynamics near cusp ends.

2.5 On computing power spectra

When the SRST approximation holds during the inflationary period (for example, if inflation takes place near a flaring end), the power spectrum can be approximated as explained in [8, 9, 13–18] (see [10, 19] for recent reviews). However, a detailed study of cosmological perturbations in our models requires going beyond the SRST approximation (in particular, because the latter can fail near cusp ends). In general, this requires the use of a numerical approach such as that developed in [20–22]. Moreover, for certain classes of trajectories one might be able to find an effective one-field description using the approach of [15]. These subjects lie outside the scope of the present paper and we hope to address them in future work.

2.6 Spiral trajectories near the ends

In semi-geodesic coordinates near an end $p \in \hat{\Sigma} \setminus \Sigma$, we have:

$$\mathrm{d}s^2_{\mathcal{G}} \simeq_{r\gg 1} 3\alpha \left[\mathrm{d}r^2 + \left(\frac{c_p}{4\pi}\right)^2 e^{2\epsilon_p r}\mathrm{d}\theta^2\right] \quad ,$$

where c_p and ϵ_p are given in equation (D.6) and the ideal point p corresponds to $r \to +\infty$. Using this asymptotic form, equations (A.4) give:

$$\Gamma^r_{\theta\theta} = -3\epsilon\alpha \left(\frac{c_p}{4\pi}\right)^2 e^{2\epsilon_p r} \quad , \quad \Gamma^\theta_{r\theta} = \Gamma^\theta_{\theta r} = \epsilon_p \quad .$$

Substituting in (1.5), we find that the equation of motion in a vicinity of the end reduces to the system:

$$\ddot{r} - 3\epsilon\alpha \left(\frac{c_p}{4\pi}\right)^2 e^{2\epsilon_p r}\dot{\theta}^2 + 3H\dot{r} + \frac{1}{3\alpha}\partial_r\Phi = 0 \quad , \tag{2.14}$$

$$\ddot{\theta} + 2\epsilon_p \dot{r}\dot{\theta} + 3H\dot{\theta} + \frac{1}{3\alpha}\left(\frac{4\pi}{c_p}\right)^2 e^{-2\epsilon_p r}\partial_\theta\Phi = 0 \quad . \tag{2.15}$$

The generic solution of this system has $\dot{r} \neq 0$ and $\dot{\theta} \neq 0$, thus being a portion of a spiral which "winds" around the ideal point. This gives a form a spiral inflation in our class of models. As already clear from Subsection 2.4, cosmological dynamics depends markedly on the type of end under consideration, i.e. on the values of ϵ_p and c_p allowed by equation (D.6). Note that this type of spiral inflation differs from that discussed in [38, 39] (since, unlike the present paper, loc. cit. considers two-field cosmological models with flat target space). With the exception of the single case when (Σ, G) is the Poincaré disk $\mathbb{D}$, the type of spiral inflation discussed here also differs from that studied in references [40–42], where only the Poincaré disk was considered. As explained in Appendix D.6, the Poincaré disk $\mathbb{D}$ is the *only* geometrically finite hyperbolic surface which admits a plane end. Hence the case $c_p = 2\pi$ with $\epsilon_p = +1$ in equations (2.14) and (2.15) (which makes those equations consistent with the equations of motion considered in references [40–42]) arises *only* for those spiral trajectories on the Poincaré disk $\mathbb{D}$ which are close to the conformal boundary of $\mathbb{D}$.

Let us consider the system (2.14)-(2.15) for various types of ends.

- For flaring ends, we have $\epsilon_p = +1$ and the equations of motion take the form:

$$\ddot{r} - 3\alpha \left(\frac{c_p}{4\pi}\right)^2 e^{2r}\dot{\theta}^2 + 3H\dot{r} + \frac{1}{3\alpha}\partial_r\Phi = 0 \quad , \tag{2.16}$$

$$\ddot{\theta} + 2\dot{r}\dot{\theta} + 3H\dot{\theta} \simeq 0 \quad , \tag{2.17}$$

  where:

$$H = \frac{1}{\sqrt{6}M}\sqrt{\frac{3\alpha}{2}\left[\dot{r}^2 + \left(\frac{c_p}{4\pi}\right)^2 e^{2r}\dot{\theta}^2\right] + 2\Phi(r,\theta)} \quad .$$

  Assuming $\dot{\theta} \neq 0$, we can write (2.17) as:

$$\frac{\mathrm{d}}{\mathrm{d}t}\ln\dot{\theta} = -\left(2\dot{r} + 3H\right) \quad .$$

- For cusp ends, we have $\epsilon_p = -1$ and $c_p = 2$, thus the equations of motion become:

$$\ddot{r} + 3H\dot{r} + \frac{1}{3\alpha}\partial_r\Phi \simeq 0 \quad , \tag{2.18}$$

$$\ddot{\theta} - 2\dot{r}\dot{\theta} + 3H\dot{\theta} + \frac{4\pi^2}{3\alpha}e^{2r}\partial_\theta\Phi = 0 \quad , \tag{2.19}$$

  where:

$$H = \frac{1}{\sqrt{6}M}\sqrt{\frac{3\alpha}{2}\left[\dot{r}^2 + \frac{e^{-2r}}{(2\pi)^2}\dot{\theta}^2\right] + 2\Phi(r,\theta)} \quad .$$

Remark. As already mentioned above, certain types of spiral trajectories in two-field cosmological models whose scalar manifold (Σ, G) is the Poincaré disk $\mathbb{D}$ were discussed in references [40–42], which consider various explicit scalar potentials and/or make certain special assumptions. Unlike the present paper, none of those references discusses spiral trajectories near the ends of a hyperbolic surface which differs from the Poincaré disk, hence the results of loc. cit. cannot apply without modification[11] for the cusp, funnel or horn ends (see Appendix D.6) of a geometrically finite hyperbolic surface (Σ, G) which differs from $\mathbb{D}$. Since the Poincaré disk is the *only* geometrically finite hyperbolic surface which has a plane end, all other cases of spiral inflation considered above have not yet been discussed in the literature. We stress once again that the class of hyperbolic surfaces considered in this paper is vastly more general than the Poincaré disk and that the geometry of such surfaces differs markedly from that of $\mathbb{D}$ — as illustrated by the presence of the parameters c_p and ϵ_p in the equations of motion (2.14) and (2.15) above and by the different behavior of the SRST conditions at cusp and flaring ends. In particular, the parameters c_p and ϵ_p (which are defined in equation (D.6)) depend on the hyperbolic type of the end of Σ near which the trajectory spirals and they lead to different cosmological dynamics near each type of end. It would be interesting to adapt some of methods and ideas of references [40–42] to the wider setting of spiral trajectories nearby cusp, funnel and horn ends of a general hyperbolic surface and to apply them to the special types of trajectories and scalar potentials to which they might be relevant. More conceptually, one can ask what is the class of trajectories in two-field generalized α-attractor models to which one could apply the methods of [15] (which in certain cases allow one to build an effective one-field description of two-field models) — a problem which we hope to address in future work. However (given that all approximation methods which are currently available for two-field models depend on various assumptions) we are of the opinion that a complete understanding of general trajectories and of the corresponding cosmological perturbations for the class of two-field models considered in the present paper requires a numerical approach.

[11] Reference [40] considered spiral trajectories on the Poincaré disk $\mathbb{D}$ in the so-called *angular inflation* regime, an approximation in which the radial coordinate r is fixed while the slow-roll approximation is assumed to apply to the angular coordinate θ; notice that such an approximation can only apply to special portions of certain particular spiral trajectories nearby the conformal boundary of $\mathbb{D}$. Reference [41] studies so-called "sidetracked inflation" in two-field models, an inflationary scenario which is highly sensitive to the precise form of the target space metric $\mathcal{G}$ and of the scalar potential Φ of the model. For the special case of the Poincaré disk and using a rather special form for the scalar potential, loc. cit. shows that the background dynamics can be described by a certain effective single field model. Those conclusions of [41] are quite model-dependent and it is unclear to what extent they could apply to the much more general situation considered herein, given that our scalar potentials are considerably more general than those considered in loc. cit. and since the local form of the hyperbolic metric close to an end of a geometrically finite hyperbolic surface which differs from the Poincaré disk depends on whether that end is a cusp, a funnel or a horn end (see Appendix D.6) and differs from the hyperbolic metric on $\mathbb{D}$. Finally, the brief note [42] points out some general features of inflation in models whose target space is the Poincaré disk $\mathbb{D}$, features which are a direct consequence of the special behavior of auto-parallel curves on $\mathbb{D}$. It is well-known that auto-parallel curves on $\mathbb{D}$ behave quite differently from auto-parallel curves on more general hyperbolic surfaces.

2.7 An example of spiral trajectory near a cusp end

In Figures 1 and 2, we show a numerical solution of the system (2.18)-(2.19), which corresponds to a spiral trajectory near a cusp end (for such an end, one has $c_p = 2$ and $\epsilon_p = -1$ by equation (D.6)). For simplicity, we took $\Phi = 0$ and $\alpha = \frac{1}{3}$, $r(0) = 10$, $\dot{r}(0) = 1$, $\theta(0) = 0$ and $\dot{\theta}(0) = 1$. Both figures represent the same solution, but in Figure 1 we follow the trajectory for a shorter time for reasons of clarity of the plot.

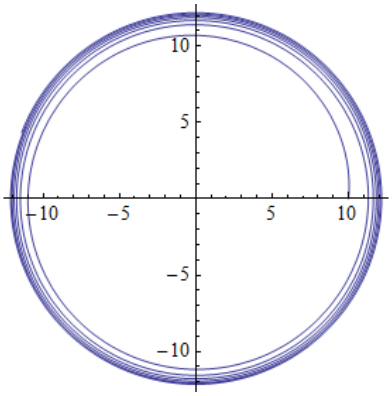

Figure 1: Numerical plot of the pair $(r(t)\cos\theta(t), r(t)\sin\theta(t))$ (with the initial conditions indicated in the text) for $t \in [0, 50]$.

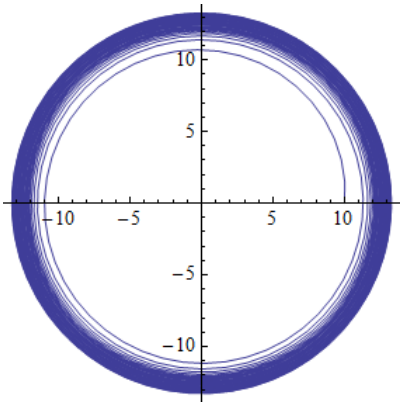

Figure 2: Numerical plot of solution $(r(t)\cos\theta(t), r(t)\sin\theta(t))$ (with the initial conditions indicated in the text) for $t \in [0, 500]$.

Figures 3 and 4 show the increase of r and the decrease of the norm of $\dot{\varphi}$ with the cosmological time t, for the trajectory with the initial conditions given above.

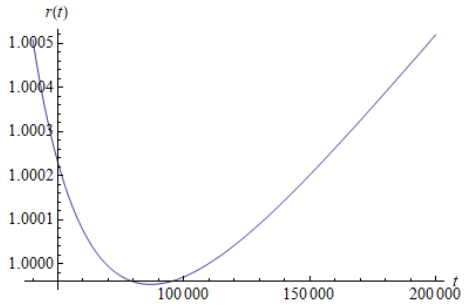

Figure 3: Plot of $\frac{1}{6.8580}\frac{r(t)}{(\ln t)^{0.3411}}$ as a function of t for $t/10^4 \in [4, 20]$. The plot shows that $r(t)$ increases at least as fast as $(\ln t)^{0.3411}$ with a 0.5% discrepancy.

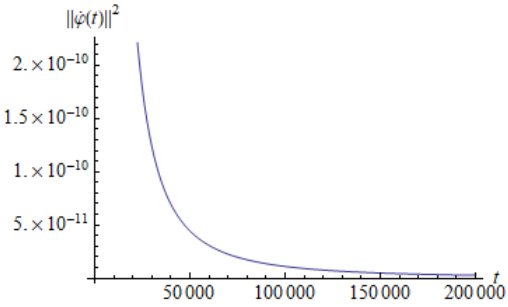

Figure 4: Plot of $||\dot{\varphi}||^2_{\mathcal{G}}$ as a function of t. The plot shows that the norm of $\dot{\varphi}$ decreases toward zero as the trajectory spirals around the cusp end.

Remark. Other examples of spiral trajectories (including their global behavior away from cusp, funnel and plane ends) in certain explicit generalized two-field α-attractor models can be found in references [31, 32].

3 Lift of generalized two-field α-attractor models to the disk and upper half plane

This section makes free use of mathematical terminology and material summarized in Appendix B.

3.1 Lift to the Poincaré disk

Let $\Delta \subset \mathrm{PSU}(1,1)$ be the uniformizing group of (Σ, G) to the disk and $\pi_{\mathbb{D}} : \mathbb{D} \to \Sigma = \mathbb{D}/\Delta$ denote the holomorphic covering map. Let $\tilde{\Phi} \overset{\text{def.}}{=} \Phi \circ \pi_{\mathbb{D}} : \mathbb{D} \to \mathbb{R}$ denote the lift of the scalar potential to $\mathbb{D}$, which is Δ-invariant:

$$\tilde{\Phi}(\delta u) = \tilde{\Phi}(u) \quad , \quad \forall u \in \mathbb{D}\,, \quad \forall \delta \in \Delta \quad .$$

Let $||\cdot||_{\mathbb{D}}$ denote the fiberwise norm induced by the Poincaré metric on the tangent bundle $T\mathbb{D}$ and $\mathrm{grad}_{\mathbb{D}}\tilde{\Phi}$ denote the gradient of $\tilde{\Phi}$ with respect to the Poincaré metric.

Let $\tilde{\varphi}_0 \in \mathbb{D}$ be a lift of the initial value $\varphi_0 \in \Sigma$, i.e. a point of the unit disk which satisfies:

$$\pi_{\mathbb{D}}(\tilde{\varphi}_0) = \varphi_0 \quad .$$

Since $\pi_{\mathbb{D}}$ is a local diffeomorphism, the differential $\mathrm{d}_{\tilde{\varphi}_0}\pi_{\mathbb{D}} : T_{\tilde{\varphi}_0}\mathbb{D} \to T_{\varphi_0}\Sigma$ is bijective. Hence there exists a unique tangent vector $\tilde{v}_0 \in T_{\tilde{\varphi}_0}\mathbb{D}$ which satisfies:

$$(\mathrm{d}_{\tilde{\varphi}_0}\pi_{\mathbb{D}})(\tilde{v}_0) = v_0 \quad .$$

Proposition. Let $\mathcal{G} = 3\alpha G$. Then the solution $\varphi : \mathfrak{I} \to \Sigma$ of (1.9) satisfying the initial conditions (1.10) can be written as $\varphi = \pi_{\mathbb{D}} \circ \tilde{\varphi}$, where $\tilde{\varphi} : \mathfrak{I} \to \mathbb{D}$ is a solution of the equation:

$$\nabla_{\dot{t}}\dot{\tilde{\varphi}}(t) + \frac{1}{M}\sqrt{\frac{3}{2}}\left[3\alpha||\dot{\tilde{\varphi}}(t)||^2_{\mathbb{D}} + 2\tilde{\Phi}(\tilde{\varphi}(t))\right]^{1/2}\dot{\tilde{\varphi}}(t) + \frac{1}{3\alpha}(\mathrm{grad}_{\mathbb{D}}\tilde{\Phi})(\tilde{\varphi}(t)) = 0 \tag{3.1}$$

which satisfies the initial conditions:

$$\tilde{\varphi}(t_0) = \tilde{\varphi}_0 \quad , \quad \dot{\tilde{\varphi}}(t_0) = \tilde{v}_0 \quad . \tag{3.2}$$

The solution $\tilde{\varphi} : \mathfrak{I} \to \mathbb{D}$ of (3.1) is called the *lift* of the solution $\varphi : \mathfrak{I} \to \Sigma$ through the point $\tilde{\varphi}_0 \in \pi_{\mathbb{D}}^{-1}(\{\varphi_0\})$.

Proof. Since $\pi_{\mathbb{D}}$ is a universal covering map, the smooth curve $\varphi : \mathfrak{I} \to \Sigma$ which satisfies $\varphi(t_0) = \varphi_0$ lifts uniquely to a curve $\tilde{\varphi} : \mathfrak{I} \to \mathbb{D}$ satisfying $\pi_{\mathbb{D}} \circ \tilde{\varphi} = \varphi$ and $\tilde{\varphi}(t_0) = \tilde{\varphi}_0$. Moreover, the condition $\dot{\varphi}(t_0) = v_0$ is equivalent with $\dot{\tilde{\varphi}}(t_0) = \tilde{v}_0$ since $\pi_{\mathbb{D}}$ is a local diffeomorphism. The lift $\tilde{\varphi}$ satisfies equation (3.1) since φ satisfies (1.9) while $\pi_{\mathbb{D}}$ is a local isometry between $(\mathbb{D}, 3\alpha G_{\mathbb{D}})$ and $(\Sigma, \mathcal{G})$, where $G_{\mathbb{D}}$ is the Poincaré metric of $\mathbb{D}$.

Remark. Since Δ is an infinite discrete group, there exists a countable infinity of choices of lifts $\tilde{\varphi}_0$ of φ_0. These lifts form an orbit of Δ on $\mathbb{D}$. The set of accumulation points of this orbit coincides with the limit set $\Lambda_{\mathbb{D}} \subset \partial_\infty \mathbb{D}$ of Δ.

In semi-geodesic coordinates $u = \tanh(\frac{r}{2})e^{i\theta}$ on $\mathbb{D}$, the Poincaré metric has the form (A.3) with $H(r) = \sinh(r)$. Using (A.4), we find:

$$\Gamma^r_{\theta\theta} = -\frac{1}{2}\sinh(2r) \quad , \quad \Gamma^\theta_{r\theta} = \Gamma^\theta_{\theta r} = \coth(r) \quad ,$$

which gives:

$$\nabla_t \dot{r} = \ddot{r} - \frac{1}{2}\sinh(2r)\dot{\theta}^2 \quad , \quad \nabla_t \dot{\theta} = \ddot{\theta} + 2\coth(r)\dot{r}\dot{\theta} \quad .$$

Thus (3.1) takes the following form in semi-geodesic coordinates on $\mathbb{D}$:

$$\begin{aligned} &\ddot{r} - \frac{1}{2}\sinh(2r)\dot{\theta}^2 + \frac{1}{M}\sqrt{\frac{3}{2}\left[3\alpha(\dot{r}^2 + \sinh^2(r)\dot{\theta}^2) + 2\tilde{\Phi}(r,\theta)\right]}\dot{r} + \frac{1}{3\alpha}\partial_r\tilde{\Phi}(r,\theta) = 0 \quad , \\ &\ddot{\theta} + 2\coth(r)\dot{r}\dot{\theta} + \frac{1}{M}\sqrt{\frac{3}{2}\left[3\alpha(\dot{r}^2 + \sinh^2(r)\dot{\theta}^2) + 2\tilde{\Phi}(r,\theta)\right]}\dot{\theta} + \frac{1}{3\alpha}\frac{\partial_\theta\tilde{\Phi}(r,\theta)}{\sinh^2(r)} = 0 \ . \end{aligned} \tag{3.3}$$

3.2 Lift to the upper half plane

One can also lift to the upper half plane using a holomorphic covering map $\pi_{\mathbb{H}} : \mathbb{H} \to \Sigma = \mathbb{H}/\Gamma$ (recall that $\pi_{\mathbb{D}} = \pi_{\mathbb{H}} \circ f$ and $\Delta = Q^{-1}\Gamma Q$, where f is the Cayley map (B.4) and Q is the Cayley element (B.5)). The Poincaré metric of $\mathbb{H}$ in Cartesian coordinates $x = \mathrm{Re}\tau$ and $y = \mathrm{Im}\tau$ takes the form (B.2) and has Christoffel symbols:

$$\Gamma^y_{xx} = \frac{1}{y} \quad , \quad \Gamma^y_{yy} = \Gamma^x_{xy} = \Gamma^x_{yx} = -\frac{1}{y} \quad ,$$

which gives:

$$\nabla_t \dot{x} = \ddot{x} - \frac{2}{y}\dot{x}\dot{y} \quad , \quad \nabla_t \dot{y} = \ddot{y} + \frac{1}{y}(\dot{x}^2 - \dot{y}^2) \quad .$$

Thus (3.1) takes the following form in Cartesian coordinates on $\mathbb{H}$:

$$\begin{aligned} &\ddot{x} - \frac{2}{y}\dot{x}\dot{y} + \frac{1}{M}\sqrt{\frac{3}{2}}\left[3\alpha\frac{\dot{x}^2 + \dot{y}^2}{y^2} + 2\tilde{\Phi}(x,y)\right]^{1/2}\dot{x} + \frac{1}{3\alpha}y^2\partial_x\tilde{\Phi}(x,y) = 0 \quad , \\ &\ddot{y} + \frac{1}{y}(\dot{x}^2 - \dot{y}^2) + \frac{1}{M}\sqrt{\frac{3}{2}}\left[3\alpha\frac{\dot{x}^2 + \dot{y}^2}{y^2} + 2\tilde{\Phi}(x,y)\right]^{1/2}\dot{y} + \frac{1}{3\alpha}y^2\partial_y\tilde{\Phi}(x,y) = 0 \quad . \end{aligned} \tag{3.4}$$

Remark. Given that every generalized two-field α-attractor model can be lifted to $\mathbb{H}$, it may naively appear that we have gained nothing by considering general geometrically finite hyperbolic surfaces. Notice, however, that the covering map $\pi_{\mathbb{H}}$ is quite non-trivial, because $\Gamma \subset \mathrm{PSL}(2,\mathbb{R})$ is an *infinite* discrete group, whose orbits have accumulation points on the set $\Lambda_{\mathbb{H}} \subset \partial_\infty\mathbb{H}$. In practice, the effect of the projection through $\pi_{\mathbb{H}}$ can be described by computing a fundamental polygon[12] for the action of Γ on $\mathbb{H}$ (see below). Determining a

[12] For example, a Dirichlet domain for Δ centered at the origin of $\mathbb{D}$, which is known as a Ford domain.

fundamental polygon for a given Fuchsian group is a classical but highly non-trivial problem. When Σ has finite hyperbolic area (i.e., when Γ is of the first kind) and when the elements of Γ have entries belonging to an algebraic extension of $\mathbb{Q}$, a stopping algorithm for finding a Ford domain was given in [43]. When Σ has infinite hyperbolic area, no general stopping algorithm for computing a fundamental polygon of Γ is currently known. Some models for which a fundamental polygon (as well as the uniformizing map) is explicitly known are discussed in detail in references [31, 32].

3.3 Describing the projection using a fundamental polygon

Let $\Delta \subset \mathrm{PSU}(1,1)$ be the uniformizing group of a geometrically finite hyperbolic surface (Σ, G). Provided that a fundamental polygon $\mathfrak{D}_{\mathbb{D}} \subset \mathbb{D}$ of Δ is known, the integral curves of (1.9) for $\mathcal{G} = 3\alpha G$ can be determined by computing their lift to the interior of $\mathfrak{D}_{\mathbb{D}}$ as follows:

1. The Δ-orbit of the lifted initial value $\tilde{\varphi}_0 \in \mathbb{D}$ intersects $\mathfrak{D}_{\mathbb{D}}$ in exactly one point. Hence by applying a Δ-transformation if necessary, we can assume without loss of generality that $\tilde{\varphi}_0$ belongs to $\mathfrak{D}_{\mathbb{D}}$. By slightly changing the initial time t_0, we can assume that $\tilde{\varphi}_0$ belongs to the interior $\mathrm{Int}\mathfrak{D}_{\mathbb{D}}$ of $\mathfrak{D}_{\mathbb{D}}$.
2. Assuming $\tilde{\varphi}_0 \in \mathfrak{D}_{\mathbb{D}}$, compute a solution $\tilde{\boldsymbol{\varphi}}$ of equation (3.1) with initial conditions (3.2). Stop the computation at the first value $t_1 > t_0$ for which $\tilde{\boldsymbol{\varphi}}(t)$ meets the relative frontier $\mathrm{Fr}\mathfrak{D}_{\mathbb{D}}$ of $\mathfrak{D}_{\mathbb{D}}$ in $\mathbb{D}$.
3. Since $\mathfrak{D}_{\mathbb{D}}$ is a fundamental polygon, there exists a unique element $\delta_1 \in \Delta$ which maps the point $\tilde{\boldsymbol{\varphi}}(t_1) \in \mathrm{Fr}\mathfrak{D}_{\mathbb{D}}$ into a point $\tilde{\varphi}_1 \overset{\text{def.}}{=} \delta_1 \tilde{\boldsymbol{\varphi}}(t_1)$ which lies on $\mathrm{Fr}\mathfrak{D}_{\mathbb{D}}$. Since δ_1 acts as an isometry of $(\mathbb{D}, \mathrm{d}s^2_{\mathbb{D}})$, the velocity vector $\dot{\tilde{\boldsymbol{\varphi}}}(t_1) \in T_{\tilde{\boldsymbol{\varphi}}(t_1)}\mathbb{D}$ is transported by δ_1 to a congruent vector $\tilde{v}_1 \overset{\text{def.}}{=} (\delta_1)_*(\dot{\tilde{\boldsymbol{\varphi}}}(t_1)) \in T_{\tilde{\varphi}_1}\mathbb{D}$ with origin at the point $\tilde{\varphi}_1$.
4. Now compute a solution $\tilde{\boldsymbol{\varphi}}(t)$ of equation (3.1) with initial conditions $\tilde{\boldsymbol{\varphi}}(t_1) = \tilde{\varphi}_1$ and $\dot{\tilde{\boldsymbol{\varphi}}}(t_1) = \tilde{v}_1$ and follow it to the first time $t_2 > t_1$ for which $\tilde{\boldsymbol{\varphi}}(t_2)$ lies in the relative frontier of $\mathfrak{D}_{\mathbb{D}}$. Then repeat the process above.

This algorithm produces an infinite sequence of times $t_0 < t_1 < t_2 < t_3 < \ldots$ and a map $\tilde{\boldsymbol{\varphi}} : [t_0, a) \setminus T \to \mathfrak{D}_{\mathbb{D}}$ (where $T \overset{\text{def.}}{=} \{t_i | i \geq 1\}$ and $a \in \mathbb{R} \sqcup \{+\infty\}$ satisfies $a \geq \sup T$) which is smooth inside each interval (t_i, t_{i+1}) $(i \geq 0)$ and satisfies $\tilde{\boldsymbol{\varphi}}(t_0) = \tilde{\varphi}_0$ and $\dot{\tilde{\boldsymbol{\varphi}}}(t_0) = \tilde{v}_0$. Moreover, it produces a sequence of elements $\delta_i \in \Delta$ (with $i \geq 1$) such that $\delta_i \tilde{\boldsymbol{\varphi}}(t_i-) = \tilde{\boldsymbol{\varphi}}(t_i+)$ and $(\delta_i)_*(\dot{\tilde{\boldsymbol{\varphi}}}(t_i-)) = \dot{\tilde{\boldsymbol{\varphi}}}(t_i+) = \tilde{v}_i$ for all $i \geq 1$, where $\tilde{\boldsymbol{\varphi}}(t_i-)$ and $\tilde{\boldsymbol{\varphi}}(t_i+)$ denote the lower and upper limits of $\tilde{\boldsymbol{\varphi}}$ at the point t_i, with a similar notation for the partial limits of $\dot{\tilde{\boldsymbol{\varphi}}}$. It is clear from the above that $\tilde{\boldsymbol{\varphi}}$ provides a lift of the forward solution $\varphi : \mathfrak{I} \cap [t_0, +\infty) \to \Sigma$ to the interior of the fundamental polygon $\mathfrak{D}_{\mathbb{D}}$. In general, the algorithm must be continued indefinitely to obtain a full lift to $\mathrm{Int}\mathfrak{D}_{\mathbb{D}}$, because the tessellation of $\mathbb{D}$ by Δ-images of the fundamental polygon has an infinite number of tiles. In particular, the errors in a numerical implementation of this algorithm will accumulate as i grows and the precision of the lifted trajectory provided by a numerical solver will decrease for large t.

A different but equivalent approach is to compute a single full trajectory $\tilde{\varphi}$ of (3.1) on $\mathbb{D}$ and then determine its projection to Σ by computing a tessellation of $\mathbb{D}$ through

Δ-images of the fundamental domain $\mathfrak{D}_{\mathbb{D}}$. Since Δ is an infinite group, the tessellation has an infinite number of tiles, which accumulate toward the conformal boundary $\partial_\infty \mathbb{D}$. As a consequence, the error made in determining the projection $\varphi(t)$ of $\tilde{\varphi}(t)$ to Σ increases as $\tilde{\varphi}(t)$ approaches $\partial_\infty \mathbb{D}$, i.e when $\varphi(t)$ approaches an ideal point of Σ. In this region, one can use instead the explicit form of the hyperbolic metric on a small punctured neighborhood of the ideal point (see Appendix D.6), which allows one to compute an approximate trajectory on such a neighborhood, thus avoiding the problem of accumulating tiles. Of course, similar algorithms can be formulated for the lift to the upper half plane.

3.4 Characterization of potentials which are well-behaved at a cusp or funnel end

Let $\Phi : \Sigma \to \mathbb{R}$ be a smooth function defined on Σ and $\tilde{\Phi} : \mathbb{H} \to \mathbb{R}$ be its Γ-invariant lift to $\mathbb{H}$. Let $\mathfrak{D}_{\mathbb{H}} \subset \mathbb{H}$ be a fundamental polygon for the uniformizing group $\Gamma \subset \mathrm{PSL}(2, \mathbb{R})$. The construction of Appendix D.4 implies:

- Φ is well-behaved at a cusp ideal point $p \in \hat{\Sigma} \setminus \Sigma$ iff there exists a smooth function $\hat{\Phi}_p : D \to \mathbb{R}$ defined on the disk $D \stackrel{\text{def.}}{=} \{z \in \mathbb{C} | \, |z| < e^{-2\pi}\}$ such that, for some (equivalently, any) ideal vertex v of $\mathfrak{D}_{\mathbb{H}}$ which corresponds to p, the restriction of the lift $\tilde{\Phi}$ to a relative cusp neighborhood $\mathfrak{C}_v$ of v in $\mathfrak{D}_{\mathbb{H}}$ has the form:

$$\tilde{\Phi}(\tau) = \hat{\Phi}_p(z_p(\tau)) \quad (\tau \in \mathfrak{C}_v) \quad ,$$

  where $z_p(\tau)$ is the cusp coordinate (D.2) near p.

- Φ is well-behaved at a funnel ideal point $p \in \hat{\Sigma} \setminus \Sigma$ iff there exists a smooth function $\hat{\Phi}_p : \mathbb{D} \to \mathbb{R}$ defined on the unit disk $\mathbb{D} = \{z \in \mathbb{C} | |z| < 1\}$ such that, for some (equivalently, any) free side E of $\mathfrak{D}_{\mathbb{H}}$ which corresponds to p, the restriction of the lift $\tilde{\Phi}$ to a relative funnel neighborhood $\mathfrak{F}_E$ of E in $\mathfrak{D}_{\mathbb{H}}$ has the form:

$$\tilde{\Phi}(\tau) = \hat{\Phi}_p \left(\frac{|z_p(\tau)| - \frac{1}{R_p}}{(1 - \frac{1}{R_p})|z_p(\tau)|} z_p(\tau) \right) \quad ,$$

  where $z_p(\tau)$ is the funnel coordinate (D.4). Here, $R_p = e^{\frac{\pi^2}{\ell_p}}$ is the displacement radius (B.8), where ℓ_p is the width of the hyperbolic funnel corresponding to p.

The condition for the cusp ideal points is obvious, while that for funnel ideal points follows from the fact that, for each $R > 1$, the map $z \to \frac{|z| - \frac{1}{R}}{(1 - \frac{1}{R})|z|} z$ is a diffeomorphism from the annulus $\mathbb{A}(R)$ of inner radius $1/R$ and outer radius 1 to the punctured unit disk $\mathbb{D}^*$.

4 Morse theory and multi-path inflation

In this section, we give a qualitative general discussion of the cosmological model in the gradient flow approximation (see Section 1) for the case when the scalar potential is globally well-behaved and the scalar manifold is geometrically finite and non-elementary (i.e. it is not a disk, a punctured disk or an annulus). In the gradient flow approximation,

the qualitative features of the model are determined by the critical points and level sets of the scalar potential Φ. Let (Σ, G) be a geometrically finite non-elementary surface and $\hat{\Sigma} = \Sigma \sqcup \{p_1, \ldots, p_n\}$ be its end compactification (see Appendix C). This section assumes some familiarity with elementary results in Morse theory. These are briefly recalled in the text for convenience of the reader.

4.1 Compactly Morse potentials

Recall that a smooth function $f : \hat{\Sigma} \to \mathbb{R}$ is called *Morse* if all its critical points have non-degenerate Hessian. In this case, the critical points are isolated and they must form a finite set since $\hat{\Sigma}$ is compact. Morse functions are generic in the space $\mathcal{C}^\infty(\hat{\Sigma}, \mathbb{R})$ of all smooth functions from $\hat{\Sigma}$ to $\mathbb{R}$ (when the latter is endowed with the compact-open topology) in the sense that they form an open and dense subset of that topological space. Hence any smooth function $f : \hat{\Sigma} \to \mathbb{R}$ can be deformed to a Morse function by an infinitesimally small perturbation.

We say that a smooth function $\Phi : \Sigma \to \mathbb{R}$ is *compactly Morse* if there exists a smooth Morse function $\hat{\Phi} : \hat{\Sigma} \to \mathbb{R}$ such that $\Phi = \hat{\Phi}|_\Sigma$ and such that $p_1, \ldots, p_n$ are critical points of $\hat{\Phi}$. In this case, the remaining critical points of $\hat{\Phi}$ lie inside Σ and they form the critical set $\mathrm{Crit}\Phi$ of Φ. We have:

$$\mathrm{Crit}\hat{\Phi} = \mathrm{Crit}\Phi \sqcup \{p_1, \ldots, p_n\} \quad ,$$

where $\mathrm{Crit}\hat{\Phi}$ denotes the critical set of $\hat{\Phi}$. Notice that compactly Morse potentials are globally well-behaved in the sense of Subsection 2.2. In particular, the extension $\hat{\Phi}$ of Φ to $\hat{\Sigma}$ is uniquely determined by Φ through continuity. Since any smooth real-valued function defined on $\hat{\Sigma}$ can be infinitesimally deformed to a Morse function, any well-behaved scalar potential on Σ can be infinitesimally deformed to a compactly Morse potential. Since infinitesimal deformations cannot be detected observationally, one can safely assume that a physically-realistic well-behaved scalar potential is compactly Morse.

4.2 Reconstructing the topology of Σ

Let Φ be a compactly Morse potential and $\hat{\Phi}$ be its extension to $\hat{\Sigma}$. Recall that a critical point $c \in \mathrm{Crit}\hat{\Phi}$ is either:

- a local minimum of $\hat{\Phi}$, when the Hessian of $\hat{\Phi}$ at c is positive-definite, i.e. when c has Morse index 0.
- a saddle point of $\hat{\Phi}$, when the Hessian operator of $\hat{\Phi}$ at c has one positive eigenvalue and one negative eigenvalue, i.e when c has Morse index 1.
- a local maximum of $\hat{\Phi}$, when the Hessian of $\hat{\Phi}$ at c is negative-definite, i.e. when c has Morse index 2.

The local minima, saddles and local maxima of Φ coincide with those local minima, saddles and local maxima of $\hat{\Phi}$ which lie in Σ. Let $\hat{N}_m$, $\hat{N}_M$ and $\hat{N}_s$ denote the number of local minima, local maxima and saddles of $\hat{\Phi}$ and N_m, N_M and N_s denote the number of local

minima, local maxima and saddles of Φ. Let n_m, n_M and n_s be the numbers of ideal points $p_1, \ldots, p_n$ which are local minima, local maxima and saddles of $\hat{\Phi}$. We have:

$$n = n_m + n_M + n_s \quad , \quad \hat{N}_m = N_m + n_m \quad , \quad \hat{N}_M = N_M + n_M \quad , \quad \hat{N}_s = N_s + n_s \quad . \tag{4.1}$$

Morse's theorem applied to $\hat{\Phi}$ shows that the Euler characteristic of $\hat{\Sigma}$ is given by:

$$\chi(\hat{\Sigma}) = 2 - 2g = \hat{N}_m + \hat{N}_M - \hat{N}_s = N_M + N_m - N_s + n_M + n_m - n_s \quad , \tag{4.2}$$

where g is the genus of Σ (which by definition equals the genus of $\hat{\Sigma}$). In particular, the quantity $2 + \hat{N}_s - \hat{N}_M - \hat{N}_m$ is an even non-negative integer and the genus of $\hat{\Sigma}$ is given by:

$$g = 1 + \frac{\hat{N}_s - \hat{N}_M - \hat{N}_m}{2} = 1 + \frac{N_s - N_M - N_m + n_s - n_M - n_m}{2} \quad . \tag{4.3}$$

Recall that Σ is determined up to diffeomorphism by its genus g and by the number $n = n_M + n_m + n_s$ of its ends. Hence (4.3) implies that the topology of Σ can be reconstructed from knowledge of the numbers n_M, n_m, n_s and N_M, N_m and N_s. In principle, these numbers could be determined observationally by comparing cosmological correlators computed in the model with observational data, thus allowing one to reconstruct the topology of the scalar manifold Σ.

4.3 The topological decomposition induced by a compactly Morse potential

A compactly Morse potential Φ induces a topological decomposition:

$$\hat{\Sigma} = Y_1 \cup \ldots \cup Y_{2g-2+n} \quad ,$$

where Y_j are (possibly degenerate) topological pairs of pants, i.e. surfaces diffeomorphic with a sphere with three holes, where any of the holes is allowed to degenerate to a point. For any regular value $a \in \hat{\Phi}(\hat{\Sigma}) - \hat{\Phi}(\mathrm{Crit}\hat{\Phi}) \subset \mathbb{R}$, the preimage $\hat{\Phi}^{-1}(\{a\})$ is a finite disjoint union of closed connected curves, each of which is diffeomorphic with a circle. When a is a critical value such that $\hat{\Phi}^{-1}(\{a\})$ contains a single critical point, one has two possibilities:

- One of the circles degenerates to a single point $p \in \hat{\Sigma}$, which is a local minimum or local maximum of $\hat{\Phi}$.
- Two of the circles touch at a single point $p \in \hat{\Sigma}$, which is a saddle point of $\hat{\Phi}$.

Two pants of a given pair of pants Y_j meet at a saddle point and each saddle point lies on a single pair of pants. Moreover, every local maximum or local minimum of $\hat{\Phi}$ corresponds to a degenerate bounding circle of a pair of pants.

One can isolate the local maxima and local minima of $\hat{\Phi}$ by cutting out small open disks $D_1, \ldots, D_{\hat{N}_M + \hat{N}_m}$ around the local maximum and local minimum points, such that the closure of each disk D_k does not meet the closure of any other disk or any other critical point. Then $Z \stackrel{\mathrm{def.}}{=} \hat{\Sigma} \setminus (\cup_{k=1}^{\hat{N}_M + \hat{N}_m} D_k)$ is a compact surface with boundary and the restriction of $\hat{\Phi}$ to Z is a Morse function whose critical points are saddles and lie in the interior of

Z. Using the Morse decomposition for surfaces with boundary, one can decompose Z as a union:

$$Z = Z_1 \cup \ldots \cup Z_{2g-2+n}$$

of a number $|\chi(\hat{\Sigma})| = 2g - 2 + n$ of pairs of pants Z_j, all of whose bounding circles are non-degenerate. This gives a decomposition:

$$\hat{\Sigma} = Z_1 \cup \ldots \cup Z_N \cup D_1 \cup \ldots \cup D_{\hat{N}_M + \hat{N}_m} \quad .$$

Notice that this decomposition is entirely determined by the topology of Σ and by the scalar potential Φ (since D_i and Z_j are determined by that data) and hence is independent of the hyperbolic metric on Σ and on the parameter α of the cosmological model.

4.4 Qualitative features and multipath inflation in the gradient flow approximation

The gradient flow approximation allows one to give a qualitative picture of cosmological trajectories when the potential Φ is compactly Morse. If the scalar field φ starts rolling from an initial value near a point $p \in \hat{\Sigma}$ which is a local maximum of $\hat{\Phi}$, then to first approximation the model has inflationary behavior as long as φ lies inside some neighborhood D of p. In general, inflation ends after φ exits D, after which the field generally evolves in a complicated manner radiating its energy and either settles in one of the local minima of Φ or evolves further toward an ideal point which is a local minimum of $\hat{\Phi}$. The full evolution can be quite complicated in general, since Φ can have many critical points.

The gradient flow of Φ bifurcates at the saddle points, where the level sets of Φ consist of two simple closed curves meeting at the saddle (see Figure 5). In the gradient flow approximation, this implies that certain integral curves will bifurcate within the topological pants components Z_j determined by Φ, entering through one of the boundary components of Z_j, hitting the unique saddle point contained inside Z_j, then following one of the two trajectories which start from that saddle point to exit through either of the other two boundary components of Z_j. In particular, this gives a realization of multipath inflation in our class of models.

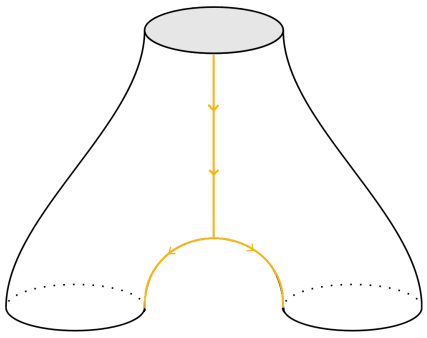

Figure 5: Example of a gradient flow trajectory (the orange line) in the gradient flow approximation, shown within a topological pair of pants determined by the scalar potential Φ.

Remark. For a detailed study beyond the gradient flow approximation, one could instead use a *hyperbolic* pants decomposition (see Appendix D.3). If a hyperbolic pants decomposition $N = X_1 \cup \ldots \cup X_{2g-2+n}$ of (Σ, G) is known, then one can study the dynamics of the cosmological model separately inside each pair of hyperbolic pants X_j. The latter can be computed by presenting X_j as the result of gluing two hyperbolic hexagons, which reduces the problem to studying the model on a hyperbolic hexagon and making appropriate identifications.

5 Examples and phenomenological implications

Unlike one-field α-attractors [1–4], the models considered in this paper are genuine two-field cosmological models. As such, they allow for deviations from the traditional paradigm of inflationary cosmology, which assumes the inflaton to be a single real scalar field. Current cosmological data are well accounted for by various one-field models, but they can also be fit using multi-field models. It is generally believed that improved measurements in the future might detect deviations from one-field predictions, a possibility which lead to renewed interest in multi-field models [14–19] and in particular to interest in numerical methods for computing cosmological perturbations in such models [20–22] beyond the limitations of the SRST approximation [8, 9]. See [23] for an investigation of constraints imposed on two-field models by Planck 2015 data [7].

As explained in Subsection 2.3, a generalized two-field α-attractor model based on a non-compact geometrically finite hyperbolic surface (Σ, G) and with a well-behaved scalar potential Φ has universal behavior near each end of Σ where the extended scalar potential has a local maximum, in a certain 'radial' one-field truncation near that end. Within the slow-roll approximation for 'radial' trajectories close to such an end of Σ, these models predict the same spectral index n_s and tensor to scalar ratio r as ordinary one-field α-attractors, namely (see Section 2.3):

$$n_s \approx 1 - \frac{2}{N} \quad , \quad r \approx \frac{12\alpha}{N^2} \quad ,$$

where N denotes the number of e-folds. Hence generalized two-field α-attractors are as promising observationally as ordinary one-field α-attractors, which are known to be in good agreement with current cosmological data [1–4].

In references [31] and [32], we study certain explicit examples of generalized two-field α-attractor models, which differ topologically from the oft-studied case of the Poincaré disk. Namely, reference [31] considers generalized two-field α-attractors based on the punctured hyperbolic disk $\mathbb{D}^*$ and on hyperbolic annuli $\mathbb{A}(R)$ of modulus $\mu = 2\ln R > 0$, for certain natural choices of globally well-behaved scalar potentials. On the other hand, reference [32] studies generalized two-field α-attractor models based on the hyperbolic triply-punctured sphere (which is also known as the modular curve $Y(2)$), for a few natural choices of scalar potential. References [31, 32] give numerous examples of numerically computed cosmological trajectories for the models considered therein, showing that generalized two-field α-attractors display intricate cosmological dynamics due to the delicate interplay between

the effects of the hyperbolic metric, the scalar potential and the topology of the scalar manifold Σ. The last effect was not considered previously in the literature — given that, until now, studies of two-field α-attractors were limited to models based on the Poincaré disk.

In the models of reference [31], the universal behavior of Subsection 2.3 arises for the radial trajectories on the punctured disk $\mathbb{D}^*$ and on the annulus $\mathbb{A}(R)$ when inflation happens close to any of the two components of the conformal boundary. In fact, reference [31] gives explicit examples of such trajectories which produce between $50 - 60$ e-folds, thereby showing that generalized two-field α-attractor models based on $\mathbb{D}^*$ or on $\mathbb{A}(R)$ are compatible with current observational data. In the same reference, we also give examples of non-geodesic cosmological trajectories with $50 - 60$ e-folds. The latter trajectories are *not* of the special type considered in Subsection 2.3; this shows that generalized two-field α-attractor models based on the hyperbolic surfaces $\mathbb{D}^*$ and $\mathbb{A}(R)$ can fit current cosmological data even for trajectories with genuine two-field behavior.

Generalized two-field α-attractor models based on the hyperbolic triply-punctured sphere $Y(2)$ are discussed in reference [32]. As shown in loc. cit., such models are again compatible with current cosmological constraints. In that reference, we again display cosmological trajectories producing between $50 - 60$ e-folds. This shows that generalized two-field α-attractor models based on $Y(2)$ are also compatible with current observational constraints.

We remark that generalized two-field α-attractors are interesting for studies of post-inflationary dynamics, a problem for which generic two field models have low predictive power (since they involve the choice of an arbitrary metric for the scalar manifold Σ). Indeed, generalized α-attractors form a mathematically *natural* class of two-field models with universal behavior in the 'radially truncated' inflationary regime near the ends. Moreover, they show remarkable dynamical complexity beyond that regime, as illustrated in detail in references [31, 32]. Such models could form a useful testing ground for two-field model technology.

6 Conclusions and further directions

We proposed a wide generalization of ordinary two-field α-attractor models obtained by promoting the Poincaré disk to a geometrically finite hyperbolic surface as well as a general procedure for studying such models through uniformization techniques; we also discussed certain general aspects of such models, using the well-developed machinery of uniformization and two-dimensional hyperbolic geometry. Our generalized models are parameterized by a positive constant α, by the choice of a surface group $\Gamma \subset \mathrm{PSL}(2, \mathbb{R})$ and by the choice of a smooth scalar potential. Despite being extremely general, we showed that such models have the same universal behavior as ordinary α-attractors for certain special trajectories, in a *naive* one-field truncation near each end and in the slow-roll approximation for such trajectories, provided that the scalar potential is well-behaved near that end. We also discussed certain qualitative features of such models in the gradient flow approximation and commented briefly on some phenomenological aspects and on some examples which are

studied in detail in references [31, 32]. The present work sets the ground for more detailed investigations of such models. There exist numerous directions for further study of such models, of which we point out a few.

First, one could investigate cosmological perturbation theory in such models, adapting the numerical approach developed in [20–22]; using numerical methods seems to be necessary within the compact core of Σ as well as near cusp ends (where the SRST approximation can fail, as showed in Subsection 2.4). In particular, the algorithm proposed in Section 3 could be combined with existing code in order to perform numerical studies of cosmological correlators.

Second, one could study in detail the particular case when Σ is a modular curve. When Γ is an arithmetic subgroup of $\mathrm{PSL}(2,\mathbb{Z})$, an algorithm for finding a fundamental polygon was given in [43] (and was implemented in `Sage` as part of the *KFarey* package [44]). In this case, the hyperbolic surface (Σ, G) has only cusp ends and the scalar potential can be expanded in Maass wave forms [45]. In general, this special subclass of two-field generalized α-attractor models leads to connections with Teichmüller theory and number theory and relates to the framework of automorphic inflation which was developed in [46, 47]. A simple example of this type (namely the model whose scalar manifold is the hyperbolic triply punctured sphere (also known as the modular curve $Y(2)$) is studied in reference [32]; as explained there, the generalized two-field α-attractor model having $Y(2)$ as its scalar manifold is related to — but does *not* coincide with – the "modular invariant j-model" considered in [11, 12].

One could also study the F-term embedding of our theories into $\mathcal{N} = 1$ supergravity with a single chiral multiplet. When Γ is an arithmetic group, this leads to connections with the theory of automorphic forms. It would be interesting to study the extension of our models to the case when Σ is a non-orientable surface. In that situation, the uniformizing surface group Γ is replaced by a non-Euclidean crystallographic group [48, 49]. It would also be interesting to consider the case when Σ is not topologically finite.

We refer the interested reader to reference [31] for a detailed study of cosmological trajectories in two-field generalized α-attractor models based on elementary hyperbolic surfaces and to [32] for a similar study in the model based on the hyperbolic triply punctured sphere. As shown in those references, it is quite easy in such models to obtain the observationally favored range of $50 - 60$ e-folds for various inflationary trajectories. This shows that the class of models proposed in the present paper could be of phenomenological interest. Unlike ordinary two-field α-attractor models (which are based on the Poincaré disk), generalized two-field α attractors can have much richer post-inflationary dynamics, as illustrated qualitatively in Section 4 of this paper and quantitatively in [31, 32] through numerical computation of various trajectories. The surprising complexity of such trajectories indicates rich possibilities which may be of interest to cosmological model building. While much work remains to be done before ascertaining the phenomenological viability of such models, it may well be worth stepping into the world of general hyperbolic surfaces as a natural special class of scalar manifolds for cosmological two-field models. Indeed, hyperbolic surfaces form a family of two-dimensional Riemannian manifolds to which two-field model technology can be applied in a non-generic manner and usefully combined with the

powerful results of uniformization theory.

Acknowledgments

The work of C.I.L. was supported by grant IBS-R003-S1. C.S.S. thanks the CERN Theory Division for hospitality during the preparation of this work and R. Kallosh for comments. C.I.L and C.S.S. thank A. Marrani for participation during the early stages of the project and for interesting discussions.

A Isothermal and semi-geodesic coordinates on Riemann surfaces

In this paper, we often use two special kinds of local coordinate systems on Σ:

- **Isothermal coordinates**. Let $x = \mathrm{Re} z$ and $y = \mathrm{Im} z$ be the real coordinates defined by a local holomorphic coordinate z on a complex curve (Σ, J). In such coordinates, any Hermitian (and hence Kähler) metric $\mathcal{G}$ on (Σ, J) takes the local form:

$$\mathrm{d}s^2 = \lambda^2(z,\bar{z})|\mathrm{d}z|^2 = \lambda^2(\mathrm{d}x^2 + \mathrm{d}y^2) \quad , \text{ where } \quad \lambda(z,\bar{z}) > 0 \tag{A.1}$$

  and the Gaussian curvature of $\mathcal{G}$ is given by:

$$K = -\Delta_{\mathcal{G}} \log \lambda \quad ,$$

  where:

$$\Delta_{\mathcal{G}} = \frac{1}{\lambda^2}\left(\frac{\partial^2}{\partial x^2} + \frac{\partial^2}{\partial y^2}\right) = \frac{4}{\lambda^2}\frac{\partial^2}{\partial z \partial \bar{z}}$$

  is the Laplacian of $\mathcal{G}$. The metric $\mathcal{G}$ is hyperbolic iff $K = -1$, which amounts to the condition:

$$\Delta_{\mathcal{G}} \log \lambda = 1 \iff 4\frac{\partial^2 \log \lambda}{\partial z \partial \bar{z}} = \lambda^2 \iff \left(\frac{\partial^2}{\partial x^2} + \frac{\partial^2}{\partial y^2}\right) \log \lambda = \lambda^2 \quad . \tag{A.2}$$

  Any Riemannian metric $\mathcal{G}$ on an oriented surface Σ determines a unique orientation-compatible complex structure J on Σ such that $\mathcal{G}$ is Kähler with respect to J; this complex structure depends only on the conformal class of $\mathcal{G}$. In this case, the isothermal coordinates x, y determined by a local J-holomorphic coordinate z defined on an open subset $U \subset \Sigma$ are called *local isothermal coordinates* for $\mathcal{G}$. The smooth function $\lambda : U \to \mathbb{R}_{>0}$ defined through (A.1) in such coordinates is called the *local density of* $\mathcal{G}$ with respect to z. When $\mathcal{G}$ is hyperbolic, λ satisfies (A.2) and is called the *Poincaré density* of $\mathcal{G}$.

- **Semi-geodesic coordinates.** Any point of a Riemann surface $(\Sigma, \mathcal{G})$ admits an open neighborhood U supporting semi-geodesic coordinates, in which the metric takes the form:

$$\mathrm{d}s^2 = \mathrm{d}r^2 + H(r,\theta)^2 \mathrm{d}\theta^2 \quad , \quad \text{where} \quad H(r,\theta) > 0 \quad . \tag{A.3}$$

Such coordinates are characterized by the property that the curves $\theta = \text{constant}$ are geodesics (with natural parameter r) which are orthogonal to the surfaces $r = \text{constant}$. The Gaussian curvature is given by:

$$K = -\frac{1}{H}\frac{\partial^2 H}{\partial r^2} \quad ,$$

while the non-vanishing Christoffel symbols are [50, p. 389]:

$$\begin{aligned} \Gamma^r_{\theta\theta} &= -H\partial_r H \quad , \\ \Gamma^\theta_{r\theta} &= \Gamma^\theta_{\theta r} = \partial_r \log H \quad , \\ \Gamma^\theta_{\theta\theta} &= \partial_\theta \log H \quad . \end{aligned} \tag{A.4}$$

The metric $\mathcal{G}$ is hyperbolic when $K = -1$, which amounts to the condition:

$$\frac{\partial^2 H}{\partial r^2} = H \quad .$$

B Uniformization of smooth Riemann surfaces

In this appendix, we summarize some well-known results of uniformization theory and of the theory of hyperbolic surfaces which are used in various sections of the paper. Some standard references for this classical subject are [30, 51–53].

B.1 Hyperbolic surfaces

Let Σ be an oriented surface, which need not be compact. A complete Riemannian metric G on Σ is called *hyperbolic* if its Gaussian curvature $K(G)$ equals -1. In this case, the pair (Σ, G) is called a *hyperbolic surface*. Each conformal class $\mathfrak{c}$ on Σ contains at most one hyperbolic metric. The uniformization theorem of Koebe and Poincaré [29] implies that such a hyperbolic metric exists in $\mathfrak{c}$ iff (Σ, J) is covered holomorphically by the unit disk, where J is the orientation-compatible complex structure determined by $\mathfrak{c}$. A compact oriented surface admits a hyperbolic metric iff its genus g is strictly greater than one; in that case, there exists a continuous infinity of hyperbolic metrics which form a moduli space of complex dimension $3g-3$ (real dimension $6g-6$). The case when Σ is non-compact is discussed below.

B.2 The Poincaré upper half plane

The open upper half plane:

$$\mathbb{H} \stackrel{\text{def.}}{=} \{\tau \in \mathbb{C} | \mathrm{Im}\tau > 0\}$$

with complex coordinate τ admits a unique complete metric of constant Gaussian curvature -1, known as the *Poincaré plane metric*. This metric is given by:

$$\mathrm{d}s^2_{\mathbb{H}} = \lambda_{\mathbb{H}}(\tau,\bar\tau)^2 |\mathrm{d}\tau|^2 \quad \text{with} \quad \lambda_{\mathbb{H}}(\tau,\bar\tau) = \frac{1}{\mathrm{Im}\tau} \quad . \tag{B.1}$$

The Cartesian coordinates $x = \mathrm{Re}\tau$ and $y = \mathrm{Im}\tau$ are isothermal (see Appendix A) and we have:

$$\mathrm{d}s^2_{\mathbb{H}} = \frac{\mathrm{d}x^2 + \mathrm{d}y^2}{y^2} \quad . \tag{B.2}$$

Notice that $\mathbb{H}$ is a non-compact manifold *without boundary* (an open manifold), which has infinite area with respect to the metric (B.1). However, $(\mathbb{H}, \mathrm{d}s^2_{\mathbb{H}})$ (which is isometric with the Poincaré disk $(\mathbb{D}, \mathrm{d}s^2_{\mathbb{D}})$ discussed below) has a *conformal compactification* $\bar{\mathbb{H}}$ (see Appendix C.2). The latter is a manifold with boundary which is diffeomorphic with the closed unit disk $\bar{\mathbb{D}}$. Thus $\mathbb{H}$ has a *conformal boundary* $\partial_\infty\mathbb{H}$ which is diffeomorphic with the unit circle S^1. The latter can be obtained from the real axis $\mathrm{Im}\tau = 0$ by adding the point at infinity:

$$\partial_\infty\mathbb{H} \simeq \mathrm{S}^1 \simeq \{\tau \in \mathbb{C} \,|\, \mathrm{Im}\tau = 0\} \sqcup \{\infty\} \quad .$$

The group of orientation-preserving isometries of $\mathbb{H}$ is isomorphic with $\mathrm{PSL}(2,\mathbb{R})$, acting on $\mathbb{H}$ from the left by fractional linear transformations:

$$\tau \to A\tau \overset{\text{def.}}{=} \frac{a\tau + b}{c\tau + d} \quad , \quad \forall A = \begin{bmatrix} a & b \\ c & d \end{bmatrix} \in \mathrm{SL}(2,\mathbb{R}) \quad . \tag{B.3}$$

The geodesics of $\mathbb{H}$ are as follows (see Figure 6):

A. The Euclidean half-circles contained in $\mathbb{H}$ and having center on the real axis. The canonical orientation of such a geodesic is from left to right when the imaginary axis of $\mathbb{H}$ points upwards.

B. The Euclidean half-lines parallel to the imaginary axis. The canonical orientation of such a geodesic is from bottom to top when the imaginary axis of $\mathbb{H}$ points upwards.

A *horocycle* of $\mathbb{H}$ is either a Euclidean circle which is tangent to a point of the real axis or a Euclidean line parallel to the real axis. In the second case, we say that the horocycle is tangent to $\partial_\infty\mathbb{H}$ at the point ∞. The canonical orientation of a horocycle is from left to right when the imaginary axis of the Poincaré half-plane points upwards.

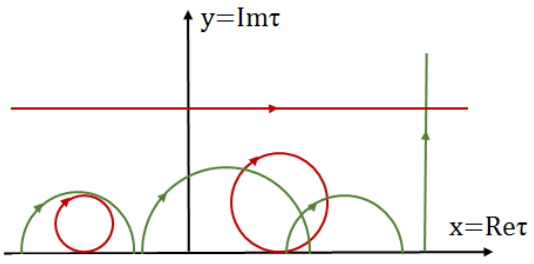

Figure 6: Some geodesics (red) and horocycles (green) on the upper half-plane.

B.3 The Poincaré disk

The open unit disk:

$$\mathbb{D} \overset{\text{def.}}{=} \{u \in \mathbb{C} \mid |u| < 1\}$$

with complex coordinate u admits a unique complete metric of constant Gaussian curvature -1. This is known as the *Poincaré disk metric* and is given by:

$$\mathrm{d}s^2_{\mathbb{D}} = \lambda^2_{\mathbb{D}}(u,\bar{u})|\mathrm{d}u|^2 \quad \text{with} \quad \lambda_{\mathbb{D}}(u,\bar{u}) = \frac{2}{1-|u|^2} \quad .$$

In particular, Reu and Imu are isothermal coordinates. The hyperbolic disk is isometric with the hyperbolic plane through the biholomorphic transformation (the *Cayley map*) $f : \mathbb{D} \to \mathbb{H}$ given by:

$$\tau = f(u) \stackrel{\text{def.}}{=} \frac{u+\mathbf{i}}{\mathbf{i}u+1} \;\Rightarrow\; u = \frac{\mathbf{i}-\tau}{\mathbf{i}\tau-1} \quad , \tag{B.4}$$

which is the action of the Cayley element:

$$Q \stackrel{\text{def.}}{=} \frac{1}{2}\begin{bmatrix} 1 & \mathbf{i} \\ \mathbf{i} & 1 \end{bmatrix} \in \mathrm{SL}(2,\mathbb{C}) \tag{B.5}$$

on τ by a fractional linear transformation. This extends to a diffeomorphism of manifolds with boundary between the conformal compactifications $\bar{\mathbb{D}}$ and $\bar{\mathbb{H}}$, which takes the center $u = 0$ of $\mathbb{D}$ into the point $\tau = \mathbf{i}$ and takes the conformal boundary point $u = \mathbf{i} \in \partial_\infty\mathbb{D}$ into the conformal boundary point $\tau = \infty \in \partial_\infty\mathbb{H}$. In particular, f identifies the conformal boundaries $\partial_\infty\mathbb{D} \simeq \mathrm{S}^1$ and $\partial_\infty\mathbb{H}$. The group of orientation-preserving isometries of $\mathbb{D}$ is $\mathrm{PSU}(1,1)$, where:

$$\mathrm{SU}(1,1) = \left\{ A = \begin{bmatrix} \eta & \sigma \\ \bar{\sigma} & \bar{\eta} \end{bmatrix} \;\middle|\; \eta,\sigma \in \mathbb{C} \;,\; |\eta|^2 - |\sigma|^2 = 1 \right\}$$

acts on $\mathbb{D}$ through:

$$u \to \frac{\eta u + \sigma}{\bar{\sigma}u + \bar{\eta}} \quad .$$

The subgroups $\mathrm{SU}(1,1)$ and $\mathrm{SL}(2,\mathbb{R})$ of $\mathrm{SL}(2,\mathbb{C})$ are conjugate through the Cayley element:

$$Q\mathrm{SU}(1,1)Q^{-1} = \mathrm{SL}(2,\mathbb{R}) \quad ,$$

which implies a similar conjugacy relation between the subgroups $\mathrm{PSU}(1,1)$ and $\mathrm{PSL}(2,\mathbb{R})$ of $\mathrm{PSL}(2,\mathbb{C})$. In particular, $\mathrm{PSU}(1,1)$ is isomorphic with $\mathrm{PSL}(2,\mathbb{R})$. Moreover, the subgroups Γ of $\mathrm{PSL}(2,\mathbb{R})$ can be identified with the subgroups Δ of $\mathrm{PSU}(1,1)$ through the *Cayley correspondence*:

$$\Delta = Q^{-1}\Gamma Q \quad . \tag{B.6}$$

The geodesics of $\mathbb{D}$ are those Euclidean half-circles contained in $\mathbb{D}$ which are orthogonal to $\partial_\infty\mathbb{D}$, together with the diameters of $\mathbb{D}$. The canonical orientation of geodesics is induced from that of geodesics in the Poincaré half-plane model. In the Poincaré disk model, horocycles correspond to those Euclidean circles contained in the closed unit disk which are tangent to $\partial_\infty\mathbb{D}$ at some point of the conformal boundary; their canonical orientation is induced from that of horocycles in the Poincaré half-plane model; the point of tangency is not part of the horocycle (see Figure 7)

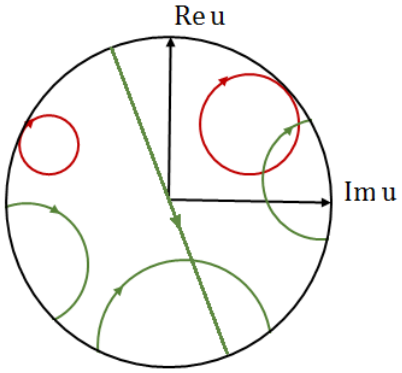

Figure 7: Some geodesics (red) and horocycles (green) on the Poincaré disc.

B.4 Classification of elements of $\mathrm{PSL}(2,\mathbb{R})$

An element $A = \begin{bmatrix} a & b \\ c & d \end{bmatrix} \in \mathrm{PSL}(2,\mathbb{R})$ is called:

- elliptic, if $|\mathrm{tr}(A)| < 2$,
- parabolic, if $|\mathrm{tr}(A)| = 2$,
- hyperbolic, if $|\mathrm{tr}(A)| > 2$.

The fixed points of $A \in \mathrm{PSL}(2,\mathbb{R})$ in $\mathbb{C}$ are the solutions $\tau_\pm = \frac{(a-d)\pm\sqrt{(a+d)^2-4}}{2c}$ of the equation:

$$c\tau^2 + (d-a)\tau - b = 0$$

(which has discriminant $\mathrm{tr}(A)^2 - 4$) and satisfy the Vieta relations:

$$\tau_+ + \tau_- = \frac{a-d}{c} \quad , \quad \tau_+\tau_- = -\frac{b}{c} \quad ,$$

as well as the relation:

$$\tau_+ - \tau_- = \frac{\sqrt{\mathrm{tr}(A)^2-4}}{c} \quad .$$

The element A is non-elliptic iff the roots belong to $\partial_\infty\mathbb{H} = \mathbb{R} \sqcup \{\infty\}$, being parabolic or hyperbolic iff the roots are respectively equal or distinct. We concentrate on parabolic and hyperbolic elements, since smooth surfaces are uniformized by Fuchsian groups without elliptic elements.

Parabolic elements and parabolic cyclic groups. The fixed point $\tau_P \in \partial_\infty\mathbb{H}$ of a parabolic element $P \in \mathrm{PSL}(2,\mathbb{R})$ can be moved to any position on $\partial_\infty\mathbb{H}$ by conjugating P inside $\mathrm{PSL}(2,\mathbb{R})$. Any horocycle tangent to $\partial_\infty\mathbb{H}$ at τ_P is stabilized by the action of P on $\mathbb{H}$. The *unit horocycle* c_P of P is the unique horocycle tangent to $\partial_\infty\mathbb{H}$ at τ_P such that the quotient closed curve $c_P/\langle P\rangle$ has hyperbolic length equal to one.

The subgroup of $\mathrm{PSL}(2,\mathbb{R})$ consisting of all elements fixing a given point $\tau_0 \in \partial_\infty\mathbb{H}$ is an infinite cyclic group $Z_{\tau_0} \subset \mathrm{PSL}(2,\mathbb{R})$ consisting of parabolic elements (called a *parabolic*

cyclic group). All parabolic cyclic groups are mutually conjugate inside $\mathrm{PSL}(2,\mathbb{R})$. Moreover, the map $\tau_0 \to Z_{\tau_0}$ is a bijection between the points of $\partial_\infty\mathbb{H}$ and the set of all parabolic cyclic subgroups of $\mathrm{PSL}(2,\mathbb{R})$. All elements $P \in Z_{\tau_0}$ satisfy $\tau_P = \tau_0$ and can be written as $P = P_{\tau_0}^m$ for some integer $m \in \mathbb{Z}$, where P_{τ_0} is a generator of Z_{τ_0}, which is called *a parabolic generator* determined by τ_0. There are exactly two parabolic generators, namely P_{τ_0} and $P_{\tau_0}^{-1}$. The *positive parabolic generator* is that parabolic generator which maps each point of the unit horocycle tangent to $\partial_\infty\mathbb{H}$ at τ_0 to a point lying forward on that horocycle with respect to the canonical orientation.

Hyperbolic elements and hyperbolic cyclic groups. The two fixed points $\tau_H^\pm$ of a hyperbolic element $H \in \mathrm{PSL}(2,\mathbb{R})$ can be moved to any distinct positions on $\partial_\infty\mathbb{H}$ (for example, to the points 0 and ∞) by conjugating H inside $\mathrm{PSL}(2,\mathbb{R})$. The *axis* of a hyperbolic element H is the unique hyperbolic geodesic c_H connecting the two fixed points of H; this geodesic is stabilized by the action of H on $\mathbb{H}$. Notice that the axis is completely determined by the two fixed points of H. The positive number $\ell(H) > 0$ defined through the relation:

$$\mathrm{tr}(H) = 2\cosh\left(\frac{\ell(H)}{2}\right) \tag{B.7}$$

is called the *displacement length* of H. It coincides with the hyperbolic distance between any point $\tau \in c_H$ and its image $H\tau \in c_H$. The *displacement radius* of H is defined through:

$$R_H \stackrel{\text{def.}}{=} e^{\frac{\pi^2}{\ell(H)}} > 1 \quad . \tag{B.8}$$

The subgroup of $\mathrm{PSL}(2,\mathbb{R})$ consisting of all elements fixing two given distinct points $\tau_1, \tau_2 \in \partial_\infty\mathbb{H}$ is an infinite cyclic group $Z_{\tau_1,\tau_2} \subset \mathrm{PSL}(2,\mathbb{R})$ consisting of hyperbolic elements (called a *hyperbolic cyclic group*). All hyperbolic cyclic groups are mutually conjugate inside $\mathrm{PSL}(2,\mathbb{R})$. Moreover, the map $\{\tau_1,\tau_2\} \to Z_{\tau_1,\tau_2}$ is a bijection between the set of two-element subsets of $\partial_\infty\mathbb{H}$ and the set of all parabolic cyclic subgroups of $\mathrm{PSL}(2,\mathbb{R})$. All elements $H \in Z_{\tau_1,\tau_2}$ satisfy $\{\tau_H^+, \tau_H^-\} = \{\tau_1,\tau_2\}$ and can be written as $H = H_{\tau_1,\tau_2}^m$ for some integer $m \in \mathbb{Z}$, where H_{τ_1,τ_2} is a generator of Z_{τ_1,τ_2}, which is called a *hyperbolic generator* determined by the set $\{\tau_1,\tau_2\}$. There are exactly two such generators, namely H_{τ_1,τ_2} and H_{τ_1,τ_2}^{-1}. The *positive hyperbolic generator* is that hyperbolic generator which maps each point of the geodesic connecting τ_1 and τ_2 to a point lying forward on that geodesic with respect to the canonical orientation.

B.5 Fuchsian and surface groups

A subgroup Γ of $\mathrm{PSL}(2,\mathbb{R})$ is discrete iff it acts properly discontinuously on the upper half plane by fractional linear transformations (B.3). In this case Γ is called a *Fuchsian group*. By definition, a *surface group* is a Fuchsian group Γ without elliptic elements.

Remark. There exists an uncountable infinity of conjugacy classes of surface groups.

B.6 Uniformization of hyperbolic surfaces

Uniformization to the hyperbolic plane. Any oriented smooth hyperbolic surface (Σ, G) can be written as the quotient $\mathbb{H}/\Gamma$ (endowed with the quotiented Poincaré metric), where $\mathbb{H}$ is the hyperbolic plane endowed with the Poincaré metric and Γ is a surface group. Notice that the groups Γ and $\pi_1(\Sigma)$ are isomorphic. Let $\pi_{\mathbb{H}} : \mathbb{H} \to \Sigma$ be the projection map (which is known as the *uniformization map*). When Σ is endowed with the complex structure corresponding to the conformal class of G and $\mathbb{H}$ is endowed with its hyperbolic complex structure, the map $\pi_{\mathbb{H}}$ is a holomorphic covering map. Conversely, any holomorphic covering map $\pi_{\mathbb{H}} : \mathbb{H} \to \Sigma$ induces a hyperbolic metric on Σ which makes $\pi_{\mathbb{H}}$ into a local isometry. Moreover, (Σ, G) determines $\pi_{\mathbb{H}}$ up to composition with an element of $\mathrm{PSL}(2, \mathbb{R})$; this implies that the uniformizing group Γ is determined by (Σ, G) up to conjugation inside $\mathrm{PSL}(2, \mathbb{R})$. Let z be a local complex coordinate on Σ. Then $\pi_{\mathbb{H}}$ has the local representation $z = z(\tau)$ and we have $\mathrm{d}s_G^2 = \lambda_\Sigma^2 |\mathrm{d}z|^2$, which gives:

$$\lambda_\Sigma(z) = \frac{1}{\mathrm{Im}\tau(z)} \left|\frac{\mathrm{d}\tau}{\mathrm{d}z}\right| \quad , \tag{B.9}$$

where $\tau(z)$ is a local inverse of $z(\tau)$.

Uniformization to the hyperbolic disk. The Cayley correspondence (B.6) identifies Fuchsian groups Γ with the discrete subgroups Δ of $\mathrm{PSU}(1,1)$. Composing $\pi_{\mathbb{H}}$ with the Cayley transformation $f : \mathbb{D} \to \mathbb{H}$ gives a holomorphic covering map $\pi_{\mathbb{D}} : \mathbb{D} \to \Sigma$ and a presentation $(\Sigma, G) = \mathbb{D}/\Delta$. The map $\pi_{\mathbb{D}}$ has the local representation $z = z(u)$ and we have $\mathrm{d}s_G^2 = \lambda_\Sigma^2 |\mathrm{d}z|^2$, which gives:

$$\lambda_\Sigma(z) = \frac{2}{1 - |u(z)|^2} \left|\frac{\mathrm{d}u}{\mathrm{d}z}\right| \quad , \tag{B.10}$$

where $u(z)$ is a local inverse of $z(u)$.

Remark. When (Σ, G) is given, the highly-nontrivial problem of determining the functions $z(u)$ (or $z(\tau)$) explicitly is known as the "explicit uniformization problem".

B.7 Classification of surface groups

Let $\bar{\mathbb{D}} \stackrel{\mathrm{def.}}{=} \mathbb{D} \sqcup \partial_\infty \mathbb{D}$ be the conformal compactification of $\mathbb{D}$ (which equals the closed unit disk). Let $\Lambda_{\mathbb{D}} \subset \partial_\infty \mathbb{D}$ denote the set of limit points (in the Euclidean topology) of the orbits of Δ on $\mathbb{D}$ and $\Lambda_{\mathbb{H}} \subset \partial_\infty \mathbb{H}$ denote the limit set of the corresponding Fuchsian group Γ. We can of course identify $\partial_\infty \mathbb{H}$ with $\partial_\infty \mathbb{D}$ and hence $\Lambda_{\mathbb{H}}$ with $\Lambda_{\mathbb{D}}$. The set $\Lambda_{\mathbb{D}}$ is closed and stabilized by the action of Δ on the complex plane given by fractional transformations. A classical theorem of Poincaré and Fricke-Klein states that one has the trichotomy [51–53]:

- $\Lambda_{\mathbb{D}}$ is finite, in which case Δ and Γ are called *elementary*.
- $\Lambda_{\mathbb{D}} = \partial_\infty \mathbb{D}$, in which case Δ and Γ are called of *the first kind*.

- $\Lambda_{\mathbb{D}}$ is a perfect and nowhere-dense[13] subset of $\partial_\infty\mathbb{D}$, in which case Δ and Γ are called of *the second kind*.

A hyperbolic surface (Σ, G) is called *elementary*, *of the first kind* or *of the second kind* if its uniformizing surface group Γ (equivalently, Δ) is of the corresponding type. For an elementary surface group Γ, the cardinality of $\Lambda_{\mathbb{D}} \simeq \Lambda_{\mathbb{H}}$ can equal 0, 1 or 2, namely:

- $\Lambda_{\mathbb{D}} = \emptyset$ iff (Σ, G) is isometric with the hyperbolic disk $\mathbb{D}$. In this case, $\Gamma = 1$ is the trivial group.
- $\Lambda_{\mathbb{D}} = \{u\}$ for some $u \in \partial_\infty\mathbb{D}$ iff (Σ, G) is isometric with the hyperbolic punctured disk[14] $\mathbb{D}^*$. In this case, $\Gamma \simeq \mathbb{Z}$ is the parabolic cyclic group consisting of all elements of $\mathrm{PSL}(2,\mathbb{R})$ which fix the point of $\partial_\infty\mathbb{H}$ corresponding to u.
- $\Lambda_{\mathbb{D}} = \{u_1, u_2\}$ with $u_1, u_2 \in \partial_\infty\mathbb{D}$ and $u_1 \neq u_2$ iff Σ is isometric with the hyperbolic annulus[15] $\mathbb{A}(R)$ for some $R > 1$. In this case, $\Gamma \simeq \mathbb{Z}$ is the hyperbolic cyclic group consisting of all elements of $\mathrm{PSL}(2,\mathbb{R})$ which fix both points of $\partial_\infty\mathbb{H}$ which correspond to u_1 and u_2.

Moreover, Γ (equivalently, Δ) is of the first kind iff $\mathrm{area}_G(\Sigma)$ is finite (see [52]); this happens iff a fundamental polygon of Δ has a finite number of vertices and sides and no free sides, where a side of a fundamental polygon is called *free* if it is a portion of the conformal boundary $\partial_\infty\mathbb{D}$ (see Appendix B.9). When Γ is of the second kind, the complement $\partial_\infty\mathbb{D} \setminus \Lambda_{\mathbb{D}} \simeq \partial_\infty\mathbb{H} \setminus \Lambda_{\mathbb{H}}$ is an open subset of S^1 and hence it is a countable disjoint union of open segments (intervals) which we denote by I_k ($k \in \mathbb{Z}_{>0}$); these are called the *intervals of discontinuity* of Γ.

B.8 Orientation-preserving isometries

For a smooth hyperbolic surface (Σ, G) uniformized by the surface group $\Gamma \subset \mathrm{PSL}(2,\mathbb{R})$, the group of orientation-preserving isometries coincides with the group of biholomorphisms (automorphisms of the underlying complex manifold (Σ, J)) and is given by:

$$\mathrm{Iso}^+(\Sigma, G) = N(\Gamma)/\Gamma \ ,$$

where:

$$N(\Gamma) \stackrel{\mathrm{def.}}{=} \{h \in \mathrm{PSL}(2,\mathbb{R}) \mid h\Gamma h^{-1} = \Gamma\}$$

is the normalizer of Γ in $\mathrm{PSL}(2,\mathbb{R})$. When Γ is elementary, this group is infinite and isomorphic with $\mathrm{U}(1)$. When Γ is non-elementary, this group is finite and its cardinality satisfies the bound [54]:

$$|\mathrm{Iso}^+(\Sigma, G)| \leq 12(g-1) + 6n \ , \quad n > 0 \ , \tag{B.11}$$

[13] I.e. a closed set with empty interior and without isolated points.

[14] The *hyperbolic punctured disk* $\mathbb{D}^*$ (also known as the *parabolic cylinder* [30]) is the non-compact hyperbolic surface obtained by endowing the open unit punctured disk $\{u \in \mathbb{C} | 0 < |u| < 1\}$ with its unique Riemannian metric of Gaussian curvature equal to -1.

[15] For each $R > 1$, the *hyperbolic annulus* $\mathbb{A}(R)$ (also known as the *hyperbolic cylinder* [30]) is the non-compact hyperbolic surface obtained by endowing the open annulus $\{u \in \mathbb{C} | \frac{1}{R} < |u| < R\}$ with its unique Riemannian metric of Gaussian curvature equal to -1. The positive quantity $\mu \stackrel{\mathrm{def.}}{=} 2\log R$ is known as the *modulus* of $\mathbb{A}(R)$.

where g is the genus of Σ and n is the number of ends. For $n = 0$ the previous formula does not apply, being replaced instead by the Hurwitz bound $|\mathrm{Iso}^+(\Sigma, G)| \leq 84(g-1)$. Notice that every finite group arises as the automorphism group of some compact hyperbolic surface.

B.9 Fundamental polygons

Let $\Gamma \subset \mathrm{PSL}(2, \mathbb{R})$ be a Fuchsian group with limit set $\Lambda_{\mathbb{H}} \subset \partial_\infty \mathbb{H}$ and let $\Sigma = \mathbb{H}/\Gamma$ be the corresponding hyperbolic surface. A subset $\mathfrak{D}_{\mathbb{H}} \subset \mathbb{H}$ is called a *fundamental domain* for Γ if it satisfies the following three conditions:

1. $\mathfrak{D}_{\mathbb{H}}$ is non-empty, open and connected.
2. For any $\gamma \in \Gamma \setminus \{1\}$, we have $\gamma(\mathfrak{D}_{\mathbb{H}}) \cap \mathfrak{D}_{\mathbb{H}} = 0$.
3. We have $\sqcup_{\gamma \in \Gamma} \overline{\mathfrak{D}_{\mathbb{H}}} = \mathbb{H}$, where $\overline{\mathfrak{D}_{\mathbb{H}}}$ denotes the relative closure of $\mathfrak{D}_{\mathbb{H}}$ in $\mathbb{H}$.

A fundamental domain $\mathfrak{D}_{\mathbb{H}}$ is called a *fundamental polygon* if it satisfies certain technical conditions for which we refer the reader to [51–53, 55]. These conditions state that $\mathfrak{D}_{\mathbb{H}}$ is a convex polygon which in general may have an infinite number of vertices and sides, where sides are either geodesic segments or so-called *free sides*. A free side of $\mathfrak{D}_{\mathbb{H}}$ is an interval of $\partial_\infty \mathbb{H}$ which is contained in some interval of discontinuity of Γ. A *free vertex* is a vertex of $\mathfrak{D}_{\mathbb{H}}$ which is an endpoint of a free side. An *ideal vertex* is a vertex of $\mathfrak{D}_{\mathbb{H}}$ which lies inside the limit set $\Lambda_{\mathbb{H}}$ of Γ. Any Fuchsian group (in particular, any surface group) admits a fundamental polygon (for example, the so-called Dirichlet polygon [51–53]). Two distinct sides of a fundamental polygon $\mathfrak{D}_{\mathbb{H}}$ are called *equivalent* (or Γ-*congruent*) if there exists an element $\gamma \in \Gamma$ which maps one side into the other. This defines an equivalence relation whose equivalence classes partition the set of all sides. Each equivalence class of non-free sides contains a single (unordered) pair of distinct sides, called a *Poincaré pair*. The set of all such equivalence classes is called the *Poincaré pairing* (or *side identification* [55]) of $\mathfrak{D}_{\mathbb{H}}$. Given two Γ-congruent non-free sides, there exist exactly two elements which map these sides into each other and these elements are mutually inverse. Moreover, picking one of these elements for each pair of Γ-congruent non-free sides one obtains a set of generators for Γ [51–53].

Since in our case Σ has no orbifold points and Γ is a surface group, all vertices of $\mathfrak{D}_{\mathbb{H}}$ must be ideal vertices or free vertices. When Γ is of the first kind, we have $\Lambda_{\mathbb{H}} = \partial_\infty \mathbb{H}$. In that case, $\mathfrak{D}_{\mathbb{H}}$ has no free sides and all its vertices are ideal vertices; thus $\mathfrak{D}_{\mathbb{H}}$ is an *ideal polygon*, i.e. a hyperbolic polygon all of whose vertices lie on $\partial_\infty \mathbb{H}$.

C Topologically finite surfaces

This appendix reviews certain classical results concerning topologically finite surfaces. An oriented surface Σ is called *topologically finite* if its fundamental group $\pi_1(\Sigma)$ is finitely-generated. This happens iff Σ is homeomorphic (and hence diffeomorphic) with $\hat{\Sigma} \backslash \{p_1, \ldots, p_n\}$, where $\hat{\Sigma}$ is a compact oriented surface without boundary and $p_1, \ldots, p_n$ is a finite collection of distinct points of $\hat{\Sigma}$. In this case, $\hat{\Sigma}$ is uniquely determined by Σ up to diffeomorphism, while the diffeomorphism class of Σ is determined by that of $\hat{\Sigma}$ and by the number n.

C.1 The end compactification. Genus and Euler characteristic

Let Σ be a topologically finite surface. Then $\hat{\Sigma}$ can be identified with the end (a.k.a. Kerékjártó-Stoilow) compactification of Σ, where $p_1, \ldots, p_n$ correspond to the Kerékjártó-Stoilow ideal points. In particular, Σ has exactly n ends, one for each ideal point p_j. Moreover, Σ is determined up to diffeomorphism by n and by the genus g of $\hat{\Sigma}$, which is also called the genus of Σ. The Euler characteristic of Σ is given by:

$$\chi(\Sigma) = 2 - 2g - n \quad ,$$

while that of $\hat{\Sigma}$ is given by:

$$\chi(\hat{\Sigma}) = 2 - 2g \quad .$$

If G is a *complete* metric on Σ such that $\mathrm{area}_G(\Sigma)$ is finite, the Gauss-Bonnet theorem applies[16], giving:

$$\int_\Sigma K(G)\mathrm{vol}_G = 2\pi\chi(\Sigma) \quad .$$

In particular, Σ admits a hyperbolic metric G of finite area iff $\chi(\Sigma) = -\frac{\mathrm{area}_G(\Sigma)}{2\pi}$ is negative, i.e. iff $2g + n > 2$. In the planar case $g = 0$, which requires $n \geq 3$.

Remark. When $g = 0$ (i.e. when Σ is a planar surface), the end compactification $\hat{\Sigma}$ is the unit sphere S^2.

C.2 Prolongation of conformal structures and the conformal compactification

Let $\Sigma = \hat{\Sigma} \setminus \{p_1, \ldots, p_n\}$ be a topologically finite surface. Consider a partition:

$$\mathcal{P} : \{1, \ldots, n\} = \{i_1, \ldots, i_{n_c}\} \sqcup \{j_1, \ldots, j_{n_f}\} \quad ,$$

where $n_c \geq 0$ and $n_f \geq 0$ are natural numbers. Since any annulus is diffeomorphic with the punctured unit disk, Σ is diffeomorphic with the borderless surface $\Sigma_{\mathcal{P}} \stackrel{\mathrm{def.}}{=} \hat{\Sigma} \setminus (\{p_{i_1}, \ldots, p_{i_{n_c}}\} \cup \bar{D}_{j_1} \cup \ldots \cup \bar{D}_{j_{n_f}})$, where $\bar{D}_j$ are closed disks embedded in $\hat{\Sigma}$ and centered at the points $p_{j_1}, \ldots, p_{j_{n_f}}$, such that no two closed disks meet each other and no closed disk meets any of the points $p_{i_1}, \ldots, p_{i_{n_c}}$.

Any orientation-compatible complex structure I on $\hat{\Sigma}$ determines a complete *canonical metric* $\hat{G}_I$ on $\hat{\Sigma}$ as follows [59]:

1. When $g = 0$, $(\hat{\Sigma}, I)$ is biholomorphic with the complex projective plane $\mathbb{CP}^1$. In this case, $\hat{G}_I$ is the unique metric on $\mathbb{CP}^1$ which has Gaussian curvature $+1$, i.e. the metric which makes $\mathbb{CP}^1$ isometric with the unit round sphere S^2.
2. When $g = 1$, $(\hat{\Sigma}, I)$ is biholomorphic with an elliptic curve. In this case, $\hat{G}_I$ is the unique flat metric for which a fundamental domain has sides 1 and τ, where $\tau \in \mathbb{H}$ is chosen such that $|\tau| \geq 1$ and $|\mathrm{Re}\tau| \leq \frac{1}{2}$.
3. When $g \geq 2$, $\hat{G}_I$ is the unique complete hyperbolic metric on $\hat{\Sigma}$ whose conformal class corresponds to I.

[16] This is because the boundary contribution from the cusp ends vanishes [56].

By definition, a *closed circular disk* in $\hat{\Sigma}$ relative to I is a closed subset of $\hat{\Sigma}$ which has the form:

$$\bar{D}_I(p;r) \stackrel{\text{def.}}{=} \{q \in \hat{\Sigma} | d_I(q,p) \leq r\} \quad ,$$

where p is a point of $\hat{\Sigma}$ and d_I is the distance function defined by the canonical metric $\hat{G}_I$. A *circle domain* of $(\hat{\Sigma}, I)$ is a connected open subset of Σ obtained by removing a finite number n_c of points and a finite number n_f of closed circular disks from $\hat{\Sigma}$ (where $n_c + n_f = n$) and endowing the resulting surface with the restriction of the complex structure I. Notice that any circle domain is diffeomorphic with a surface of the form $\Sigma_{\mathcal{P}}$ for some partition $\mathcal{P}$ as above.

Let J be an orientation-compatible complex structure on Σ. Then it was shown in [58, 59] that there exists a unique complex structure $\hat{J}$ on $\hat{\Sigma}$ such that (Σ, J) is biholomorphic with a circle domain Σ_J of $(\hat{\Sigma}, \hat{J})$. Moreover, Σ_J is uniquely determined up to a biholomorphism of $(\hat{\Sigma}, \hat{J})$. We say that $\hat{J}$ is the *prolongation* of J to $\hat{\Sigma}$. If $\mathfrak{c}$ and $\hat{\mathfrak{c}}$ are the conformal structures defined by J and $\hat{J}$ on Σ and $\hat{\Sigma}$, then we say that $\hat{\mathfrak{c}}$ is the prolongation of $\mathfrak{c}$ to $\hat{\Sigma}$.

By definition, the *conformal compactification* $\overline{\Sigma}_J$ of Σ with respect to J is the surface obtained by taking the closure of Σ_J inside $\hat{\Sigma}$. The topological boundary $\partial^J_\infty \Sigma = \overline{\Sigma}_J \setminus \Sigma$ of Σ_J consists of n_c isolated points and n_f disjoint simple closed curves; this is called the *conformal boundary* of (Σ, J). In particular, $(\overline{\Sigma}_J, \hat{J}|_{\overline{\Sigma}_J})$ is a bordered Riemann surface with n_c interior marked points and n_f boundary components. When J is of hyperbolic type, one has $n_f = 0$ iff the area of Σ (computed with respect to the hyperbolic metric determined by J) is finite. When a hyperbolic metric G on Σ is given, we define $\partial^G_\infty \Sigma \stackrel{\text{def.}}{=} \partial^J_\infty \Sigma$, where J is the complex structure determined by G. We sometimes write this simply as $\partial_\infty \Sigma$, when the hyperbolic metric G is understood.

Remark. Suppose that Σ is a planar surface, i.e. $g = 0$. In this case, $\hat{\Sigma} = \mathrm{S}^2$ admits a unique orientation-compatible complex structure I (which makes it biholomorphic with the Riemann sphere $\mathbb{CP}^1$) and the result above reduces to the classical statement that any topologically finite planar Riemann surface is biholomorphic with a circle domain in the Riemann sphere.

D Geometrically finite hyperbolic surfaces

This appendix contains a brief review of basic results on geometrically finite hyperbolic surfaces, i.e. those hyperbolic surfaces whose underlying 2-manifold is topologically finite. An important advantage of such surfaces (which makes them especially useful for applications to cosmology) is that each end of a geometrically finite hyperbolic surface admits a canonical neighborhood on which the hyperbolic metric can be brought to one of a small number of standard forms in semi-geodesic coordinates. A standard reference for this subject is [30].

D.1 Basics

Proposition-definition [30] Let (Σ, G) be a hyperbolic surface uniformized by the surface group $\Gamma \subset \mathrm{PSL}(2,\mathbb{R})$. Then the following statements are equivalent:

(a) Σ is topologically finite.

(b) Γ is finitely-generated.

(c) Γ admits a fundamental domain which is a convex polygon with a finite number of sides (some of which may be free sides).

In this case, one says that Γ and (Σ, G) are *geometrically finite*.

All elementary hyperbolic surfaces (the Poincaré disk, the hyperbolic punctured disk and the hyperbolic annuli) are geometrically finite. Moreover, a result due to Siegel states that any hyperbolic surface of the first kind (i.e. with finite area) is geometrically finite (see [52]); in particular, all compact hyperbolic surfaces are geometrically finite. A hyperbolic surface of the second kind may be either geometrically finite or geometrically infinite.

Elementary hyperbolic surfaces are special in that the isometry type of their ends can be exceptional. Due to this fact, we start by discussing non-elementary geometrically finite hyperbolic surfaces, whose ends admit a uniform classification up to isometry [30].

D.2 Hyperbolic type of ends of non-elementary geometrically finite hyperbolic surfaces

A non-elementary geometrically finite hyperbolic surface (Σ, G) can have only two types of ends, namely *cusp* or *funnel* ends. The cusp ends correspond to isolated points of the conformal boundary $\partial^G_\infty \Sigma$, while the funnel ends correspond to the simple closed curve components of $\partial^G_\infty \Sigma$.

Hyperbolic cusps. Given a parabolic element $P \in \mathrm{PSL}(2,\mathbb{R})$, the *cusp domain* $\mathcal{C}_P \subset \mathbb{H}$ defined by P is the interior of the disk bounded by the unit horocycle c_P of P (see Appendix B.4). The *hyperbolic cusp* defined by P is the quotient $\mathrm{C}_P = \mathcal{C}_P/\langle P\rangle$ (endowed with the quotient metric), where $\langle P\rangle$ denotes the infinite cyclic group generated by P. The cusp defined by any parabolic element $P \in \mathrm{PSL}(2,\mathbb{R})$ is isometric with a sub-disk of the hyperbolic punctured disk $\mathbb{D}^*$ which contains the origin (see Appendix D.4). In particular, the cusp is independent of the choice of the parabolic element P up to isometry. A hyperbolic cusp is non-compact but has finite hyperbolic area.

Hyperbolic funnels. Given a hyperbolic element $H \in \mathrm{PSL}(2,\mathbb{R})$, the *funnel domain* $\mathcal{F}_H \subset \mathbb{H}$ defined by H is the region bounded by $\partial_\infty\mathbb{H}$ and by the axis c_H of H. The *hyperbolic funnel* defined by H is the quotient $\mathrm{F}_H = \mathcal{F}_H/\langle H\rangle$ (endowed with the quotient metric), where $\langle H\rangle$ denotes the infinite cyclic group generated by H. Up to isometry, F_H depends only on the displacement length $\ell(H)$ of H and can be identified with the "inner half" of the hyperbolic annulus $\mathbb{A}(R_H)$ of modulus $\mu_H = 2\log R_H = \frac{2\pi^2}{\ell(H)}$, where R_H is the

displacement radius of H (see (B.8)). The displacement length $\ell(H)$ is called the *width* of the hyperbolic funnel. A hyperbolic funnel is non-compact and of infinite hyperbolic area.

The Nielsen and truncated Nielsen regions. Let $\Gamma \subset \mathrm{PSL}(2,\mathbb{R})$ be a non-elementary finitely-generated surface group and $\Sigma \stackrel{\text{def.}}{=} \mathbb{H}/\Gamma$. For each such group, we define the *cusp domains* $\mathcal{C}_j := \mathcal{C}_j(\Gamma)$, *funnel domains* $\mathcal{F}_k := \mathcal{F}_k(\Gamma)$, *Nielsen region* $\mathcal{N}_\Gamma$ and *truncated Nielsen region* $\mathcal{K}_\Gamma$ as follows. Let $\Lambda_{\mathbb{H}} \subset \partial_\infty\mathbb{H}$ denote the limit set of Γ. The set of points of $\partial_\infty\mathbb{H}$ which are fixed by some parabolic cyclic subgroup of Γ is a countable subset of $\Lambda_{\mathbb{H}}$ called the set of *cusp points of* Γ. For each cusp point $\tau_j \in \Lambda_{\mathbb{H}}$, let P_j be the positive generator of the parabolic cyclic subgroup of Γ which fixes τ_j and let $\mathcal{C}_j \stackrel{\text{def.}}{=} \mathcal{C}_{P_j} \subset \mathbb{H}$ be the cusp domain defined by P_j. It can be shown (see [30, Lemma 2.12]) that $\overline{\mathcal{C}_{j_1}} \cap \overline{\mathcal{C}_{j_2}} = \emptyset$ for $j_1 \neq j_2$ and that an element $\gamma \in \Gamma$ satisfies $\gamma(\mathcal{C}_j) \cap \mathcal{C}_j \neq \emptyset$ iff $\gamma(\mathcal{C}_j) = \mathcal{C}_j$ iff γ belongs to the parabolic cyclic group $\langle P_j \rangle$ generated by P_j. Distinguish the cases:

A. When Γ is of the first kind, we have $\Lambda_{\mathbb{H}} = \partial_\infty\mathbb{H}$. In this case, define:

$$\mathcal{N}_\Gamma \stackrel{\text{def.}}{=} \mathbb{H} \quad , \quad \mathcal{K}_\Gamma \stackrel{\text{def.}}{=} \mathbb{H} \setminus (\sqcup_j \mathcal{C}_j) \quad .$$

B. When Γ is of the second kind, the complement $\partial_\infty\mathbb{H} \setminus \Lambda_{\mathbb{H}}$ is a countable union of intervals of discontinuity of Γ. For each such interval I_k, let H_k be the generator of the hyperbolic cyclic group consisting of all hyperbolic elements of $\mathrm{PSL}(2,\mathbb{R})$ which fix the two endpoints of I_k and let $\mathcal{F}_k \stackrel{\text{def.}}{=} \mathcal{F}_{H_k} \subset \mathbb{H}$ denote the funnel domain defined by H_k. It can be shown (see [30, Lemma 2.12]) that the closure of $\mathcal{F}_k$ does not meet any $\mathcal{F}_{k'}$ with $k' \neq k$ and also does not meet the union of the cusp regions $\cup_j \mathcal{C}_j$. Define:

$$\mathcal{N}_\Gamma \stackrel{\text{def.}}{=} \mathbb{H} \setminus (\sqcup_j \mathcal{F}_j) \quad , \quad \mathcal{K}_\Gamma \stackrel{\text{def.}}{=} \mathcal{N}_\Gamma \setminus (\sqcup_j \mathcal{C}_j) \quad .$$

It is easy to see the set $\mathcal{N}_\Gamma$ is geodesically convex, being the geodesic convex hull of $\Lambda_{\mathbb{H}}$.

The canonical decomposition of Σ.

Definition. The *convex core* of Σ is the bordered surface:

$$N_\Sigma \stackrel{\text{def.}}{=} \mathcal{N}_\Gamma/\Gamma \quad ,$$

endowed with the quotient hyperbolic metric. The *compact core* of Σ is the bordered compact surface:

$$K_\Sigma \stackrel{\text{def.}}{=} \mathcal{K}_\Gamma/\Gamma \quad ,$$

endowed with the quotient hyperbolic metric. The *cusp regions* $\mathrm{C}_1, \ldots, \mathrm{C}_{n_c}$ of Σ are the distinct regions of Σ obtained from the sequence of hyperbolic cusps $\mathcal{C}_j/\langle P_j \rangle$ under the full quotient by Γ. The *funnel regions* $\mathrm{F}_1, \ldots, \mathrm{F}_{n_f}$ of Σ are the distinct regions of Σ obtained from the sequence of hyperbolic funnels $\mathcal{F}_k/\langle H_k \rangle$ under the full quotient by Γ. The quotient of $\mathbb{H}$ by Γ identifies those hyperbolic cusps $\mathcal{C}_{j_1}/P_{j_1}$ and $\mathcal{C}_{j_2}/P_{j_2}$ for which P_{j_1} is conjugate to P_{j_2} inside Γ, and similarly for hyperbolic funnels.

We have:

$$N_\Sigma = K_\Sigma \sqcup \mathrm{C}_1 \sqcup \ldots \sqcup \mathrm{C}_{n_c} \quad .$$

The convex core N_Σ is the largest geodesically convex subset of Σ.

Theorem. [30] A non-elementary geometrically finite hyperbolic surface (Σ, G) admits a disjoint union decomposition $\Sigma = N_\Sigma \sqcup \mathrm{F}_1 \sqcup \ldots \sqcup \mathrm{F}_{n_f} = K_\Sigma \sqcup \mathrm{C}_1 \sqcup \ldots \sqcup \mathrm{C}_{n_c} \sqcup \mathrm{F}_1 \sqcup \ldots \sqcup \mathrm{F}_{n_f}$.

In particular, each end of sigma corresponds to a cusp or a funnel region, being either a cusp end or a funnel end. We have:

$$n = n_c + n_f \quad ,$$

where n is the total number of ends. Moreover:

- (Σ, G) has no funnel ends ($n_f = 0$) iff it is of the first kind, i.e. iff (Σ, G) has finite area.
- (Σ, G) has no cusp ends ($n_c = 0$) iff the convex core N_Σ is compact.
- (Σ, G) is compact iff it has no ends ($n = 0$).

A geometrically finite hyperbolic surface with two cusp ends and one funnel end is sketched in Figure 8.

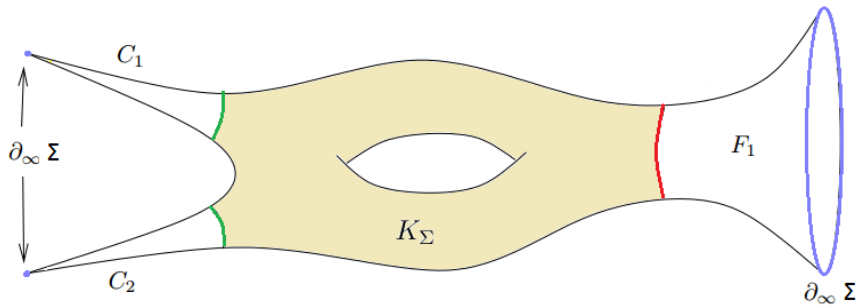

Figure 8: A geometrically finite hyperbolic surface with two cusp ends and one funnel end, where K_Σ indicates the compact core. In this example, the ideal boundary consists of $n = 3$ points while the conformal boundary $\partial_\infty \Sigma$ consists of two points (the blue dots corresponding to the cusp ends) and a circle (the blue circle corresponding to the funnel end). The two green lines are the horocycles which separate the compact core K_Σ from the two cusp regions C_1 and C_2, while the red line is the geodesic which separates K_Σ from the funnel region F_1.

D.3 Hyperbolic pants decompositions of the convex core

Recall that a (topological) *pair of pants* X is a genus zero surface with boundary which is diffeomorphic with a sphere with three holes, where the boundaries of the holes (each of which is diffeomorphic with a circle and is called a *cuff*) are the boundary components of X.

Such a surface has genus zero and 3 ends, thus $\chi(X) = -1$. In particular, the fundamental group $\pi_1(X)$ is free on two generators. A *hyperbolic pants metric* is a hyperbolic metric G on X for which each boundary component is a geodesic. When endowed with such a metric, the Riemannian manifold with boundary (X, G) is called a *hyperbolic pair of pants*. This has area 2π and the hyperbolic metric G is uniquely determined by the hyperbolic lengths (called the *cuff lengths*) ℓ_1, ℓ_2, ℓ_3 of the boundary components. A cuff length vanishes iff the corresponding cuff is collapsed to a point; such a generated pair of pants is called *tight*. The non-negative real numbers ℓ_1, ℓ_2 and ℓ_3 determine (X, G) up to isometry, so we shall use the notation $X(\ell_1, \ell_2, \ell_3)$ for the latter. The uniformizing group of $X(\ell_1, \ell_2, \ell_3)$ is a free group on two generators. Moreover, $X(\ell_1, \ell_2, \ell_3)$ can be obtained by gluing two copies of a right angled hyperbolic hexagon $\mathcal{H} \subset \mathbb{H}$ with three alternating sides of lengths $\ell_1/2$, $\ell_2/2$ and $\ell_3/2$, where the gluing is performed along the other three sides. Such a hyperbolic hexagon is uniquely-determined by ℓ_1, ℓ_2 and ℓ_3 up to the action of $\mathrm{PSL}(2, \mathbb{R})$. The following is a fundamental result in Teichmüller theory [30, 36]:

Theorem. Let (Σ, G) be a non-elementary geometrically finite hyperbolic surface. Then the convex core N_Σ of (Σ, G) can be decomposed as a finite union of hyperbolic pairs of pants $X_1, \ldots, X_m$, where $m = -\chi(\Sigma) = n + 2g - 2$ and the hyperbolic pants metric of X_j is given by restricting G:

$$N_\Sigma = X_1 \cup \ldots \cup X_{n+2g-2} \quad .$$

The hyperbolic pairs of pants in the theorem are separated by geodesics of (Σ, G). One can order these such that $X_1, \ldots, X_{n_c}$ are tight pairs of pants, each of which has precisely one vanishing cuff length; this isolates each cusp end of Σ within a tight pair of pants. Notice that the hyperbolic pants decomposition of (Σ, G) is not unique.

D.4 Cusp and funnel coordinates

Consider a geometrically finite hyperbolic surface $\Sigma = \mathbb{H}/\Gamma$, where $\Gamma \subset \mathrm{PSL}(2, \mathbb{R})$ is a surface group with limit set $\Lambda_\mathbb{H} \subset \partial_\infty \mathbb{H}$. Recall that $\partial_\infty \mathbb{H} \setminus \Lambda_\mathbb{H}$ is a countable union of intervals of discontinuity I_k. Since $\partial_\infty \mathbb{H}$ and $\Lambda_\mathbb{H}$ are stabilized by the action of Γ, this action permutes the intervals I_k.

Ideal vertices and free sides of a fundamental polygon. Let $\mathfrak{D}_\mathbb{H}$ be a fundamental polygon for Γ. The Euclidean closure of $\mathfrak{D}_\mathbb{H}$ touches $\partial_\infty \mathbb{H}$ at a finite number of ideal vertices and along a finite number of free sides. Each ideal vertex lies in $\Lambda_\mathbb{H}$ while each free side is contained in one of the intervals I_k. Two ideal vertices or two free sides of $\mathfrak{D}_\mathbb{H}$ are called equivalent if they are related by the action of an element of Γ. This defines equivalence relations on the sets of ideal vertices and free sides of $\mathfrak{D}_\mathbb{H}$, which partition these sets into equivalence classes called *ideal vertex cycles* and *free side cycles*. Equivalent vertices project through $\pi_\mathbb{H}$ to the same isolated point of the conformal boundary $\partial_\infty \Sigma$, while equivalent free sides project to the same circle component of $\partial_\infty \Sigma$. It follows that cusp points and circle components of $\partial_\infty \Sigma$ are respectively in bijection with ideal vertex cycles and free side cycles.

Cusp coordinates. At each ideal vertex v of the fundamental polygon, two sides of $\mathfrak{D}_{\mathbb{H}}$ (which are hyperbolic geodesic segments of $\mathbb{H}$) meet with a vanishing angle, being paired by a parabolic element $P_v \in \Gamma$. This element is a generator of the parabolic cyclic group consisting of all elements of $\mathrm{PSL}(2,\mathbb{R})$ which fix v, and we can take it to be the positive generator of that group. The *relative cusp neighborhood* of v in $\mathfrak{D}_{\mathbb{H}}$ is the intersection:

$$\mathfrak{C}_v \stackrel{\text{def.}}{=} \mathfrak{D}_{\mathbb{H}} \cap \mathcal{C}_v$$

of $\mathfrak{D}_{\mathbb{H}}$ with the cusp domain $\mathcal{C}_v \stackrel{\text{def.}}{=} \mathcal{C}_{P_v}$ of P_v. It can be shown that no vertex of $\mathfrak{D}_{\mathbb{H}}$ except v meets the Euclidean closure of $\mathfrak{C}_v$. The holomorphic covering map $\pi_{\mathbb{H}}$ maps $\mathcal{C}_v$ onto the cusp region $\mathrm{C}_p = \mathcal{C}_v/\langle P_v\rangle$ of Σ, which is a holomorphically embedded disk punctured at the corresponding ideal point $p = \pi_{\mathbb{H}}(v) \in \hat{\Sigma} \setminus \Sigma$ (see Figure 9). There exists a unique element $T_v \in \mathrm{PSL}(2,\mathbb{R})$ such that $T_v P_v T_v^{-1}$ equals the translation $\tau \to \tau + 1$. The local holomorphic coordinate z_p on C_p which identifies the latter with the punctured disk:

$$\dot{D} \stackrel{\text{def.}}{=} \{z \in \mathbb{C} \,|\, 0 < |z| < e^{-2\pi}\} \tag{D.1}$$

is called a *local cusp coordinate* for Σ near p and is given by[17]:

$$z_p = e^{2\pi i T_v \tau} \quad (\tau \in \mathcal{C}_v)\ . \tag{D.2}$$

Notice that z_p depends only on the ideal point p. Indeed, if v' is another ideal vertex of $\mathfrak{D}_{\mathbb{H}}$ such that $\pi_{\mathbb{H}}(v') = \pi_{\mathbb{H}}(v) = p$, then we have $v' = \gamma v$ for some $\gamma \in \Gamma$ and hence $P_{v'} = \gamma P_v \gamma^{-1}$ and $\mathcal{C}_{v'} = \gamma \mathcal{C}_v$. Thus $T_{v'} = T_v \gamma^{-1}$ and $T_{v'}\tau' = T_v(\gamma^{-1}\tau') = T_v\tau$ for any $\tau' = \gamma\tau \in \mathcal{C}_{v'}$, where $\tau \in \mathcal{C}_v$. With respect to the coordinate z_p, the ideal point p corresponds to $z_p = 0$ and the restriction of the hyperbolic metric G to the cusp region C_p of Σ corresponds to the restriction of the hyperbolic metric of the punctured disk $\mathbb{D}^*$ to the punctured disk (D.1).

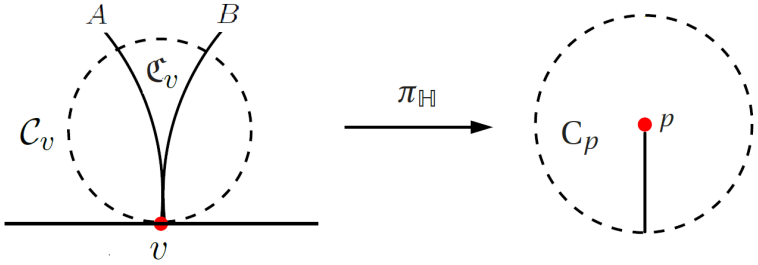

Figure 9: Two sides A and B of a fundamental polygon $\mathfrak{D}_{\mathbb{H}}$ meeting at an ideal vertex $v \in \partial_\infty \mathbb{H}$ and the unit horocycle of the parabolic generator P_v. The relative cusp neighborhood $\mathfrak{C}_v$ of v in $\mathfrak{D}_{\mathbb{H}}$ is the region lying between the sides and the horocycle (represented by the dashed circle). The holomorphic covering $\pi_{\mathbb{H}}$ maps the cusp domain $\mathcal{C}_v$ bounded by the unit horocycle to the hyperbolic cusp region C_p of Σ, which can be identified with a punctured disk of radius $e^{-2\pi}$, centered at the corresponding ideal point $p = \pi_{\mathbb{H}}(v) \in \hat{\Sigma}$ (shown in red). The covering map identifies the two sides of $\mathfrak{D}_{\mathbb{H}}$ which meet at v.

[17] We have $T_v(v) = \infty$ and $T_v(\mathcal{C}_v) = \{\tau' \in \mathbb{H} \mid \mathrm{Im}\tau' > 1\}$.

Funnel coordinates. The ends of each free side E of $\mathfrak{D}_{\mathbb{H}}$ lie on two non-free sides of $\mathfrak{D}_{\mathbb{H}}$ (which are hyperbolic geodesic segments in $\mathbb{H}$). These meet $\partial_\infty\mathbb{H}$ orthogonally, being paired by a hyperbolic element $H_E \in \Gamma$. Let $e \stackrel{\text{def.}}{=} \pi_{\mathbb{H}}(E)$ denote the circle component of the conformal boundary $\partial^G_\infty\Sigma$ which corresponds to the free side E and let $p \in \hat{\Sigma} \setminus \Sigma$ be the corresponding ideal point. Let I_E be the unique interval of discontinuity of Γ which contains E. Then H_E is a generator of the hyperbolic cyclic subgroup of Γ consisting of all elements of $\mathrm{PSL}(2,\mathbb{R})$ which fix each of the endpoints of I_E, and we can take H_E to be the positive generator of this group. The *relative funnel neighborhood* of E in $\mathfrak{D}_{\mathbb{H}}$ is defined as the intersection:

$$\mathfrak{F}_E \stackrel{\text{def.}}{=} \mathfrak{D}_{\mathbb{H}} \cap \mathcal{F}_E$$

of $\mathfrak{D}_{\mathbb{H}}$ with the funnel domain $\mathcal{F}_E \stackrel{\text{def.}}{=} \mathcal{F}_{H_E}$ of H_E. It can be shown that no vertex of $\mathfrak{D}_{\mathbb{H}}$ except the two endpoints of E meets the Euclidean closure of $\mathfrak{F}_E$. Let $\ell_E \stackrel{\text{def.}}{=} \ell(H_E)$ and $R_E \stackrel{\text{def.}}{=} R_{H_E} = e^{\frac{\pi^2}{\ell_E}}$ be the displacement length and displacement radius of H_E (see (B.7) and (B.8)). The holomorphic covering map $\pi_{\mathbb{H}}$ projects $\mathcal{F}_E$ onto the funnel region F_p of Σ corresponding to p, which is a holomorphically embedded open annulus, whose inner boundary corresponds to e (see Figure 10). There exists a unique element $T_E \in \mathrm{PSL}(2,\mathbb{R})$ such that $T_E H_E T_E^{-1}$ is the dilation $\tau \to e^{\ell_E}\tau$. The local holomorphic coordinate z_p on F_p which identifies the latter with the open annulus:

$$A_{R_E} \stackrel{\text{def.}}{=} \{z \in \mathbb{C} \,\big|\, \frac{1}{R_E} < |z| < 1\} \tag{D.3}$$

is called a *local funnel coordinate* on Σ near p and is given by[18]:

$$z_p = e^{\frac{2\pi i}{\ell_E}\log(T_E\tau)} \quad (\tau \in \mathcal{F}_E) \quad . \tag{D.4}$$

Again notice that z_p depends only on the ideal point p. With respect to this coordinate, e corresponds to the circle of radius $|z_p| = \frac{1}{R_E}$ and the restriction of the hyperbolic metric G to the funnel region F_p of Σ corresponds to the restriction of the hyperbolic metric of $\mathbb{A}(R_E)$ to the annulus (D.3).

[18] We have $T_E(E) = \{\tau' \in \mathbb{H} \mid \mathrm{Re}\tau' = 0\}$ and $T_E(\mathcal{F}_E) = \{\tau' \in \mathbb{H} \mid \mathrm{Re}\tau' > 0\}$.

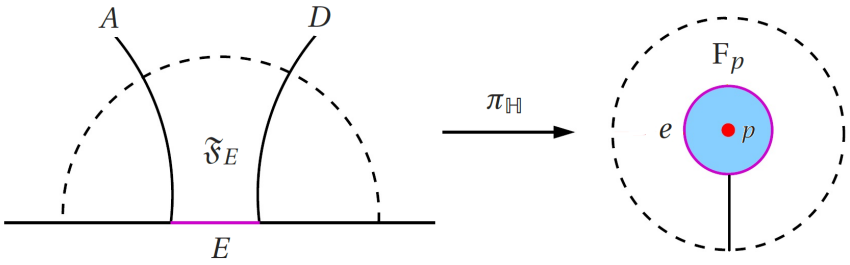

Figure 10: A free side E of a fundamental polygon is shown in magenta. The dashed half-circle is the axis of the hyperbolic transformation H which pairs the two non-free sides A and D of $\mathfrak{D}_{\mathbb{H}}$ which meet the endpoints of E; this axis meets $\partial_\infty\mathbb{H}$ at the endpoints of the interval of discontinuity I_E which contains E. The relative funnel neighborhood $\mathfrak{F}_E$ of E in $\mathfrak{D}_{\mathbb{H}}$ is the region lying between E, these two non-free sides and the dashed half-circle. The holomorphic covering $\pi_{\mathbb{H}}$ maps E to the inner circle (continuous line e of radius $1/R_E$) of the annulus A_{R_E} which corresponds to the funnel region F_p. The dashed boundary of the funnel neighborhood is mapped to the outer circle (radius 1) of this annuls, while the sides A and D of the fundamental polygon are identified by the projection. The ideal point p corresponding to the funnel end is depicted in red. The shadowed disk shown in blue is *not* part of Σ or of its conformal compactification $\partial^G_\infty\Sigma$.

D.5 Ends of elementary hyperbolic surfaces

Elementary hyperbolic surfaces can have special types of hyperbolic ends, known as the *plane* and *horn* ends. The plane end is the only end of the Poincaré disk $\mathbb{D}$, while the horn end is one of the two hyperbolic ends of the hyperbolic punctured disk $\mathbb{D}^*$ (the other being a cusp end). On the other hand, a hyperbolic annulus $\mathbb{A}(R)$ has two ends, both of which are hyperbolic funnels. More details about these ends and some applications of elementary hyperbolic surfaces to cosmology can be found in [31, 32].

D.6 Explicit form of the hyperbolic metric on a canonical neighborhood of each end

The ends of a geometrically finite hyperbolic surface admit semi-geodesic coordinate neighborhoods on which the hyperbolic metric takes a canonical form [30, 57]:

1. (**cusp ends**) The cusp region C_p of Σ corresponding to a cusp ideal point $p \in \hat{\Sigma}\setminus\Sigma$ is isometric with $\mathbb{R}_{>0}\times\mathbb{R}/(2\pi\mathbb{Z})$, equipped with the following metric:

$$\mathrm{d}s^2_G = \mathrm{d}r^2 + e^{-2r}\frac{\mathrm{d}\theta^2}{(2\pi)^2} \quad .$$

   On this region, $r > 0$ and $\theta \in (0, 2\pi)$ are semi-geodesic coordinates. The boundary of this region relative to Σ is a horocycle of length 1 placed at $r = 0$, while the ideal point p corresponds to $r \to +\infty$.

2. (**funnel ends**) The funnel region F_p of Σ corresponding to a funnel ideal point $p \in \hat{\Sigma} \setminus \Sigma$ is isometric with $\mathbb{R}_{>0} \times \mathbb{R}/(2\pi\mathbb{Z})$, equipped with the following metric:

$$\mathrm{d}s_G^2 = \mathrm{d}r^2 + \ell_p^2 \cosh(r)^2 \frac{\mathrm{d}\theta^2}{(2\pi)^2} \quad ,$$

where ℓ_p is the width of the funnel. On this region, $r > 0$ and $\theta \in (0, 2\pi)$ are semi-geodesic coordinates. The boundary of this region relative to Σ is a closed geodesic of length ℓ_p placed at $r = 0$, while the ideal point p (and the associated circle of the conformal boundary $\partial_\infty^G \Sigma$) correspond to $r \to +\infty$.

3. (**horn end**) A canonical punctured neighborhood in[19] $\widehat{\mathbb{D}^*}$ of the ideal point corresponding to the horn end of $\mathbb{D}^*$ is isometric to $\mathbb{R}_{>0} \times \mathbb{R}/(2\pi\mathbb{Z})$, equipped with the following metric:

$$\mathrm{d}s_G^2 = \mathrm{d}r^2 + e^{2r} \frac{\mathrm{d}\theta^2}{(2\pi)^2} \quad .$$

On such a neighborhood, $r > 0$ and $\theta \in (0, 2\pi)$ are semi-geodesic coordinates. The boundary of such a neighborhood relative to $\mathbb{D}^*$ is a horocycle of length 1 placed at $r = 0$. The ideal point (and the associated circle of the conformal boundary $\partial_\infty^G \Sigma$) corresponds to $r \to +\infty$. The only hyperbolic surface which admits a horn end is the hyperbolic punctured disk $\mathbb{D}^*$.

4. (**plane end**) A canonical punctured neighborhood in $\hat{\mathbb{D}}$ of the ideal point corresponding to the plane end of $\mathbb{D}$ is isometric to $\mathbb{R}_{>0} \times \mathbb{R}/(2\pi\mathbb{Z})$, equipped with the following metric:

$$\mathrm{d}s_G^2 = \mathrm{d}r^2 + \sinh(r)^2 \mathrm{d}\theta^2 \quad .$$

On such a neighborhood, $r > 0$ and $\theta \in (0, 2\pi)$ are semi-geodesic coordinates. The ideal point (and the associated circle of the conformal boundary $\partial_\infty^G \Sigma$) corresponds to $r \to +\infty$. The only hyperbolic surface which admits a plane end is the Poincaré disk $\mathbb{D}$.

The previous list implies the following asymptotic behavior for $r \gg 1$, near an ideal point $p \in \hat{\Sigma} \setminus \Sigma$:

$$\mathrm{d}s_G^2 = \mathrm{d}r^2 + \left(\frac{c_p}{4\pi}\right)^2 e^{2\epsilon_p r} \mathrm{d}\theta^2 \quad , \tag{D.5}$$

where $\theta \in (0, 2\pi)$ and[20]:

$$c_p = \begin{cases} \ell_p \ , & \textit{funnel end} \\ 2\pi \ , & \textit{plane end} \\ 2 \ , & \textit{horn or cusp end} \end{cases} \quad , \tag{D.6}$$

$$\epsilon_p = \begin{cases} +1 & \textit{funnel, plane or horn end} \\ -1 & \textit{cusp end} \end{cases} \quad .$$

[19] Recall that the hat denotes the end compactification.

[20] The sign factor ϵ_p should not be confused with the slow-roll parameter ϵ.

A funnel, plane or horn end will be called a *flaring end*. Flaring ends are characterized by the fact that the size of horocycles in (Σ, G) grows exponentially towards the end ($\epsilon_p = +1$); such an end corresponds to a circle boundary component of the conformal compactification of (Σ, G). The only non-flaring ends are cusp ends, each of which corresponds to a point added when passing to the conformal compactification; for such ends, the length of horocycles in (Σ, G) tends to zero as one approaches the ideal point.

References

[1] R. Kallosh, A. Linde, D. Roest, *Superconformal Inflationary α-Attractors*, JHEP **11** (2013) 098, arXiv:1311.0472 [hep-th].

[2] R. Kallosh, A. Linde, D. Roest, *Large field inflation and double α-attractors*, JHEP **08** (2014) 052, arXiv:1405.3646 [hep-th].

[3] R. Kallosh, A. Linde, D. Roest, *A universal attractor for inflation at strong coupling*, Phys. Rev. Lett. **112** (2014) 011303, arXiv:1310.3950 [hep-th].

[4] M. Galante, R. Kallosh, A. Linde, D. Roest, *The Unity of Cosmological Attractors*, Phys. Rev. Lett. **114** (2015) 141302, arXiv:1412.3797 [hep-th].

[5] J. J. M. Carrasco, R. Kallosh, A. Linde, D. Roest, *The hyperbolic geometry of cosmological attractors*, Phys. Rev. D **92** (2015) 4, 41301, arXiv:1504.05557 [hep-th].

[6] R. Kallosh, A. Linde, *Escher in the Sky*, Comptes Rendus Physique **16** (2015) 914, arXiv:1503.06785 [hep-th].

[7] P. A. R. Ade et al. [Planck Collaboration], Astron. Astrophys. **594** (2016) A20 doi:10.1051/0004-6361/201525898, arXiv:1502.02114 [astro-ph.CO]

[8] C. M. Peterson, M. Tegmark, *Testing Two-Field Inflation*, Phys. Rev. D **83** (2011) 023522, arXiv:1005.4056 [astro-ph.CO].

[9] C. M. Peterson, M. Tegmark, *Non-Gaussianity in Two-Field Inflation*, Phys. Rev. D **84** (2011) 023520, arXiv:1011.6675 [astro-ph.CO].

[10] A. Achucarro, Y. Welling, *Multiple field inflation and signatures of heavy physics in the CMB*, arXiv:1502.04369 [gr-qc].

[11] R. Schimmrigk, *Modular inflation observables and j-inflation phenomenology*, JHEP09 (2017) 043, arXiv:1612.09559 [hep-th].

[12] R. Schrimmrigk, *Multifield Reheating after Modular j-Inflation*, arXiv:1712.09961 [hep-ph].

[13] C. Gordon, D. Wands, B. A. Bassett, R. Maartens, *Adiabatic and entropy perturbations from inflation*, Phys. Rev D **63** (2001) 023506, astro-ph/0009131.

[14] S. G. Nibbelink, B. van Tent, *Scalar perturbations during multiple field slow-roll inflation* Class. Quant. Grav. **19** (2002) 613–640, hep-ph/0107272.

[15] S. Cremonini, Z. Lalak, K. Turzynski, *Strongly Coupled Perturbations in Two-Field Inflationary Models*, JCAP, **1103** (2011) 016, arXiv:1010.3021 [hep-th].

[16] Z. Lalak, D. Langlois, S. Pokorski, K. Turzynski, *Curvature and isocurvature perturbations in two-field inflation*, JCAP **0707** (2007) 014, arXiv:0704.0212 [hep-th].

[17] A. Achucarro, J.-O. Gong, S. Hardeman, G. A. Palma, S. P. Patil, *Features of heavy physics in the CMB power spectrum*, JCAP **1101** (2011) 030, arXiv:1010.3693 [hep-ph].

[18] A. Achucarro, J.-O. Gong, S. Hardeman, G. A. Palma, S. P. Patil, *Mass hierarchies and nondecoupling in multi-scalar field dynamics*, Phys. Rev. D **84** (2011) 043502, arXiv:1005.3848 [hep-th].

[19] J.-O. Gong, *Multi-field inflation and cosmological perturbations*, Int. J. Mod. Phys D **26** (2017) 1, 1740003, arXiv:1606.06971 [gr-qc].

[20] M. Dias, J. Frazer, D. Seery, *Computing observables in curved multifield models of inflation – A guide (with code) to the transport method*, JCAP **12** (2015) 030, arXiv:1502.03125 [astro-ph.CO].

[21] M. Dias, J. Frazer, D. J. Mulryne, D. Seery, *Numerical evaluation of the bispectrum in multiple field inflation*, JCAP **12** (2016) 033, arXiv:1609.00379 [astro-ph.CO].

[22] D. J. Mulryne, *PyTransport: A Python package for the calculation of inflationary correlation functions*, arXiv:1609.00381 [astro-ph.CO].

[23] K. Kainulainen, J. Leskinen, S. Nurmi, T. Takahashi, *CMB spectral distortions in generic two-field models*, JCAP **11** (2017) 002, arXiv:1707.01300 [astro-ph.CO].

[24] N. Bartolo, D.M.Bianco, R. Jimenez, S. Matarrese, L. Verde. *Supergravity, α-attractors and primordial non-Gaussianity*, arXiv:1805.04269 [astro-ph.CO].

[25] H. Freudenthal, *Uber die Enden topologischer Räume und Gruppen*, Math. Z. **33** (1931) 692–713.

[26] G. Peschke, *The theory of ends*, Nieuw Archief voor Wiskunde **8** (1990) 1–12.

[27] I. Richards, *On the Classification of Non-Compact Surfaces*, Transactions of the AMS **106** (1963) 2, 259–269.

[28] S. Stoilow, *Leçons sur les principes topologiques de la théorie des fonctions analytiques*, Gauthier-Villars, Paris, 1956.

[29] H. P. de Saint-Gervais, *Uniformization of Riemann Surfaces: revisiting a hundred-year-old theorem*, EMS, 2016.

[30] D. Borthwick, *Spectral Theory of Infinite-Area Hyperbolic Surfaces*, Progress in Mathematics **256**, Birkhäuser, Boston, 2007.

[31] E. M. Babalic, C. I. Lazaroiu , *Generalized α-attractor models from elementary hyperbolic surfaces*, Adv. Math. Phys., Vol. 2018 (2018), Art. ID 7323090, 1-24, arXiv:1703.01650 [hep-th].

[32] E. M. Babalic, C. I. Lazaroiu, *Generalized α-attractors from the hyperbolic triply-punctured sphere*, arXiv:1703.06033 [hep-th].

[33] P. Fré, A. S. Sorin, *Axial Symmetric Kähler manifolds, the D-map of Inflaton Potentials and the Picard-Fuchs Equation*, Fortsch. Phys. **62** (2014) 26, arXiv:1310.5278 [hep-th].

[34] S. Ferrara, P. Fré, A. S. Sorin, *On the Topology of the Inflaton Field in Minimal Supergravity Models,* JHEP **1404** (2014) 095, arXiv:1311.5059 [hep-th].

[35] S. Ferrara, P. Fré, A. S. Sorin, *On the Gauged Kähler Isometry in Minimal Supergravity Models of Inflation*, Fortsch. Phys. **62** (2014) 277, arXiv:1401.1201 [hep-th].

[36] P. Buser, *Geometry and Spectra of Compact Riemann Surfaces*, Birkhäuser, 1992.

[37] A. Achucarro, R. Kallosh, A. Linde, D-G Wang, Y. Welling, *Universality of multifield α-attractors*, JCAP **04** (2018) 028, arXiv:1711.09478 [hep-th].

[38] G. Barenboim, W.-I. Park, *Spiral Inflation*, Phys. Lett. B **741** (2015) 252, arXiv:1412.2724 [hep-ph].

[39] G. Barenboim, W.-I. Park, *Spiral Inflation with Coleman-Weinberg Potential*, Phys. Rev. D **91** (2015) 6, 063511, arXiv:1501.00484 [hep-ph].

[40] P. Christodoulidis, D. Roest, E. I. Sfakianakis, *Angular inflation in multi-field α-attractors*, arXiv:1803.09841 [hep-th].

[41] S. Garcia-Saenz, S. Renaux-Petel and J. Ronayne, *Primordial fluctuations and non-Gaussianities in sidetracked inflation*, arXiv:1804.11279 [astro-ph.CO].

[42] A. R. Brown, *Hyperinflation*, arXiv:1705.03023 [hep-th].

[43] J. Voight, *Computing fundamental domains for cofinite Fuchsian groups*, J. Théorie Nombres Bordeaux **21** (2009) 2, 467–489, see also *Errata: Computing fundamental domains for cofinite Fuchsian groups*, https://math.dartmouth.edu/ jvoight/articles/funddom-errata.pdf

[44] SageMath mathematics software, available online at: http://www.sagemath.org/.

[45] D. Bump, *Automorphic Forms and Representations*, Cambridge Studies in Advanced Mathematics **55**, Cambridge Univ. Press, 1997.

[46] R. Schimmrigk, *Automorphic inflation*, Phys. Lett. B **748** (2015) 376, arXiv:1412.8537 [hep-th].

[47] R. Schimmrigk, *A geneneral framework of automorphic inflation*, JHEP **05** (2016) 140, arXiv:1512.09082 [hep-th].

[48] H. C. Wilkie, *On non-Euclidean crystallographic groups*, Mathematische Zeitschrift **91** (1966) 87–102.

[49] E. Bujalance, F. J. Cirre, J. M. Gamboa, G. Gromadzki, *Symmetries of Compact Riemann Surfaces*, Lecture Notes in Mathematics **2007**, Springer, 2010.

[50] S. P. Novikov, I. A. Taimanov, *Modern Geometric Structures and Fields*, Graduate Studies in Mathematics **71**, AMS, 2006.

[51] A. F. Beardon, *The geometry of discrete groups*, Graduate Texts in Mathematics **91**, Springer, 1983.

[52] S. Katok, *Fuchsian Groups*, U. Chicago Press, 1992.

[53] W. Fenchel, J. Nielsen, *Discontinuous Groups of Isometries in the Hyperbolic Plane*, de Gruyter, 2003.

[54] K. Oikawa, *Notes on conformal mappings of a Riemann surface onto itself*, Kodai Math. Sem. Rep. **8** (1956) 1, 23–30.

[55] B. Maskit, *On Poincaré's Theorem for Fundamental Polygons*, Adv. Math **7** (1971) 219–230.

[56] S. Rosenberg, *Gauss-Bonnet theorems for non-compact surfaces*, Proc. Amer. Math. Soc. **86** (1982) 1, 184–185.

[57] D. Borthwick, C. Judge, P. A. Perry, *Selberg's zeta function and the spectral geometry of geometrically finite hyperbolic surfaces*, arXiv:math/0310364.

[58] A. Haas, *Linearization and mappings onto pseudocircle domains*, Trans. Amer. Math. Soc. **282** (1984), 415–429.

[59] B. Maskit, *Canonical domains on Riemann surfaces*, Proc. Amer. Math. Soc. **106** (1989), 713–721.